KTH Land and Water
Resources Engineering

SIMULATION OF THE PARIS 1910 FLOOD WITH A LUMPED HYDROLOGICAL MODEL : THE INFLUENCE OF FROZEN SOIL

Yohann Tondu

November 2010

TRITA-LWR Degree Project 11-09
ISSN 1651-064X
ISRN KTH/LWR/Degree Project 11-09
ISBN 55-555-555-5

Degree Project in Hydraulic Engineering

Department of Land and Water Resources Engineering

Royal Institute of Technology (KTH)

SE-100 44 STOCKHOLM, Sweden

Reference should be written as: Tondu, Y. (2010) "Simulation of the Paris 1910 flood with a lumped Hydrological model : The influence of frozen soil", Trita 11-09, 120p.

SUMMARY

Svenska

Denna uppsats handlar om simulationen av en översvämning i Paris år 1910. Efter en kort redogörelse av denna händelse och dess konsekvenser beskrivs regnflödes hydrologiska modellen, GR4J, som nu används till att förutse översvämningar av Seinebassängen. I nästa del presenteras resultaten av simulationen för översvämningen 1910 framtagen av GR4J på huvudbassängen i Seine vid Paris och 4 av dess underbassänger. När dessa resultat visade sig misslyckade, togs en ny hypotes fram om den möjliga inverkan av tjäle på översvämningsformationen. Således togs en frostmodul fram, kopplad till en jord temperatur modell med luft temperaturer som inläggsdata. Resultaten av simulationen för översvämningen 1910 framtagen av GR4J kopplad till frostmodulen är slutligen presenterade. Sammanfattningsvis, nya perspektiv är presenterade för att fortsätta forskningen.

Français

Ce mémoire a pour sujet la simulation de la crue qui inonda Paris en 1910. Après une brève présentation de cet évènement et de ses conséquences, GR4J, le modèle hydrologique pluie-débit aujourd'hui utilisé par les services de prédiction des crues sur le bassin de la Seine, est décrit. Le chapitre suivant présente les résultats obtenus par ce modèle en simulation de la crue de 1910 sur les bassins de la Seine à Paris et de 4 de ses sous-bassins. Comme ces résultats n'étaient pas satisfaisants, l'hypothèse d'une possible influence du gel sur la formation de la crue a été formulée. Un module gel a donc été développé, couplé avec un modèle de simulation de la température du sol à partir de la température de l'air. Enfin, les résultats des simulations de la crue de 1910 obtenus par GR4J couplé à ce module gel sont présentés. En conclusion, de nouvelles pistes d'études sont présentées pour poursuivre les recherches.

English

This thesis deals with the simulation of the flood that took place in Paris in 1910. After a brief presentation of this event and its consequences, GR4J, the lumped hydrological model that is now used in flood prediction on the Seine basin is described. The next part is presenting the results of the 1910 flood simulation obtained by GR4J on the main Seine at Paris basin and on 4 of its sub-basins. As these results were disapointing, a new hypothesis was developed about the possible influence of frozen soil on the flood formation. A frost module is thus developed, coupled with a soil temperature model using air temperatures as input data. The results of the 1910 flood simulation by GR4J coupled with the frost module are finally presented. In the conclusion, new perspectives are presented to continue the research.

ACKNOWLEDGEMENTS

I would like to thank my two French supervisors Vazken Andréassian and Charles Perrin for their help, their advices and their incredible benevolence. I would also like to thank the whole Hydrology team in CEMAGREF for their support and their happiness. It was really nice working with you. I would then like to thank the whole DIREN team for providing the data and helping with the calculations.

Thank you also to my Swedish supervisor, Hans Bergh, for his help. I would also like to thank Peter Brokking, Eva Lindhal, Nawal Safey and Mme. Arbeille who all helped me to get this internship.

Finally, I would like to thank all my friends and family for their unconditional support during those tempestuous times. I wouldn't have finished this thesis without you.

TABLE OF CONTENT

TABLE OF FRENCH INSTITUTIONS AND ABBREVIATIONS

CEMAGREF :	French national research institute in environment. This thesis was done in internship in their laboratories.
DIREN :	Regional Direction for Environment. Organism that is in charge of the flood prediction in Paris and that owns many archives related to the flood flow in 1910.
GR4J :	Hydrologic Rainfall-Runoff model used throughout this study for flow simulation.
Grands Lacs de Seine :	Organism that manages the 4 water reservoirs upstream of Paris.
Météo France :	French national meteorological institute.
RATP :	Public transport company in the Paris region.

ABSTRACT

In 1910, Paris experienced its biggest flood in the 20th century. In 2010, for the anniversary of this event – supposed to happen every 100 years ! – the flood prediction model that is now used on the Seine basin was tested on its simulation,… and failed to reproduce the observed flood volume. This paper will try to explain, and correct, such disappointing results. Many hypotheses have been tested and based on their results, it has been decided to develop a frost module in order to assess the influence of this phenomenon – that is not taken into account by the lumped hydrological model that is used – on the flood formation. A soil temperature model using air temperature as input data was also designed because soil temperature data were not available in 1910. The addition of the frost module did not, however, bring many improvements to the 1910 flood simulation because frost is a too rare phenomenon on the Seine basin for the module to be correctly calibrated. However, new perspectives are presented to continue the research on this phenomenon.

Key words : Paris 1910 flood ; Lumped hydrological model ; Rainfall-Runoff model ; Frost

1 INTRODUCTION : THE 1910 FLOOD

In winter 1910, from January to March, Paris experienced its biggest flood of the 20th century with the Seine river reaching a maximum level of 8,62m at the Paris Austerlitz station (around 8m more than the normal level) on Januray, 28th. The 1910 flood was also named "crue centennale" (100 years flood) because it was estimated that it had a probability of 1/100 to happen in any given year. Thus 2010 was a very special anniversary for this flood and this is how the subject of this thesis was launched in order to assess whether it could be possible to predict the 1910 flood today with the available hydrologic models.

This introduction will briefly describe the 1910 flood, its causes –to the extent of the current knowledge - and its effects. A last part will present what the consequences of a similar flood would be nowadays and how the main institutions are prepared for such an event. Most of the data and figures that will be introduced here were presented by the different invited speakers during the colloquium organized by the *Société Hydrologique de France* (French Hydrologic Society) on March, 24th, 25th 2010 about this particular event. The pictures are all coming from the archives of the *Bibliothèque Historique de la Ville de Paris* (Paris Historical Library).

1.1 The 1910 flood causes

In 1909, the summer and the last trimester were particularly rainy with unusual precipitation levels that saturated the soil with water.

In January 1910, two episodes of heavy rains were reported. The first one took place from January, 18th to 21st with unusually strong precipitations on many parts of the basin. Because of the saturated soil – and maybe other factors – the Seine and its tributaries reacts immediately with unusual water levels. The peak flows of the most rapid tributaries like the Yonne river reaches Paris in a few days and the water level in Paris Austerlitz raises. Peak flows of the other tributaries like the Marne river and the Seine are expected later, around January, 28th.

But from January, 23rd to January, 25th a second episode of precipitations happens that results in a second peak flow on all the basin's rivers. Around January, 26th, the second peak flows of the rapid tributaries meet the first peak flows of the slower tributaries and of the Seine. The simultaneity of those 2 events will then result in the maximum flow of the 1910 flood that will reach Paris on January, 28th.

After 10 days of increase, the water level in Paris Austerlitz will then decrease from January, 29th but won't reach a normal level before March 1910 with the occurrence of other peak flows during February 1910.

1.2 The 1910 flood consequences

A plan of the flooded areas in Paris is displayed on figure 1.1. Of course during the 1910 flood, the water got over the river's bank and flooded the streets, but it also infiltrated in the underground tunnels like the subway lines and reaches other parts of the city that were not very elevated like, for example, the Saint-Lazare station (Fig. 1.2). Monuments (Fig. 1.3 and 1.4) and garden (Fig. 1.5) were also flooded as long as other strategic places like stations (Fig. 1.6) or the deputies chamber (Fig. 1.7). But the most famous symbol of the 1910 flood still is the Alma bridge zouave statue on which Parisians measure the water level and that will be flooded till the shoulders (Fig. 1.8).

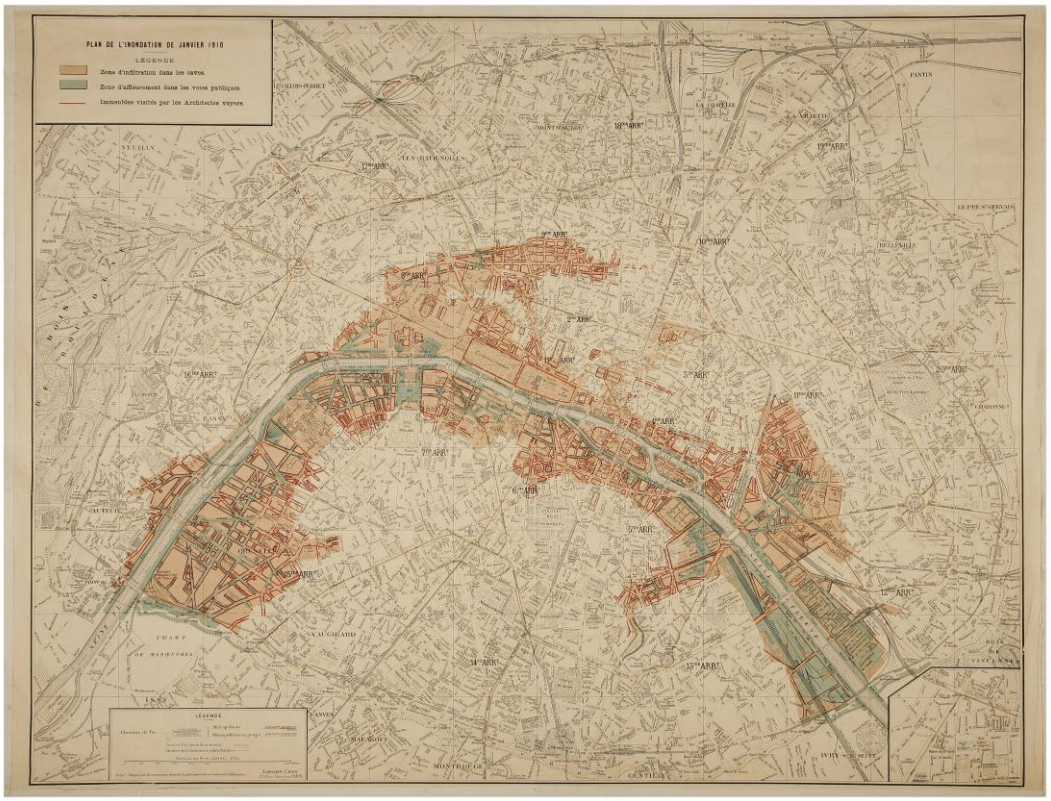

Fig. 1.1 Plan of the Flooded areas in Paris. In Orange the places where water infiltrated the caves, in blue, the places where it reached the streets.

Fig. 1.2 The Saint-Lazare station.

Fig. 1.3 Notre-Dame de Paris cathedral

The subway lines are rapidly flooded and unusable, especially near to the Seine. To move around the city, the Parisians thus mostly use horses as most of the modern energy transports are also unable to work in those conditions (Fig. 1.9). In some quarters, barks will even be used (Fig. 1.10) - the deputies will reach their chamber this way (Fig. 1.7). Finally, small plank footbridges will be built in the most flooded street to allow pedestrians to cross them (Fig. 1.11).

Only one person died because of the flood. It nevertheless had huge social and economical consequences with 20 000 of the 80 000 buildings of the capital being flooded and 150 000 people stricken. The flood did not strike Paris only and it is more than 200 000 people that immigrated from the suburb to the capital where first aid was more organized. The cost of the flood was estimated at 400 million francs-or for direct damages plus 50 million francs-or spent on aids which in total is equivalent to 1,4 billion euros (Ambroise-Rendu M. cited in DIREN, 2010).

Fig. 1.4 The Eiffel Tower

Fig. 1.5 The Jardin des plantes, the ourses' den

Fig. 1.6 Inside of the Orsay station – that will become the Orsay museum.

Fig 1.7 The deputies chamber

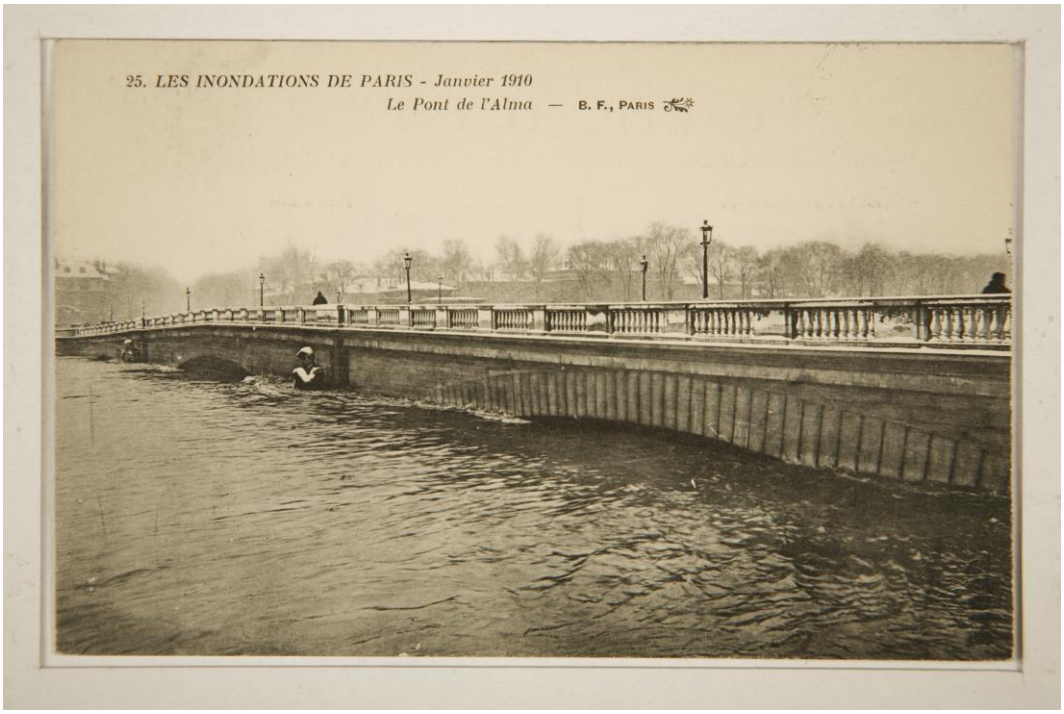

Fig. 1.8 The Alma bridge with the zouave statue.

Fig. 1.9 Horses carriage on the Faubourg Saint Antoine street

Fig. 1.10 A bark in the Surcouf street

Fig. 1.11 A footbridge in a Parisian street.

1.3 If the Flood happened today

Today, the Seine banks in Paris have been raised to the 1910 flood water level in order to limit the spreading of water in the capital if a similar flood had to happen again. The Seine bed has also been enlarged and now it would necessitate 110% of the 1910 flow for the water to reach the same level. Furthermore, several water reservoirs were built in order to limit the peak flow – even if in the case of a flood similar to the 1910 one, they will not have much effect. Finally, the different emergency scenarios designed by the *ORSEC* (Civilian Security Response Organization) are all based on the 1910 flood : the R1.0 scenario represents the case of 100% of the 1910 flow, the R0.6, 60%, the R1.15, 115%. In 2010, an exercise was launched ans it was possible to predict the peak flow 72 hours in advance with the different hydraulic and hydrologic models.

Furthermore, the main institutions have designed emergency plans based on the different scenarios cited above. The *RATP* which is in charge of the public transport in the Parisian region thus have the obligation to protect the underground subway network in order to re-open it after the flood. around 100 pumps have thus been placed in the areas liable to flooding. Furthermore, in case of a high flood, all the entrance of the 42 stations (out of 297) situated in vulnerable areas would be sealed with bricks and concrete that are already in stocks. In a similar way, the health care services have sesigned scenarios for hospital evacuation in flood cases. Finally, the Defense quarter (biggest business quarter in Europe) has also designed plans with the use of independent electric generator to allow for a minimum computer service during 36 hours.

Despite all this, it was estimated that, if the R1.0 scenario (100% of the 1910 flows) was happening today, 820 000 people would be flooded in Paris and its small suburb only, 1 220 000 would lack electricity and 1 500 000 would lack drinkable water. In Paris and its suburb, 90% of the areas liable to flooding are already built, thus adding an industrial risk, for example by chemical pollution of the water. In the Ile-de-France region 800 000 jobs would be threaten because of the damages with a cost equivalent to 30% of the regional GDP (Growth Domestic Product). In 1998, *les grands lacs de Seine* (cited in DIREN, 2010) estimated that such a flood would have a total cost of more than 12 billion euros.

1.4 Purpose of the study

In order to be able to predict a similar flood in the future, this study aims at testing the following hypotheses as explanations of the 1910 flood and of the difficulties encountered in its simulation :

- No particular causes
- Influence of the water reservoirs
- Influence of the model evaluation criterion
- Propagation of the error from selected sub-basins
- Influence of frost

and from these tests conclude on the 1910 flood causes and integrate them in the hydrological model used in flood simulation.

1.5 Method

The evaluation of the different hypotheses listed above has been made with the GR4J model ("modèle du génie rural à 4 paramètres, journalier") that is described in chapter 2. Different modules that are also described in the study were also used when necessary.

1.6 Conclusion

The 1910 flood thus was the largest flood of the 20th century. If it happened in very specific conditions, each winter there is one chance out of 100 that it would happen again. In this case, there would be even more harmful social and economical consequences than in 1910 because of the urbanization.

It is thus important to be able to predict such an event as soon as possible in order to allow for a better application of the different emergency scenarios. This study will thus focus on the simulation of the 1910 flood with GR4J which is the hydrologic model that is now used in flood prediction on the region. Indeed, if it manages to reproduce the flood satisfactorily then the model can be expected to accurately predict a similar event much more in advance than any hydraulic model because GR4J uses rain as input data while hydraulic models use upstream flows.

In the next chapter, the GR4J model will be described. Then it will be used on the 1910 flood to assess the way it can simulate it on the main Paris Austerlitz basin and then on several sub-basins. Finally, in front of the poor results obtained in simulation, it was thought that frost could have played a role by reducing water infiltration in the soil. A new frost module will thus be designed - coupled with a soil temperature model using air temperature as input data – in order to take into account its influence on hydrology. This module will then be tested on the 1910 data.

Other References

DIREN (2010) Conditions de déclenchement de la crue de 1910. Online at http://www.ile-de-france.ecologie.gouv.fr/spip.php?article243 [accessed on 20/11/2010]

2 THE GR4J MODEL

The GR4J model which stands for "modèle du Génie Rural à 4 paramètres Journalier" (i.e. daily model for rural engineering with 4 parameters), is a daily lumped rainfall-runoff hydrological model. From precipitations and evapotranspiration data, it gives an estimation of the water flow at the outlet of the studied basin. It is used in many applications at the basin scale, especially a modified version called GR3P is currently being used for flood forecasting in the Seine basin..

The first version of the GR4J model was developed empirically in the early 1980s at CEMAGREF and has been modified several times over the last decades. The version presented in this chapter is described by Perrin et al. (2003). GR4J is a rather simple model with only four free parameters (i.e. parameters that are to be calibrated before getting results from the model) but it gives results similar to more complex models. Some modules can however be used to take into account some specificities like, for example, water reservoirs influence or snow melt.

2.1 Model description

GR4J is an empirical lumped model designed at the basin scale. It is not directly linked to physics and uses stores to represent the overall water behaviour. It is illustrated in figure 2.1.

All the equations of this chapter are provided by Perrin et al. (2003) and Perrin et al. (2007). In those equations, all the volumetric terms are expressed in mm, by dividing them by the catchment area as GR4J is a lumped model considering the basin as a whole and averaging every data on its surface.

2.1.1 Precipitation and Evapotranspiration

P_k and E are the input data :

- Pk (mm) reprensents the areal precipitation depth at day k averaged over the surface of the basin.
- E (mm) is the daily potential evapotranspiration

The net precipitation Pn is equal to 0 if $E>P_k$ and equal to P_k-E otherwise. The net evapotranspiration En is equal to 0 if $P_k>E$ and equal to E-P_k otherwise.

2.1.2 Recharge and Discharge of the production store

If Pn>0, the net rainfall water is then divided and a part of it will go in the production store, if En>0 water is taken from this production store. This store stands for the humidity or moisture of the basin and is often confused with the soil although there is no direct link. It is aimed at dividing the rainwater - in a part that will actually reach the rivers and a part that will go back to the atmosphere by evapotranspiration or percolate later - by taking into account the past conditions over the basin (past precipitations and evapotranspiration). The production store is basically a stock of water S_k (in mm at the beginning of day k) that will increase or decrease due to rainfall and evapotranspiration. Part of this water will also percolate to the rivers.

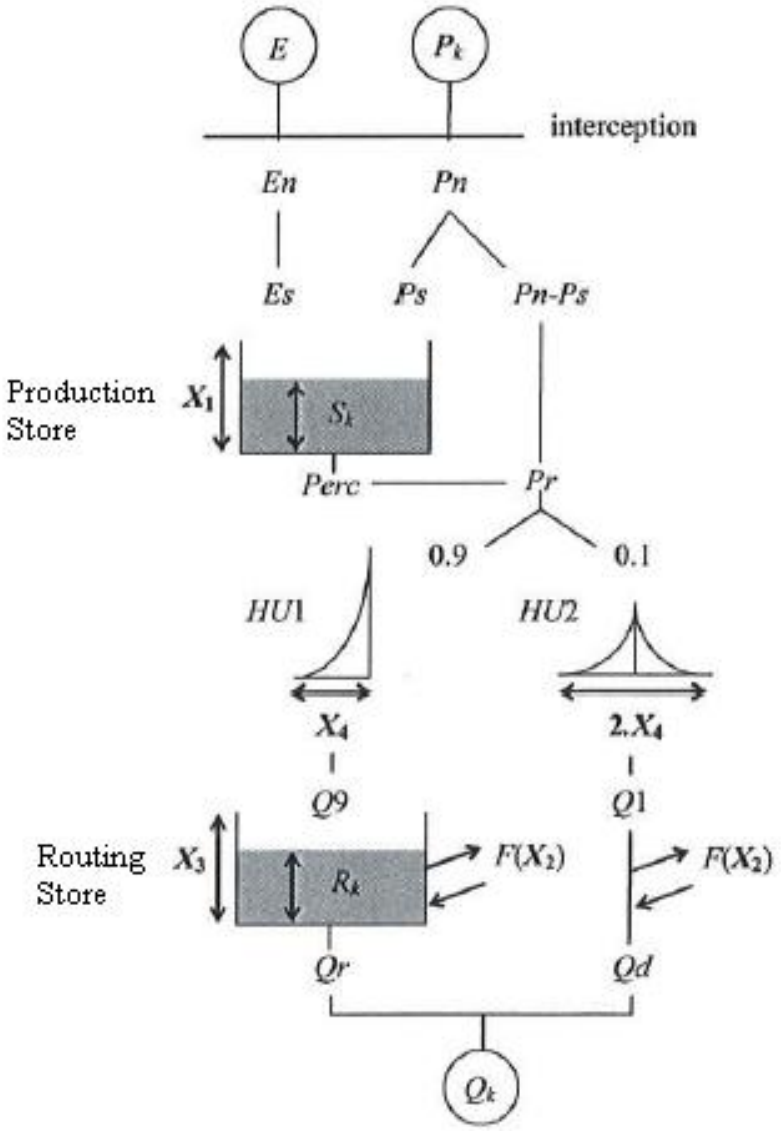

Fig. 2.1 scheme of the GR4J model principle (source : Perrin et al. (2003)

If Pn>0, the production store is thus recharged by a part of the rainfall Ps expressed in mm. Ps is given by :

$$Ps = \frac{X_1\left[1-\left(\frac{S_k}{X_1}\right)^2\right]\tanh\left(\frac{Pn}{X_1}\right)}{1+\frac{S_k}{X_1}\tanh\left(\frac{Pn}{X_1}\right)} \qquad \text{(Eq. 2.1)}$$

Where X_1 (in mm) is the maximum capacity of the production store and is the first parameter of the GR4J model.

CEMAGREF (1991) provides a brief development of the calculation that leads to this result for Ps. During a day, it is considered that only a

fraction $\left(1-\frac{S^2}{X_1^2}\right)$ of the net precipitation Pn will be brought to the production store, and that this fraction will fall on the store following a uniform temporal distribution along the day. We can then integrate the mass-balance equation of the production store under those conditions on a day to obtain S_{k+1} function of S_k. Ps is then deduced by the equation : $Ps = S_{k+1} - S_k$. As an example, the calculation of Ps is shown in annexe 2.1.

If En>0, the production store is discharged of a quantity of water Es expressed in mm and given by the equation :

$$Es = \frac{S_k\left(2-\frac{S_k}{X_1}\right)\tanh\left(\frac{En}{X_1}\right)}{1+\left(1-\frac{S_k}{X_1}\right)\tanh\left(\frac{En}{X_1}\right)} \qquad \text{(Eq. 2.2)}$$

There again, CEMAGREF (1991) offers an explanation for this calculation. It is considered that only a fraction $\frac{S}{X_1}\left(2-\frac{S}{X_1}\right)$ of the net evapotranspiration En is actually effective, and that the effect will follow a continuous temporal distribution along the day. The mass-balance equation of the production store is then integrated on a day to obtain S_{k+1} function of S_k and Es can then be deduced with $Es = S_{k+1} - S_k$.

Finally, the new store stock S' (mm) is then :

$$S' = S_k + Ps - Es \qquad \text{(Eq. 2.3)}$$

2.1.3 Percolation

The percolation Perc is a quantity of water (in mm) that is taken from the production store to end up in the rivers. This term is small related to store content and was actually not present in the first versions of the GR4J model. It was added later as a corrective term that gives better results (i.e. results that fit more to the reality) especially for low flows. It is given by the equation :

$$Perc = S'\left\{1-\left[1+\left(\frac{4}{9}\frac{S'}{X_1}\right)^4\right]^{-\frac{1}{4}}\right\} \qquad \text{(Eq. 2.4)}$$

And thus the new store stock S_{k+1} becomes :

$$S_{k+1} = S' - Perc \qquad \text{(Eq. 2.5)}$$

2.1.4 Unit Hydrographs

The upstream water Pr (in mm) that reaches the routing part of our model is thus :

$$Pr = Pn - Ps + Perc \quad \text{(Eq. 2.6)}$$

This water is then divided : 90% will be routed via a unit hydrograph UH1 and a routing store and the other 10% will be routed by a symmetric unit hydrograph UH2.

Those hydrographs mainly aim at delaying the arrival of water to the outlet by taking into account and weighting the importance of the previous days' precipitations. They have been designed empirically. The 90%-10% division is also an empirical result. Making this splitting variable from basin to basin, with the introduction of a 5th free parameter does not bring any improvement (Perrin, 2000).

Unit hydrographs ordinates are calculated using the S-curves SH1 and SH2 :

$$SH1(t) = \begin{cases} 0 \ if \ t \le 0 \\ \left(\frac{t}{X_4}\right)^{\frac{5}{2}} \ if \ 0 < t < X_4 \\ 1 \ if \ t \ge X_4 \end{cases} \quad \text{(Eq. 2.7)}$$

and :

$$SH2(t) = \begin{cases} 0 \ if \ t \le 0 \\ \frac{1}{2}\left(\frac{t}{X_4}\right)^{\frac{5}{2}} \ if \ 0 < t \le X_4 \\ 1 - \frac{1}{2}\left(2 - \frac{t}{X_4}\right)^{\frac{5}{2}} \ if \ X_4 < t < 2X_4 \\ 1 \ if \ t \ge 2X_4 \end{cases} \quad \text{(Eq. 2.8)}$$

Where X_4 is the time base for UH1 expressed in days and is a parameter of the GR4J model that needs to be calibrated.

We can then define UH1 and UH2 :

$$UH1(j) = SH1(j) - SH1(j\text{-}1) \quad \text{(Eq. 2.9)}$$

$$UH2(j) = SH2(j) - SH2(j\text{-}1) \quad \text{(Eq. 2.10)}$$

With j an integer.

Finally, at day k, Q9 and Q1, the water flows (in mm/day) that are getting out of the 2 hydrographs are given by the equations :

$$Q9(k) = 0{,}9\sum_{j=1}^{l}\left(UH1(j) \times \Pr(k - j + 1)\right) \quad \text{(Eq. 2.11)}$$

$$Q1(k) = 0{,}1\sum_{j=1}^{m}\left(UH2(j) \times \Pr(k - j + 1)\right) \quad \text{(Eq. 2.12)}$$

Where l = int(X_4)+1 and m=int($2X_4$)+1 with int(.) the integer part.

2.1.5 Routing store and water exchange

The routing store is characterised by R_k, the stock of water at the beginning of the day k (in mm) and by X_3 its capacity (in mm) that is a parameter of the model. The routing store is used to simulate the flow dynamic and the recession of a flow peak some days after a heavy rain. It smoothes the flow curve resulting from the model.

The exchange term applied to the routing store replicates the water exchange with other basins due to groundwater aquifers. This exchange F, that can be positive or negative, is given by the equation :

$$F = X_2\left(\frac{R_k}{X_3}\right)^{\frac{7}{2}} \quad \text{(Eq. 2.13)}$$

Where X_2 is the exchange coefficient in mm. It is the last parameter of the model.

The stock of water in the routing store R' then becomes :

$$R' = \max(0; R_k + Q9(k) + F) \quad \text{(Eq. 2.14)}$$

Some of this water Qr (in mm/day) is released from the routing store to reach the flow at the outlet of the basin :

$$Qr = R'\left\{1 - \left[1 + \left(\frac{R'}{X_3}\right)^4\right]^{-\frac{1}{4}}\right\} \quad \text{(Eq. 2.15)}$$

CEMAGREF (1991) also describes this calculation. If, within a day, we call Q(t) the water flow exiting the routing store at time t, R(t) the stock of water in this store at time t and Δt the duration of one day, then the result shown above is coming from the integration of the mass-balance equation in the routing store supplemented by the empirical equation : $Q(t) = \frac{R(t)^5}{4\Delta t X_3^4}$.

And the stock of water in the routing store becomes :

$$R_{k+1} = R' - Qr \quad \text{(Eq. 2.16)}$$

2.1.6 Total flow at the bottom of the basin

The flow Q1 also exchanges water with the others basins with the same exchange term F. The resulting amount of water Qd (in mm/day) that reaches the river is thus given by :

$$Qd = \max(0; Q1(k) + F) \quad \text{(Eq. 2.17)}$$

Finally the amount of water flowing at the outlet of the basin at day k, Q_k (in mm/ day) is :

$$Q_k = Qr + Qd \quad \text{(Eq. 2.18)}$$

2.2 Method to run the model

2.2.1 The different steps

In the ideal situation, to run the model, we need two data sets at two different time periods of at least 5 years. The data needed are daily precipitations and evapotranspiration (in mm) averaged on the basin - using reference stations where the data are available, as well as daily flow values at the outlet of the basin (in m^3/s.).

On the first data set, the model will be calibrated : the four parameters will be given values that give the best results when matching the simulated and the observed water flow values. The length of the calibration period can have a small influence on the calibrated values of the free parameters but this influence becomes negligible when the calibration period is long enough (at least 5 years). Generally, the longer the calibration period, the more robust the calibration as more hydrological events happening on the basin are likely to occur and thus are likely to be taken into account in the calibration process (Perrin, 2000).

On the second data set, the values of the four parameters are used and the model is run to control that those values give good results when matching the observed and simulated flows in order to validate the calibration.

The process is summarized in figure 2.2.

It can be interesting at the end of this process to reverse it, using the second data set to calibrate the model and the first one to validate it. It can then be seen how the different parameters values evolve. A big difference can then have many interpretations : change in the basins conditions, unreliability of our model, other unknown factors,…

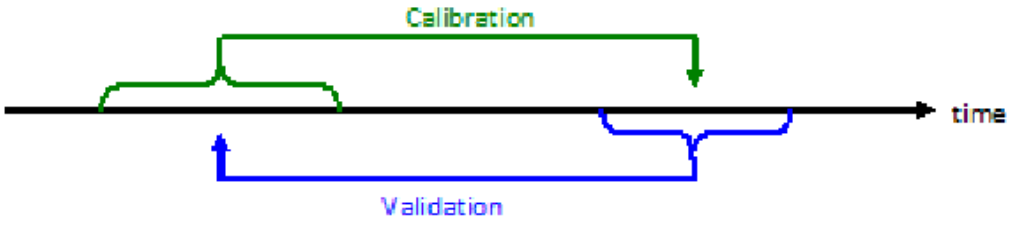

Fig. 2.2 process of calibration and control for GR4J

2.2.2 Evaluation Criteria

Calibration

The model has 4 parameters that are summarized in table 2.1 (Perrin et al., 2007)

During the calibration process we will vary those 4 parameters in order to find the combination that reaches the best fit between the simulated and the observed water flows. Several evaluation criteria exist to assess this fit between the 2 ranges of data (see for examples, Perrin, 2000 and Perrin et al., 2003). Generally the Nash-Sutcliffe Efficiency (NSE) is used. Its formula is given by Nash and Sutcliffe (1970) :

$$NSE = 1 - \frac{\sum_{k=1}^{n}(x_{o,k} - x_{s;k})^2}{\sum_{k=1}^{n}(x_{o,k} - \mu_o)^2} \qquad \text{(Eq. 2.19)}$$

Where n is the number of values, $x_{o,k}$ is the observed value at time k (the observed flow), $x_{s,k}$ is the simulated value at time k (the simulated flow), and μ_o is the mean of the observed values. NSE is often given in %.

NSE varies between $-\infty$ and 1. If it is negative, then the simulated results are worse than the mean observed values and a constant would give better results than the model which is thus considered useless. If the NSE is equal to 1 then the observed and simulated values are exactly equal. Thus during the calibration process, one must try to reach an NSE as close as possible to 1 i.e. as high as possible. In this case the calibration process is an optimization of the 4 parameters X_1, X_2, X_3 and X_4 to maximize NSE.

Other criteria exist using, for example, the square root or the logarithm of flows in the NSE formula as observed and simulated values. The use of those different criteria will be discussed in chapter 3.

Validation

In the validation process, the same criteria or new ones can be used to assess the quality of the calibration of our 4 parameters on a new data set. Several criteria can be used at that step - whereas the calibration is generally made to optimize one criterion only even if, nowadays, more and more works develop a multi-criteria approach.

2.2.3 Influence of the initial values of S and R

Before running the model, for calibration or control, initial values of S and R (i.e. S_0 and R_0) must be set. Le Moine (2008) has shown that the setting of those values could influence the efficiency of the model. In practice, we initialize the values of S_0/X_1 and R_0/X_3 arbitrarily between 0 and 1. The influence of those initial values are shown on figure 2.3.

Table 2.1 GR4J parameters and their statistical values

Parameter	Description	Median	Confidence Interval at 80%
X_1	Production store capacity (mm)	350	100 to 1200
X_2	Exchange coefficient (mm)	0	-5 to 3
X_3	Routing store capacity (mm)	90	20 to 30
X_4	Base time of UH1 (day)	1,7	1,1 to 2,9

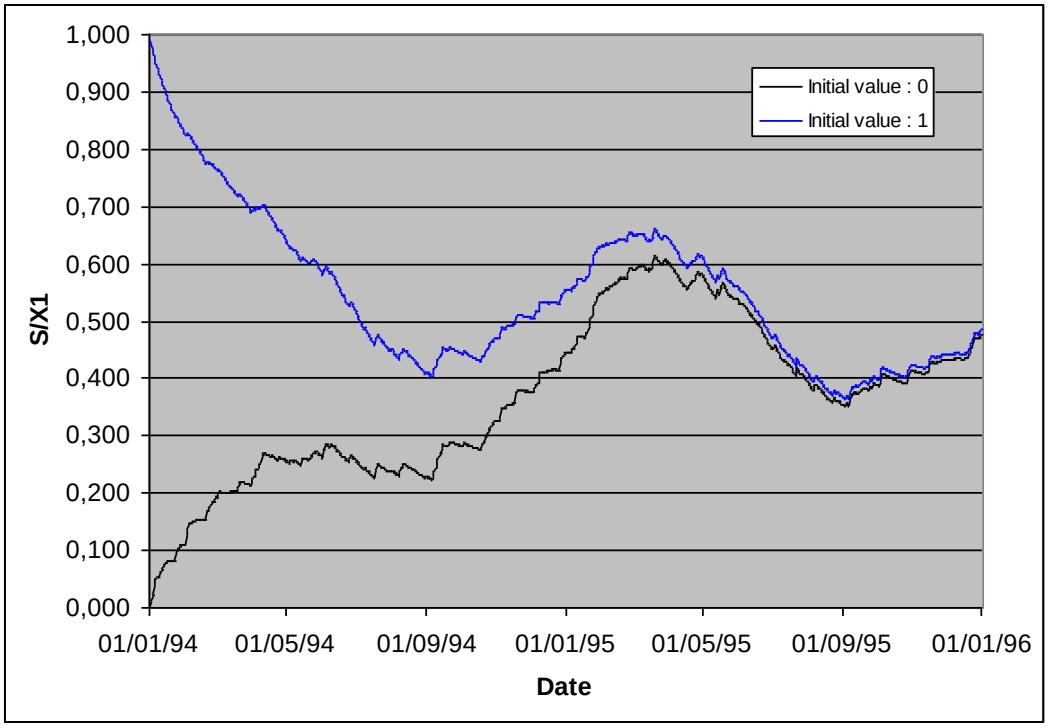

Fig. 2.3 filling ratio S/X1 evolution with time in the GR4J model with the parameters values : X1=776,90mm, X2=0,48mm, X3=75,41mm, and X4=3,62 days for initial values of S/X1 of 0 and 1..

It can be seen in figure 2.3 that the filling ratio curves are almost identical after a certain amount of time (around one year here) whether their initial value S_0/X_1 was set to 0 or to 1. Indeed Le Moine (2008) shows that after some time, S/X_1 will reach a state of steady evolution independent of initial values. Ideally, the model should be run after this state is reached but that can take some time, especially in case of important production store capacity (X_1) which will allow a larger variability for the store level S. The same results can be obtained with R_0/X_3 although the routing store generally has a smaller capacity, thus allowing less variability and a quicker reach of the steady evolution state.

Thus, in practice, when running the model for calibration or for control, no result is accounted for during a defined period – warm-up period - which is only used to settle the values of S and R. During this period, no observed values of flows are necessary since S and R are only influenced by precipitations and evapotranspiration. The flow values (simulated and observed) belonging to this period are not taken into account in the calculation of the efficiency of the model – for example with the NSE criterion - or for any other calculation.

Le Moine (2008) has designed a specific method for initialisation of S_0/X_1 that allows the model to reach the state of steady evolution more quickly and thus to reduce the warm-up period –or give better results than an arbitrary S_0/X_1 value with an equal warm-up period. However, Perrin (2000) using a model very similar to GR4J for a test on 595 calibration on 17 different basins concludes that after one year of initialisation, only 8% of the parameters values change with different initial values of S_0/X_1 and R_0/X_3.

In this study, the influence of the initial value set to S_0/X_1 and R_0/X_3 will thus be neglected after around one year. If not stated otherwise, during

this whole study, the values $S_0/X_1 = 0{,}60$ and $R_0/X_3 = 0{,}70$ will thus be taken with a warm-up period of one year.

2.2.4 Software used

To run the GR4J model, two softwares were mainly used in this study : Microsoft Office Excel – named Excel in this study, and Compaq Visual Fortran – named Fortran in this study.

Excel

All the formulas – to run the model and calculate its efficiency - are put in different cells. The data are completed by the operator and the calculation is instantaneous. For Calibration, the solver tool was used.

Fortran

Fortran is a programming language that is able to open and read many different files in a very quick time. The program used in this study is also able to handle other models than GR4J with different numbers of parameters. Additional modules can also be integrated in those models to simulate snow influence in the basin.

A "step-by-step" optimization method is used in the program for calibration (Mathevet, 2005, Perrin, 2000). For GR4J, the four parameters X_1, X_2, X_3 and X_4 are given an arbitrary initial value. The efficiency criterion (e.g. NSE) is then calculated based on those parameters values. One by one, each parameter value is then added and subtracted a constant step ΔX and the efficiency criterion is recalculated with this different set of parameters values and compared to the previous result. The set of parameters values that give the best result is then selected and taken as a basis for another iteration of the optimization process and so on. The variation step ΔX is raised to accelerate the process when several consecutive improvements are found in the same direction. Reversely, it is diminished if, during an iteration, no better result than the initial set of values could be found in order to allow for a more precise research around this set of values. The optimum is said to be found when the variation step ΔX becomes lower than the minimum variation step decided in advance.

The efficiency criteria's variation with the parameters values is generally simple, without secondary optimum, in the GR4J model. The "step-by-step" method has thus proven to be effective both in optimization time and in results compared to other methods – implying several initial parameters values, for example (Perrin, 2000).

Appendix 2.1 : Calculation of Ps in the GR4J model.

This calculation is shown as an example of the developments that have led to the equations of the GR4J model. It is largely inspired from CEMAGREF (1991).

Within day k, we call P(t) the net amount of water falling per unit of time on the basin at time t and S(t) the volume of the production store at time t. We consider that P(t) follows a uniform distribution along the day. Thus $P(t) = \frac{Pn}{u}$, with Pn the total net precipitation during the day and u the duration of one day. We consider that only a fraction $\left(1 - \frac{S^2}{X_1^2}\right)$ of P(t) actually reaches the production store. Finally we don't take into account the percolation that is calculated separately.

The mass balance equation on the volume S(t) gives :

$$dS = \left(1 - \frac{S^2}{X_1^2}\right)\frac{Pn}{u}dt$$

$$dt = \frac{dS}{\frac{Pn}{u} - \frac{Pn}{uX_1^2}S^2}$$

$$d\left(\frac{t}{u}\right) = \frac{dS}{Pn - \frac{Pn}{X_1^2}S^2}$$

With $\frac{Pn}{X_1^2} = \frac{1}{h}$ we get by integration :

$$\frac{t}{u} = \sqrt{\frac{h}{Pn}}\left[Argth\left(\frac{S(t)}{\sqrt{hPn}}\right) - Argth\left(\frac{S(0)}{\sqrt{hPn}}\right)\right]$$

We then have $S(0) = S_k$ (initial condition) and $S(u) = S_{k+1}$. Then for $t = u$:

$$\sqrt{\frac{Pn}{h}} = Argth\left(\frac{S_{k+1}}{\sqrt{hPn}}\right) - Argth\left(\frac{S_k}{\sqrt{hPn}}\right)$$

$$\frac{S_{k+1}}{\sqrt{hPn}} = th\left[\sqrt{\frac{Pn}{h}} + Argth\left(\frac{S_k}{\sqrt{hPn}}\right)\right]$$

$$S_{k+1} = \frac{\sqrt{hPn} \times th\left(\sqrt{\frac{Pn}{h}}\right) + S_k}{1 + \frac{S_k}{\sqrt{hPn}}th\left(\sqrt{\frac{Pn}{h}}\right)}$$

We can then replace h by $\frac{X_1^2}{Pn}$ and calculate Ps which is the amount of water brought to the production store during the day so :

$$Ps = S_{k+1} - S_k$$

$$Ps = \frac{X_1 th\left(\frac{Pn}{X_1}\right) + S_k - S_k - \frac{{S_k}^2}{X_1} th\left(\frac{Pn}{X_1}\right)}{1 + \frac{S_k}{X_1} th\left(\frac{Pn}{X_1}\right)}$$

$$Ps = \frac{X_1 th\left(\frac{Pn}{X_1}\right) \times \left(1 - \frac{{S_k}^2}{{X_1}^2}\right)}{1 + \frac{S_k}{X_1} th\left(\frac{Pn}{X_1}\right)}$$

References

CEMAGREF (1991) *Hydrologie appliquée aux petits bassins ruraux*, CEMAGREF, Groupement d'Antony, division : Hydrologie.

LE MOINE, N. (2008) Le bassin versant de surface vu par le souterrain : une voie d'amélioration des performances et du réalisme des modèles pluie-débit ? , UNIVERSITE PIERRE ET MARIE CURIE PARIS VI, CEMAGREF ANTONY HBAN. 348 p.

MATHEVET, T. (2005) Quels modèles pluie-débit globaux au pas de temps horaire ? Développements empiriques et comparaison de modèles sur un large échantillon de bassins versants. Ecole Nationale Du Genie Rural Des Eaux Et Des Forets, Cemagref Antony, Hban. 463 p.

NASH, J. E. & SUTCLIFFE, J. V. (1970) River flow forecasting through conceptual models part I -- A discussion of principles. *Journal of Hydrology,* 10**,** 282-290.

PERRIN, C., MICHEL, C. & ANDREASSIAN, V. (2007) Modèles hydrologiques du Génie Rural (GR). CEMAGREF, UR Hydrosystèmes et Bioprocédés.

PERRIN, C., MICHEL, C. & ANDREASSIAN, V. (2003) Improvement of a parsimonious model for streamflow simulation. *Journal of Hydrology,* 279**,** 275-289.

PERRIN, C. (2000) Vers une amélioration d'un modèle global pluie-débit au travers d'une approche comparative. Institut National Polytechnique de Grenoble, Cemagref Antony, Qhan, 530 p.

3 MODELLING THE 1910 FLOOD WITH THE GR4J MODEL

The GR4J model has proved in the past years to be rather robust and reliable and is now at the basis for the flood forecasting model used in the Seine basin by the DIrection Régionale de l'ENvironnement (DIREN : regional direction for environment). At the occasion of the anniversary of the "crue centennale" (100-years flood), the DIREN tried to run the model to simulate this phenomenal flood. This was the first time that the model was run on those data. The experiment and its results are described in the first part of this chapter.

In front of the poor results obtained during this simulation, and before further investigations, the model - especially the calibration process - was questioned in order to find an explanation to the large difference between observed and simulated values. Two tests were thus conducted about artificial influences between 1910 and 1994 and statistical criteria used for optimization, based on previous studies showing that those factors could influence the results of models (Payan, 2007, Gupta et al., 2009). The experiments and their results are described in the second and third part of this chapter.

3.1 The simulation of the 1910 flood

The experiment was conducted with the GR4J model as described in chapter 2 without any modification of its structure, the aim being to assess its efficiency in modelling the 1910 flood.

3.1.1 Data

The following data were used :

- For Calibration : observed flow values at Paris Austerlitz (in m^3/s) as well as precipitation, and evapotranspiration values (in mm) averaged on the Seine basin upstream of Paris Austerlitz – of a surface of 43800 km^2. for conversion of volumetric values. Precipitation and evapotranspiration values covered the period from January 1st 1994 to December 31st, 2009. Flow values covered the period from January 2nd, 1995 to December 31st, 2009. Those data were provided by the "Banque Hydro" (French national data base for hydrological data).
- Observed flow values at the station of Paris Austerlitz in m^3/s from November 1st, 1909 to February 28th, 1910. Those data were given by the DIREN. The peak flow was traditionally believed to be around 2400 m^3/s which happened to be inconsistent with the data available upstream and downstream from Paris. In the set of data used this mistake was corrected and the peak flow was estimated at 2649 $m^3./s$.
- Precipitation and evapotranspiration (in mm) averaged on the whole Seine Basin upstream of Paris Austerlitz and covering the period from January 1st, 1909 to December 31st, 1910. Those data were extracted from paper archives available at DIREN or provided by Météo France (French National Institute for meteorology). The calculation method for the average precipitation on the basin is described in appendix 3.1.

3.1.2 Method

The GR4J model as described in chapter 2 was used with the Excel software.

For calibration, the range of data covering the period from 01/01/1994 to 31/12/2009 was used, with one year (1994) used to settle the values

of S and R and not taken into account for the efficiency computation (one year model warm-up). The 4 parameters X_1, X_2, X_3 and X_4 were calibrated so as to maximize the NSE criterion calculated on flow values (NSE calibration).

The parameters calibrated as seen above were used to run the model with the 1909 – 1910 data. The year 1909 was used to settle the values of S and R and the simulation covered the period from 01/01/1910 to 28/02/1910.

Finally, a calibration of the model on the 1909 – 1910 period was made by maximizing the NSE criterion calculated on the flow values. The first year (1909) was used to settle S and R values and was not taken into account in the calculations.

3.1.3 Results

The model calibration on the period 1994 – 2009 gave the parameters values presented in table 3.1. When using those parameters on the 1909 – 1910 period as described in part 3.1.2 the efficiency results given in table 3.2 were obtained

The observed and simulated flow values are shown on figure 3.1.

By simple integration of the curve presented on figure 3.1, the observed and simulated volumes of water that flowed at Paris Austerlitz between 01/01/1910 and 28/02/1910 are calculated : the observed volume is $7{,}3483.10^9 m^3$ and the calculated volume is $5{,}6326.10^9 m^3$, and the difference between observed and simulated volumes thus represents 23,35% of the observed volume.

Finally, after calibration on the 1909 – 1910 period as described in part 3.1.2, the parameters took the values presented in table 3.3.

3.1.4 Discussion

The Nash-Sutcliffe efficiencies obtained on the period covering January and February 1910 after calibration on the 1994 – 2009 period, are all very low (below 0,30) as we can see in table 3.2. The figure 3.1 also shows a large difference between simulated and observed flows with a clear underestimation by the model.

Table 3.1 parameters values after NSE calibration on 1994 - 2009

Parameter	Unit	Value after calibration
Production store capacity : X_1	mm	777
Exchange coefficient : X_2	mm	0,48
Routing store capacity : X_3	mm	75
Time basis for UH1 : X_4	days	3,6
NSE obtained with those parameters on 1995 - 2009	.	0,825

Table 3.2 efficiency results obtained on the 1910 flood with NSE calibration on 1994 2009

Criteria	Abreviation	Result of simulation
NSE calculated on flow values	NSE(Q)	0,229
NSE calculated on the square-root of flow values	NSE (VQ)	0,227
NSE calculated on the logarithm of flow values	NSE (ln(Q))	0,295

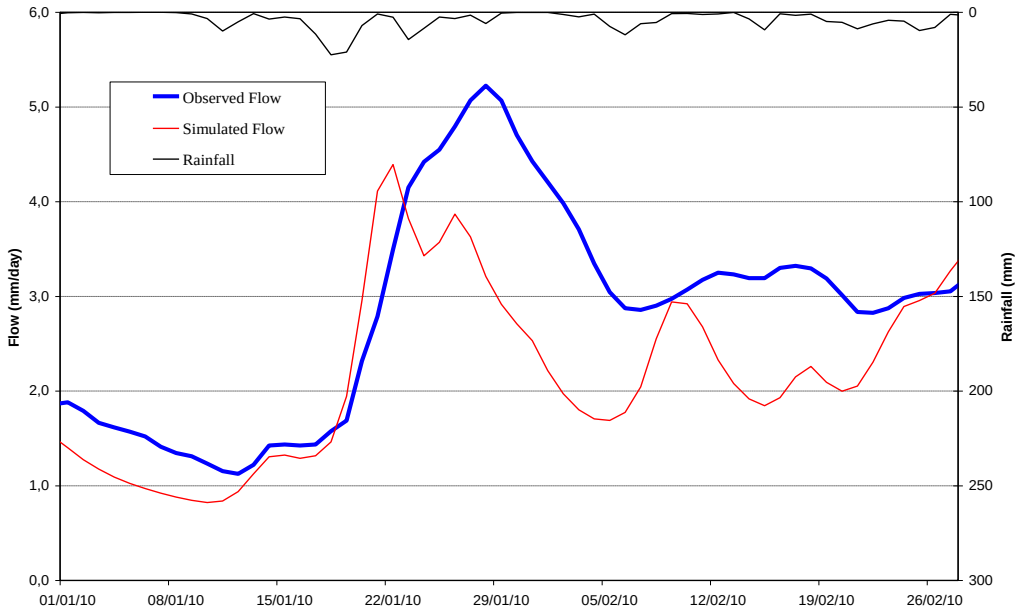

Fig. 3.1 rainfall, observed and simulated flow from 01/01/1910 to 28/02/1910 with NSE calibration on 1994 – 2009

The underestimation of the flow can be directly translated in an underestimation of the level of the Seine river and of the water volume that flowed in Paris – the simulation lacking 23,35% of this volume i.e. more than 1,7 billions cubic meter of water between January 1st and February 28th 1910. In case of such a natural catastrophe like the 1910 flood, it is important for the authority to be accurately informed in advance of the extent of the flood. Such an error in the simulation that would have led to a tremendous underestimation of the situation gravity is thus completely unacceptable.

There are three possible explanations to those very poor results :

- Data could be wrong.
- The model can be unable to simulate such a flood, and will always give false results in those conditions of precipitation and evapotranspiration
- There is something that happened in 1910 or between 1910 and 1994, that is not taken into account in our model, and that is leading to those wrong results.

The data source are rather well-documented and are less likely to be false than the model. It has thus been decided to investigate further the 2nd and 3rd possibilities.

Table 3.3 parameters obtained after NSE calibration on the 1909 – 1910 period

Parameter	Unit	Value after calibration
Production store capacity : X_1	mm	191
Exchange coefficient : X_2	mm	-0,19
Routing store capacity : X_3	mm	302
Time basis for UH1 : X_4	Days	6,4
NSE obtained with those parameters on jan – feb 1910	.	0,963

Finally it is interesting to compare tables 3.3 and 3.1. Table 3.1 gives relatively usual values for the parameters while in table 3.3, which actually replicate the flood with a very high NSE criterion, a huge diminution of the production store capacity, and a large augmentation of the routing store capacity can be observed. In a physical interpretation, by reducing the production store capacity, the model is allowing a faster saturation of the soil leading to increased run-off - and thus augmentation of water in the river at the end. By raising the routing store capacity, the model simulates a smoother response while reducing the loss of water into other aquifers (the exchange coefficient is negative). Those two values of the stores capacities are very unlikely, but they give clue on what must be looked for. An event, that would raise the runoff or lead to more water obtained from the soil, that is not taken into account in our model but that had happened in 1910, could explain those differences between observed and simulated values.

However, before investigating the possibility and consequences of such an event, and as a first preliminary approach, the model calibration method will be questioned. Especially, the influence of infrastructure changes on the basin between 1910 and 1994 and the statistical criteria used for optimization will be studied.

3.2 Taking into account the water reservoirs

In our previous experiment we have calibrated the model on the years 1994 – 2009 to use it on the years 1909 – 1910. One reason of the poor results we obtained could be that the conditions in the basin have changed between those two time periods so drastically that they could be considered as two independent basins.

In 1910, in the *journal d'agriculture pratique* of the French *Académie d'Agriculture* (Academy of agriculture), Paul Descombes notes that after the 1910 flood of Paris, a special budget for strive against inundation had been voted. 222 millions of ancient Francs (around 340 000 euros) would be allocated to constructions on the basin - rivers' beds enlargement and creation of water reservoirs - and 122 millions of ancient Francs (around 190 000 euros) would be allocated to reforestation (Descombes, 1910).

Four reservoirs were thus built in the second half of the 20th century on four rivers of the basin : Aube, Seine, Marne and Yonne. They are now managed by *Les Grands Lacs de Seine* institution created in 1969. Their location is shown on figure 3.2 and their main characteristics (Institution Interdépartementale des barrages-réservoirs des bassins de la Seine, 2010) are summarized in table 3.4.

The land cover changes are more difficult to appreciate as there is not much data available for 1910. Especially, whether the forest area in the basin has increased or decreased between 1910 and 1994 is not certain but this change is not assumed to be very significant. More significant could be the urbanization. Urban area in the basin has indeed certainly increased since 1910 due to population growth and national urbanization trend.

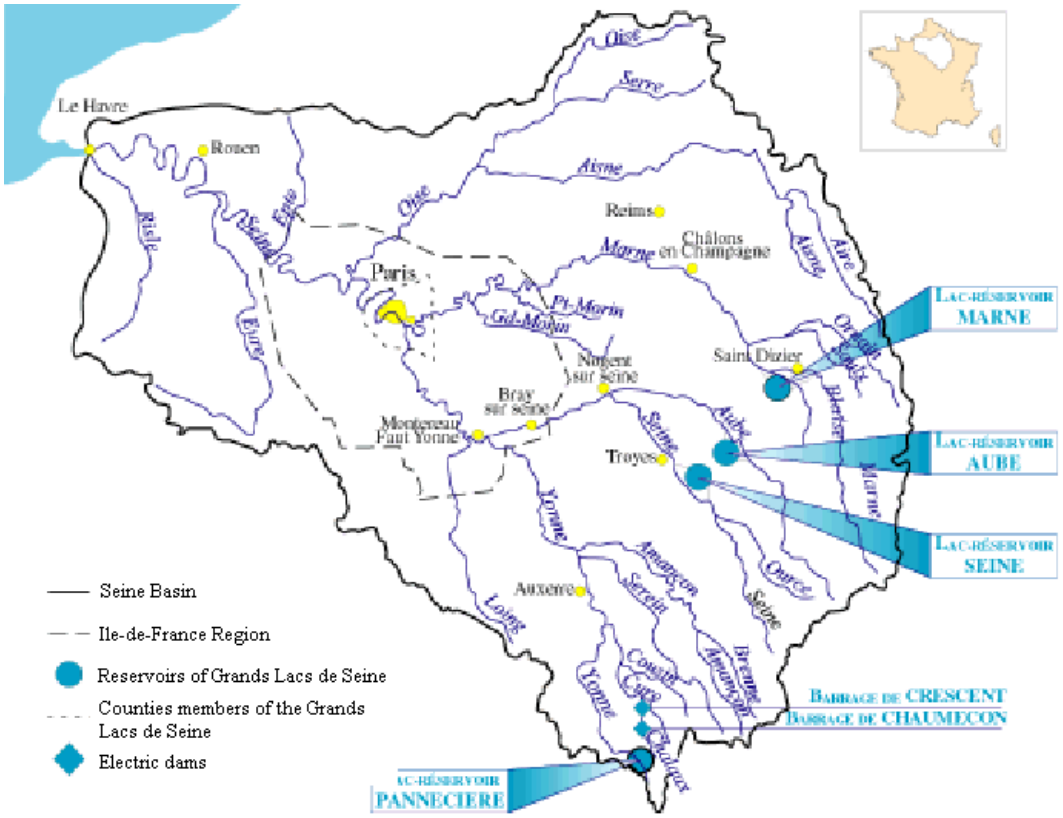

Fig. 3.2 The 4 major reservoirs on the Seine Basin (source : Institution Interdépartementale des barrages-réservoirs des bassins de la Seine, 2010)

3.2.1 Influence on the GR4J model

Urbanization definitely has an impact on the hydrology of the basin by increasing the run-off coefficient of rain water. However as the basin was more urbanized in 1994-2009 than in 1910, the parameters calibrated on this first period should allow more run-off and thus an increased flow compared to parameters of 1910. Taking only the urbanization into account, calibration on 1994-2009 should thus lead to an overestimation of the flow in 1910. As the opposite problem is occurring, influence of changing urbanization won't be considered further.

More complicated is the assessment of other land covers changes between 1910 and 1994 and particularly of forests and their influence on the basin. Andreassian (2004) presents a review of many different paired-watershed experiments run worldwide in order to assess the link between basin hydrological behaviour and forestation/deforestation. If the results of those experiments appeared to be very variable, in case of flood, a deforestation of the basin will generally increase the flood peak and volume. However, this deforestation effect appeared to be significant only during the growing season of the year. Moreover, effect of reforestation –as it may have happened between 1910 and 1994 on the Seine basin, according to M. Descombes – appears in the few studies made about it to be very limited on floods in general, with "no effect at all on the large ones" (Andreassian, 2004, p. 12). As the 1910 flood of Paris can definitely be considered a large flood and that it happened in the dormant season (January), any possible deforestation or reforestation of the basin should not have any influence on it and thus the model should be able to replicate it even though it doesn't take into account land covers.

Table 3.4 characteristics of the four storages of the Seine basin

Name of the Resevoir	Concerned Rivers	Type of Reservoir	Year of first operation	Surface of the upstream basin (km²)	Maximum Volume of the reservoir (10^6 m^3.)	Maximum inflow (from the river) (m^3./s.)	Maximum outflow (towards the river) (m^3./s.)
Marne	Marne Biaise	in derivation	1974	2900	364,5	408	50
Aube	Aube	in derivation	1989/1990	1650	185	135	35
Seine	Seine	in derivation	1966	2300	217	180	35
Panneciere	Yonne	dam accross the river	1949	220	82,5	all flow	14

Finally, Oudin et al. (2008) in a study on hydrological impacts of land cover conclude that forest areas have less influence on the results of a water balance model than arable lands and that land cover data are much more informative on small catchments (<10 km²) – the Seine basin being 43800 km².

In front of all those results, it can be considered very unlikely that any land cover change would have a greater influence on model calibration – which, if leading to an underestimation of the 1910 flow by the model, would anyway be counter-balanced, to some extent, by the influence of urbanization that should lead the model to an overestimation - than the four reservoirs put in operation between the two time periods and that directly affect the rivers flows.

The enlargement of the rivers' beds doesn't change the flow of water in the rivers but only their levels. Thus, it won't have any influence on the model that works with flow values.

The influence of reservoirs on the GR4J model has been studied by Payan (2007).The production store capacity X_1 appears to be the most affected parameter. After calibration, in the presence of water reservoirs on the basin, a significant augmentation of its value can be observed compared to the value it had when there were not any reservoirs on the basin. The exchange coefficient X_2 and the routing store capacity X_3 are moderately affected by the presence of reservoirs but whether an augmentation or a diminution of the values can be observed depends on the basin under study. Finally, the time basis for UH1 X_4 is very little affected by the presence of reservoirs and their influence can thus be neglected.

3.2.2 Model of reservoirs

To diminish the influence of those reservoirs on the calibration on our data, one must try to integrate those reservoirs in the model in order to make the values after calibration of the parameters X_1, X_2, X_3 and X_4 more independent of the presence or absence of reservoirs on the basin.

However, it is difficult to integrate site-located components such as water reservoirs in a lumped model like GR4J that considers the basin as a whole and that has no direct physical interpretation of its structure (Moulin, 2003, Payan, 2007, Payan et al., 2008).

Payan (2007) and Payan et al.(2008) have thus designed a model without describing the processes induced by the presence of reservoirs, but focusing on the volumetric variations of water stored in them. All the reservoirs are thus aggregated in a single store which volume V_k at the beginning of day k is the sum of their respective volumes at that time. The variation $\Delta V = V_{k+1} - V_k$ of this volume during day k is then considered :

- If ΔV is positive, then the volume of water stored in the reservoirs has increased and this water has been taken from the hydrological watershed. ΔV must thus be withdrawn from the model storages that are considered to represent the natural basin.
- If ΔV is negative, then the volume of water stored in the reservoirs has decreased and this water has been brought back to the watershed and must thus be added to the model storages.

After many tests, the best results were obtained by adding $|\Delta V|$ to the routing store ($R = R_k + |V_k - V_{k-1}|$) when ΔV is negative and by subtracting $|\Delta V|$ from the production store ($S = S_k - |V_k - V_{k-1}|$ if $S_k > |\Delta V|$, $S = 0$ otherwise) when ΔV is positive.

The volumes of the different reservoirs at day k thus constitute new data that must be brought to the model.

3.2.3 Influence of the model on the calibrated parameters' values

Payan (2007) after a test on 46 basins shows that when the reservoirs are integrated as explained above in the model, the value – after calibration - of the production store capacity X_1 is decreased significantly so as to get closer to the value it would have without the presence of the reservoirs in the basin. The other parameters are not very much affected by the integration of the reservoirs in the model.

Payan (2007) thus concludes that "Les valeurs de la solution [du modèle avec réservoirs] sont proches des paramètres représentatifs d'un bassin versant non influencé." (p. 193 – 194 ; The values of the solution [of the model with reservoirs] are close to the representative parameters of a non-influenced basin.).

3.2.4 Application of the model to the 1910 flood

When the model is calibrated on the time period 1994 – 2009, the parameters values that are obtained are influenced by the presence on the basin of the 4 reservoirs described above. But those reservoirs were not present in 1909 – 1910 and influenced parameters are thus not suited for a model of this period.

To mitigate this problem, the reservoirs have been integrated as described above in the model for calibration on the years 1994 – 2009 so as to get parameters values more independent from the presence of reservoirs and thus closer to the values of the parameters in the period 1909 – 1910.

3.2.5 Data

The same data as in part 3.1.1 were used plus the daily volumes of each of the four reservoirs in millions of cubic meters from January, 1st, 1994 to December, 31st, 2002. Those data were furnished by *Les Grands Lacs de Seine.*

3.2.6 Method

The GR4J model was used with the Excel software. The reservoirs volumes data were added to the model as described in part 3.2.2. When adding $|\Delta V|$ to S or R, the volumes were first converted in mm. by dividing $|\Delta V|$ by the surface of the whole basin (43800 km².).

The parameters were calibrated on the time period from 01/01/1994 to 31/12/2002 with the reservoirs integrated in the model so as to diminish their influence on the parameters. NSE-calibration was used with one-year warm-up.

The model was then run on the period from 01/01/1909 to 28/02/1910 like in part 3.1.2.

3.2.7 Results

On the calibration of the model on the period 1994 – 2002 with integration of the reservoirs in the model, the parameters values presented in table 3.5 below were obtained.

When using those parameters on the 1909 – 1910 period as described in part 3.2.6 the efficiency results given in table 3.6 below were obtained. The flow values observed and simulated are shown on figure 3.3.

Then again, the simulated volume between 01/01/1910 and 28/02/1910 is calculated by integration : 5,8919.10^{9}m^3 representing a difference with the observed volume of 19;82% of the observed volume.

Table 3.5 parameters values after NSE calibration on 1994 – 2002 with integration of the reservoirs in the model

Parameter	Unit	Value after calibration
Production store capacity : X_1	mm	573
Exchange coefficient : X_2	mm	0,17
Routing store capacity : X_3	mm	99
Time basis for UH1 : X_4	days	3,6
NSE obtained with those parameters on 1995 - 2002	.	0,885

Table 3.6 efficiency results obtained on the 1910 flood with NSE calibration integrating the reservoirs on 1994 2002

Criteria	Abreviation	Result of simulation
NSE calculated on flow values	NSE(Q)	0,350
NSE calculated on the square-root of flow values	NSE (VQ)	0,392
NSE calculated on the logarithm of flow values	NSE (ln(Q))	0,404

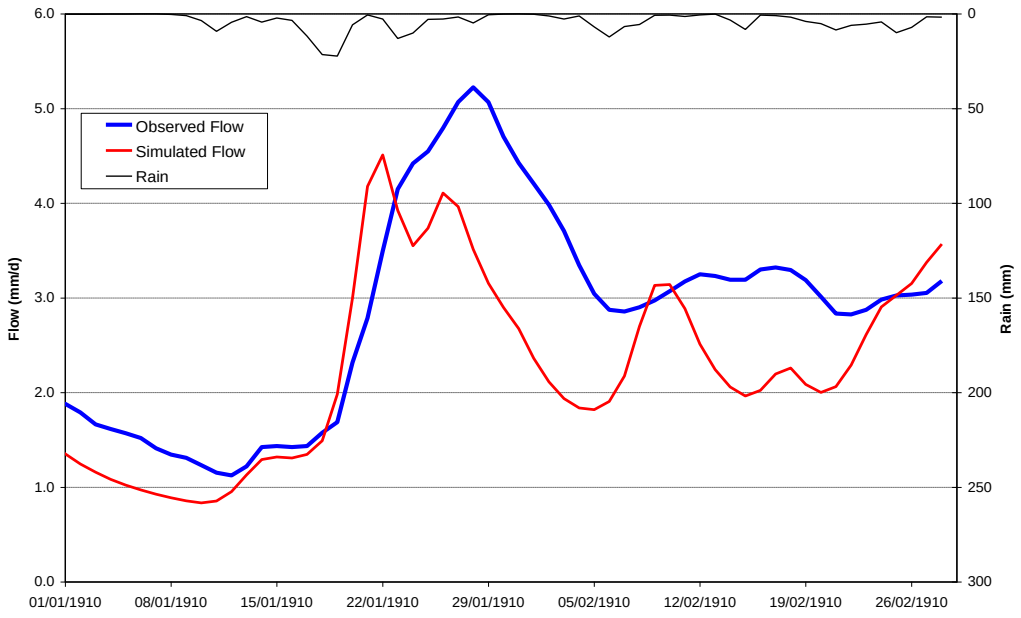

Fig. 3.3 rainfall and observed and simulated flow from 01/01/1910 to 28/02/1910 with NSE calibration integrating reservoirs on 1994 – 2002.

3.2.8 Discussion

The reservoirs data were not available on 2003 – 2009 and the calibration was thus limited on the period 1994 – 2002. However, when tables 3.5 and 3.1 are compared, it can be observed that the production store capacity X_1 has been decreased significantly which is in agreement with the results of Payan (2007) developed in part 3.2.3. X_2 and X_3 also varies while X_4 is almost constant. The NSE criterion results however cannot be compared as the two simulations were not done on the exact same period.

When comparing tables 3.2 and 3.6 however, it can be seen that the integration of the reservoirs in the calibration model has yielded better results on the 1910 flood, with a Nash-Sutcliffe efficiencies raise of around 0,16. The same observation can be made when comparing figures 3.1 and 3.3, the simulated flow peaks getting higher values (thus closer to the observed flow values) in figure G3.

However, the results presented in table 3.6 and figure 3.3 are still far from being satisfactory, the NSE still being less than 0,50 and a great volume of water – more than 1,4 billions of cubic meter - still absent from the simulation. Even if other land cover changes had an influence and that this could be integrated in the model for calibration, it still wouldn't give good results as this influence is likely to be even less significant than the reservoirs influence and would thus not be enough to explain the huge difference that remains between observed and simulated data.

Thus even if the changes of conditions between the period when the model is run (1909 – 1910) and the period when it is calibrated (1994 – 2002) could have had a small influence on the difference between observed and simulated values for the 1910 flood, the latter still remains very high when those changes are taken into account. In those conditions, it is advisable to investigate for other facts - events or model inadequacies - that could explain such a difference.

3.3 Discussion on the statistical tools used in the model

In the previous experiments, the model was calibrated by optimizing the four parameters X_1, X_2, X_3 and X_4 so as to maximize the Nash-Sutcliffe Efficiency (NSE) calculated on the flow values –observed and simulated – according to the formula given in equation 2.19. The use of the NSE criterion in calibration and evaluation of models is common practice in hydrology but has often been discussed.

In this part, based on the study from Gupta et al. (2009), the NSE criterion will be further investigated and other criteria will be tested in order to assess the statistical sensitivities of the GR4J results obtained for the 1910 flood and check if the NSE calibration method could be the explanation of the difference obtained between observed and simulated values for this flood.

3.3.1 Decomposition of the Nash-Sutcliffe Efficiency

Gupta et al. (2009) offers a decomposition of the NSE criterion. From the formula of equation 2.19, one easily get the equations :

$$NSE = 2\alpha r - \alpha^2 - \beta_n{}^2 \qquad \text{(Eq. 3.1)}$$

With :

$$r = \frac{COV(Y_O, Y_S)}{\sigma_O . \sigma_S} \quad \text{(Eq. 3.2)}$$

$$\alpha = \frac{\sigma_S}{\sigma_O} \quad \text{(Eq. 3.3)}$$

$$\beta_n = \frac{\mu_S - \mu_O}{\sigma_O} \quad \text{(Eq. 3.4)}$$

Where :

COV (Y_O,Y_S) is the covariance of the observed and simulated values :

$$COV(Y_O, Y_S) = \overline{(Y_O - \overline{Y_O})(Y_S - \overline{Y_S})} \quad \text{(Eq. 3.5)}$$

with $\overline{Z}$ the mean of the set of values Z.

σ_O and σ_S the standard deviations of the observed and simulated values respectively

μ_O and μ_S the means of the observed and simulated values respectively.

r is here the linear correlation coefficient between the simulated and the observed values, while "α is a measure of relative variability in the simulated and observed values; and β_n is the bias normalized by the standard deviation in the observed values" (Gupta et al., 2009, p. 81).

Maximizing the NSE is thus finding the best balance between those 3 components so as to get as close as possible to the ideal values : r = 1, α = 1 and β_n = 0.

However there are several problems that appear in equations 3.1 and 3.4 :

- The bias parameter β_n is a ratio where the discriminator is the standard deviation of the observed values, thus diminishing the importance of this component in case of high variability in the observed data.
- The relative variability parameter α appears twice in the NSE equation and is linked to r in the optimization as NSE will be maximized for α = r. In some cases this will lead the model to choose a value of α inferior to its optimal value at 1.

3.3.2 New efficiency criteria

To mitigate those problems, Gupta et al. (2009) have designed a new efficiency criterion, based on a multi-objective approach, and that will be maximised for the optimal values of each of the 3 components without any interplay between them. This new criterion was called Kling-Gupta Efficiency (KGE) and is given by the equations :

$$\beta = \frac{\mu_S}{\mu_O} \quad \text{(Eq. 3.6)}$$

$$KGE = 1 - \sqrt{(r-1)^2 + (\alpha-1)^2 + (\beta-1)^2} \quad \text{(Eq. 3.7)}$$

The bias parameter has been replaced by the ratio between the simulated mean and the observed mean and is now optimal for β = 1. In the KGE equation (Eq. 3.7), the Euclidian Distance between the actual values of r, α and β and their optimal values (1,1,1) is calculated and subtracted from 1, preventing any interplay between the parameters. KGE is optimal at 1 and will be optimized by maximization.

Finally, a new component k_O can be introduced. It is the slope of the regression line when regressing the simulated against the observed values, and it is given by the equation :

$$k_O = \frac{COV(Y_O, Y_S)}{\sigma_O^{\,2}} = r.\alpha \quad \text{(Eq. 3.8)}$$

Gupta et al. (2009) describes k_O as of interest in the case of peak flows where NSE will lead to underestimation as well as - but less severely - KGE. It would thus be interesting to use it to replicate the 1910 flood. Noticing the similarity between r and k_O, a new efficiency criterion has been created during this study, that will be called KGE_{mod} (KGE modified) and given by the equation :

$$KGE_{\text{mod}} = 1 - \sqrt{(k_O - 1)^2 + (\alpha-1)^2 + (\beta-1)^2} \quad \text{(Eq. 3.9)}$$

As KGE, KGE_{mod} is optimal for a value of 1 and is optimized by maximization.

As for the NSE criterion, KGE and KGE_{mod} are generally calculated on the observed and simulated flow values but can be also calculated on the logarithm or the square root of those flow values.

3.3.3 Application on the replication of the 1910 flood

In order to asses the importance of the efficiency criterion used on the simulation of the 1910 flood, it has been decided to run the calibration of the parameters on the years 1994 -2002 but with the KGE and KGE_{mod} criteria for optimization and to check if the results would be better when the model is run on the 1910 flood with those parameters. Because it gave better results, the reservoirs were still integrated in the model for calibration.

Data :

The same data as in part 3.2.5 were used.

Method :

The GR4J model was used with the Excel software. The formulas developed in the equations 3.1 to 3.9 were encoded so as to give the KGE and KGE_{mod} values. The Solver tool of Excel was then used for optimization of those criteria.

First, the four parameters X_1, X_2, X_3 and X_4 were calibrated on the time period from 01/01/1994 to 31/12/2002 with one year model warm-up, in order to maximise the KGE criterion calculated on the flow values.

The reservoirs influence was integrated in the model as described in part 3.2.

The model was then run on the period from 01/01/1909 to 28/02/1910 with the values of the parameters obtained on the calibration by maximization of the KGE criterion (KGE calibration) with one year model warm-up.

Then, the same experiment was reproduced with the only difference of making the calibration of the model by maximizing the KGE_{mod} criterion (KGE_{mod} calibration) instead of the KGE criterion.

Results :

Using the KGE and KGE_{mod} criteria for calibration of the model on the period 1994 – 2002 with integration of the reservoirs in the model, the parameters values presented in table 3.7 were obtained.

When using those parameters on the 1909 – 1910 period as described in *Method* the efficiency results given in table 3.8 were obtained. The flow values observed and simulated are shown on figure 3.4.

By integration, simulated volumes of water that flowed in Paris between 01/01/1910 and 28/02/1910 are calculated : $6{,}0270.10^9 m^3$ - representing a difference of 17,98% of observed volume – for KGE calibration and $6{,}1998.10^9 m^3$ - representing a difference of 15,63% of observed volume – for KGE_{mod} calibration

Discussion :

By comparing the results of tables 3.5 and 3.7, it can be seen that the production store capacity X_1 is diminished when the KGE and KGE_{mod} criteria are used while the time-basis for UH1 X_4 is raised, the two other parameters being more stable. Those results thus get closer to the parameters values obtained when calibrating the model on the period 1909-1910 even if they are still far from it (Table 3.3).

Table 3.7 parameters values after KGE and KGEmod calibration on 1994 – 2002 with integration of the reservoirs in the model

Parameter	Unit	Value after KGE calibration	Value after KGE_{mod} calibration
Production store capacity : X_1	mm	543	504
Exchange coefficient : X_2	mm	0,18	0,16
Routing store capacity : X_3	mm	94	95
Time basis for UH1 : X_4	days	4,2	4,2
NSE obtained with those parameters on 1995 - 2002	.	0,884	0,881
KGE obtained with those parameters on 1995 - 2002	.	0,942	0,935
KGE_{mod} obtained with those parameters on 1995 - 2002	.	0,943	0,958

Table 3.8 efficiency results obtained on the 1910 flood with KGE and KGEmod calibration integrating the reservoirs on 1994 2002

Criteria	Abreviation	Result of simulation with KGE calibration	Result of simulation with KGE_{mod} calibration
NSE calculated on flow values	NSE(Q)	0,455	0,489
NSE calculated on the square-root of flow values	NSE (VQ)	0,490	0,527
NSE calculated on the logarithm of flow values	NSE (ln(Q))	0,501	0,543

:

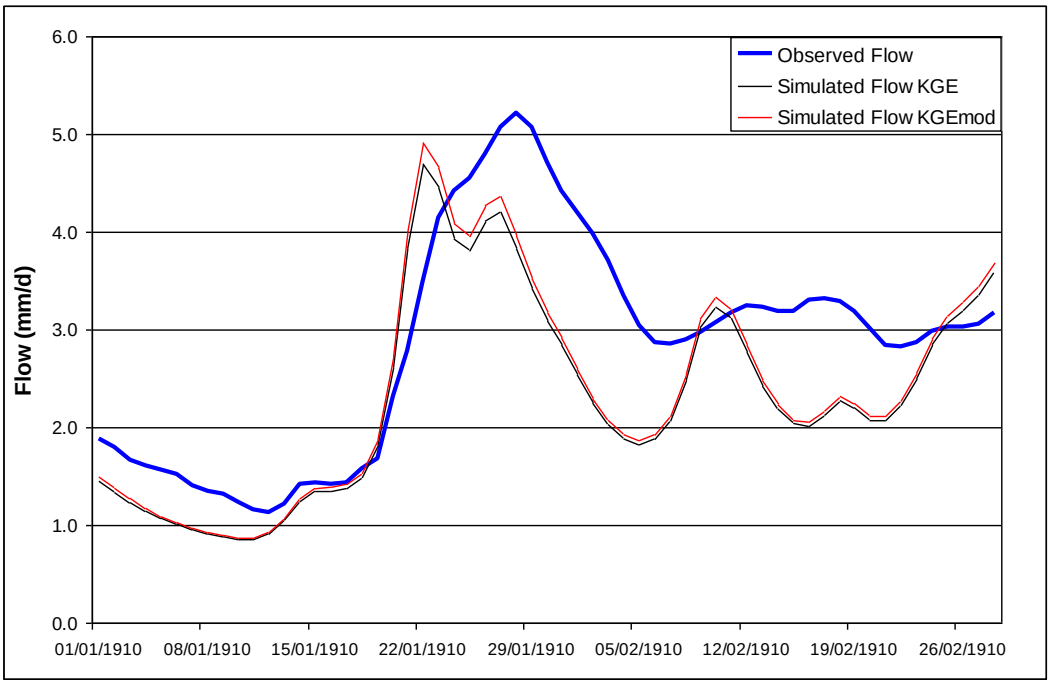

Fig. 3.4 observed and simulated flow from 01/01/1910 to 28/02/1910 with KGE and KGEmod calibration integrating reservoirs on 1994 – 2002.

Consequently, by comparing the results of tables 3.6 and 3.8 and figures 3.3 and 3.4, a significant augmentation of the Nash-Sutcliffe Efficiencies can be observed when running the model on the 1909-1910 period with parameters calibrated with KGE or KGE_{mod} criteria (of around 0,10 and around 0,14 respectively). The simulated peak flows are also getting closer to the observed value. By comparing only the results obtained with KGE and KGE_{mod} calibration, it can be seen that the parameters calibrated with the KGE_{mod} criterion give better Nash-Sutcliffe Efficiencies (augmentation of around 0,04 compared to KGE calibration). The flow graph obtained with KGE_{mod} calibration (Fig. 3.4) also shows higher peaks. However those peaks are narrower than with KGE and NSE calibrations (Fig. 3.3 and 3.4), and the contrast between high and low flow values is sharper with KGE_{mod} than with KGE and NSE (Fig. 3.4 and 3.3). Thus the KGE_{mod} calibration seems more suited for narrow flow peaks events with quick variability such as the 1910 flood which explains why it got the best results of all calibration methods. However, it is not recommended to use this KGE_{mod} calibration for other, more usual, events.

In all cases, even if the results appear to be better, they are still far from being satisfactory with more than 1 billion cubic meter of water lacking from the model in both cases. Statistical deficiencies of the model are not sufficient to explain the large difference between simulated and observed flow values on the 1910 flood. If the model is to be put into question, mistakes must thus be looked for on another part of its structure. Furthermore, this statistical solution to the 1910 flood simulation problem is not sustainable, as it is not sure that KGE and particularly KGE_{mod} calibrations would still give better results than NSE calibrations in other cases than large, rare, floods and it is thus difficult to integrate them in the model for other applications. In the coming experiments, NSE calibration will thus still be used as it is the most common statistical tool in hydrology and that it is obviously not the source of the 1910 flood problem.

Appendix 3.1 : Calculation of the 1909-1910 average precipitation on the Paris Austerlitz basin

On the period from January, 1st 1909 to February, 28th 1910, precipitation data were available on 148 stations of the Paris Austerlitz basin and its surroundings including 108 stations with complete data, 16 with less than one month of missing data and 24 with more than one month of missing data. The location of the stations is shown on figure 3.5.

A grid was then created over the basin with pixels of 8km*8km. For each of those pixels and for each day of the period, the average precipitation was calculated by inverse distance weighting using equation 3.10 :

$$P_{pixel} = \frac{\sum_{stations} \frac{P_s}{d_{s-p}^{\ 2}}}{\sum_{stations} \frac{1}{d_{s-p}^{\ 2}}} \qquad \text{(Eq. 3.10)}$$

Where :

- P_{pixel} is the average precipitation on the pixel (mm)
- P_s is the observed precipitation at station s (mm)
- d_{s-p} is the distance from station s to the pixel centre (km)

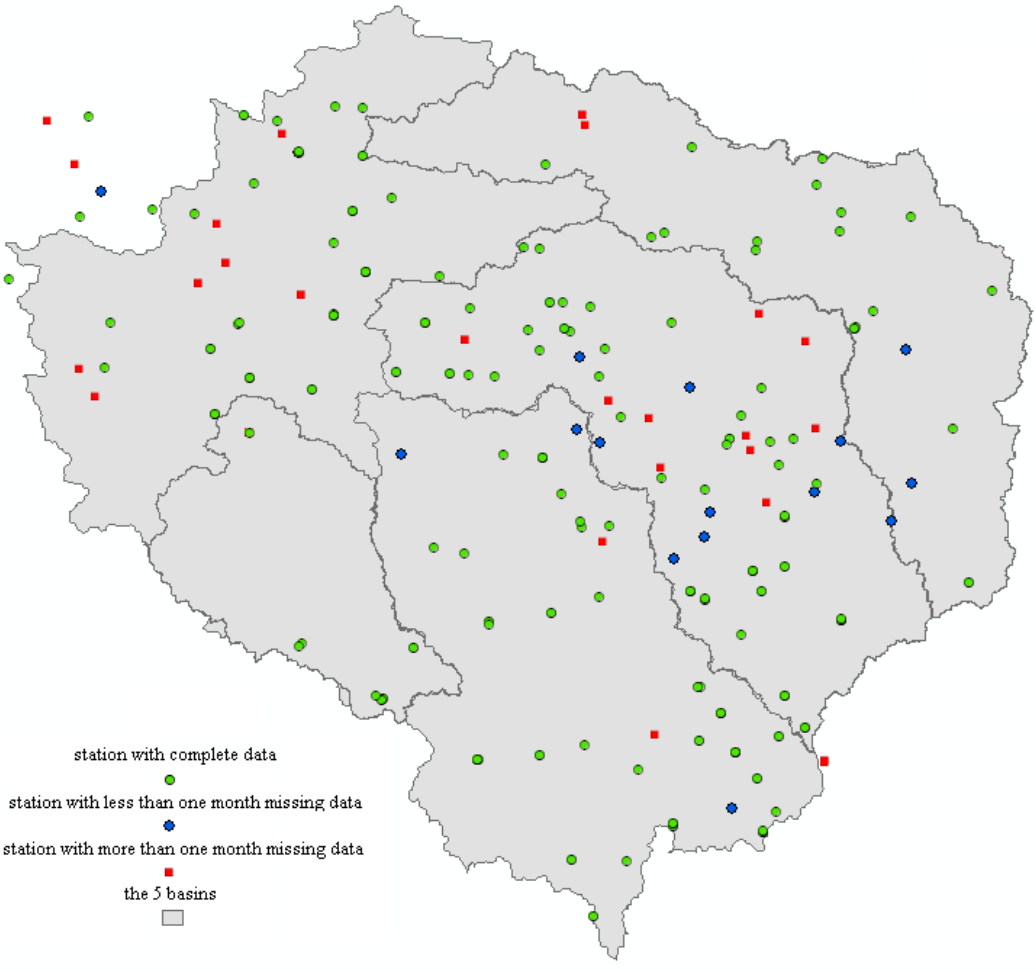

Fig. 3.5 the stations with available data for 1909-1910.

Finally, the average precipitation on the whole basin could be calculated by averaging each of the pixels precipitation value using equation 3.11.

$$P_{basin} = \frac{\sum_{pixels}\left(P_p \times S_p\right)}{\sum_{pixels} S_p} \qquad \text{(Eq. 3.11)}$$

Where :

- P_{basin} is the average precipitation on the whole basin (mm)
- P_p is the average precipitation on pixel p as calculated with equation 3.10 (mm)
- S_p is the percentage of pixel p's surface included in the basin

References

ANDREASSIAN, V. (2004) Waters and forests: from historical controversy to scientific debate. *Journal of Hydrology,* 291**,** 1-27.

DESCOMBES, P. (1910) *Journal d'agriculture pratique*, Académie de l'agriculture.

GUPTA, H. V., KLING, H., YILMAZ, K. K. & MARTINEZ, G. F. (2009) Decomposition of the mean squared error and NSE performance criteria: Implications for improving hydrological modelling. *Journal of Hydrology,* 377**,** 80-91.

MOULIN, L. (2003) Prise en compte des barrages-réservoirs dans un modèle pluie-débit global. *Unité de Recherche Qualité et Fonctionnement Hydrologique des Systèmes Aquatiques, CEMAGREF.* Antony, Université Pierre et Marie Curie, Université Paris-Sud, Ecole des Mines de Paris & Ecole Nationale du Génie Rural des Eaux et des Forêts. 55 p.

OUDIN, L., ANDREASSIAN, V., LERAT, J. & MICHEL, C. (2008) Has land cover a significant impact on mean annual streamflow? An international assessment using 1508 catchments. *Journal of Hydrology,* 357**,** 303-316.

PAYAN, J. L., PERRIN, C., ANDREASSIAN, V. & CLAUDE, M. (2008) How can man-made water reservoirs be accounted for in a lumped rainfall-runoff model? *Water Resources Research,* 44**,** 11 p.

PAYAN, J. L. (2007) Prise en compte de barrages-réservoirs dans un modèle global pluie-débit. *Unité de recherche Hydrosystèmes et Bioprocédés, CEMAGREF* Antony, Ecole Nationale du Génie Rural, des Eaux et des Forêts. 256 p.

Other Reference :

INSTITUTION INTERDÉPARTEMENTALE DES BARRAGES-RÉSERVOIRS DES BASSINS DE LA SEINE (2010) Lacs réservoirs. Online at http://www.iibrbs.fr/lacs/lac.htm [accessed at 05/04/2010].

4 TEST ON THE SUB-BASINS

In front of the disappointing results obtained when modelling the 1910 flood on the catchment of the Seine at Paris Austerlitz, it was decided to test the model on sub-basins. The goal was to assess more in detail the problem that occurs when GR4J is calibrated on recent years and validated on the 1910 flood and especially to find out whether this problem comes from the lumped nature of GR4J or from a deeper reason such as a process missing in the model.

Indeed, GR4J is a lumped model, which should be able to model the 1910 flood on the sub-basins. If it fails on all those sub-basins – like it fails on the Paris Austerlitz basin – then the reliability of the model could be questioned, at least in front of some general event that would have occurred on the whole basin in 1910 and that is not taken into account inside the model. But if it works on some sub-basins and not on others then it will show that the model can work accurately and that some site-specific event that is not taken into account by GR4J, has occurred within the Paris-Austerlitz basin.

Flow data in 1910 were available for only 4 sub-basins (Fig. 4.1) :

- the Loing river basin at Episy (3 900 km²)
- the Marne river basin at Ferté-sous-Jouarre (8 818 km²)
- the Seine river basin at Bazoches-lès-Bray (10 100 km²)
- the Yonne river basin at Courlon-sur-Yonne (10 700 km²)

The modelling of the 1910 flood on those 4 sub-basins will first be presented. Then a simplified propagation model will be used to assess the influence of the errors in those 4 modelling on the global simulated flow at Paris Austerlitz

4.1 Data and Method for tests on the sub-basins

4.1.1 Data

All the data that have been used for the different tests on the sub-basins, and their sources, are summarized in table 4.1 below. The water reservoirs have been taken into account in some of the tests during calibration (since they did not exist in 1910, see chapter 3). Indeed, the Marne reservoir is situated upstream of the Ferté-sous-Jouarre station, the Aube and Seine reservoirs are situated upstream of the Bazoches-lès-Bray station and the Panneciere dam is situated upstream of the Courlon-sur-Yonne station.

4.1.2 Method

For each of the sub-basins, the Excel software was used to run the GR4J model. When water reservoirs were present on the basin, calibration on the recent years was performed first using the NSE criterion, then using the NSE, KGE and KGEmod criteria respectively with the water reservoirs model. For the Loing at Episy basin which does not include any water reservoir, the calibration was performed on the recent years using the NSE, KGE and KGEmod criteria respectively. One year warm-up was taken for both calibration and validation on 1910.

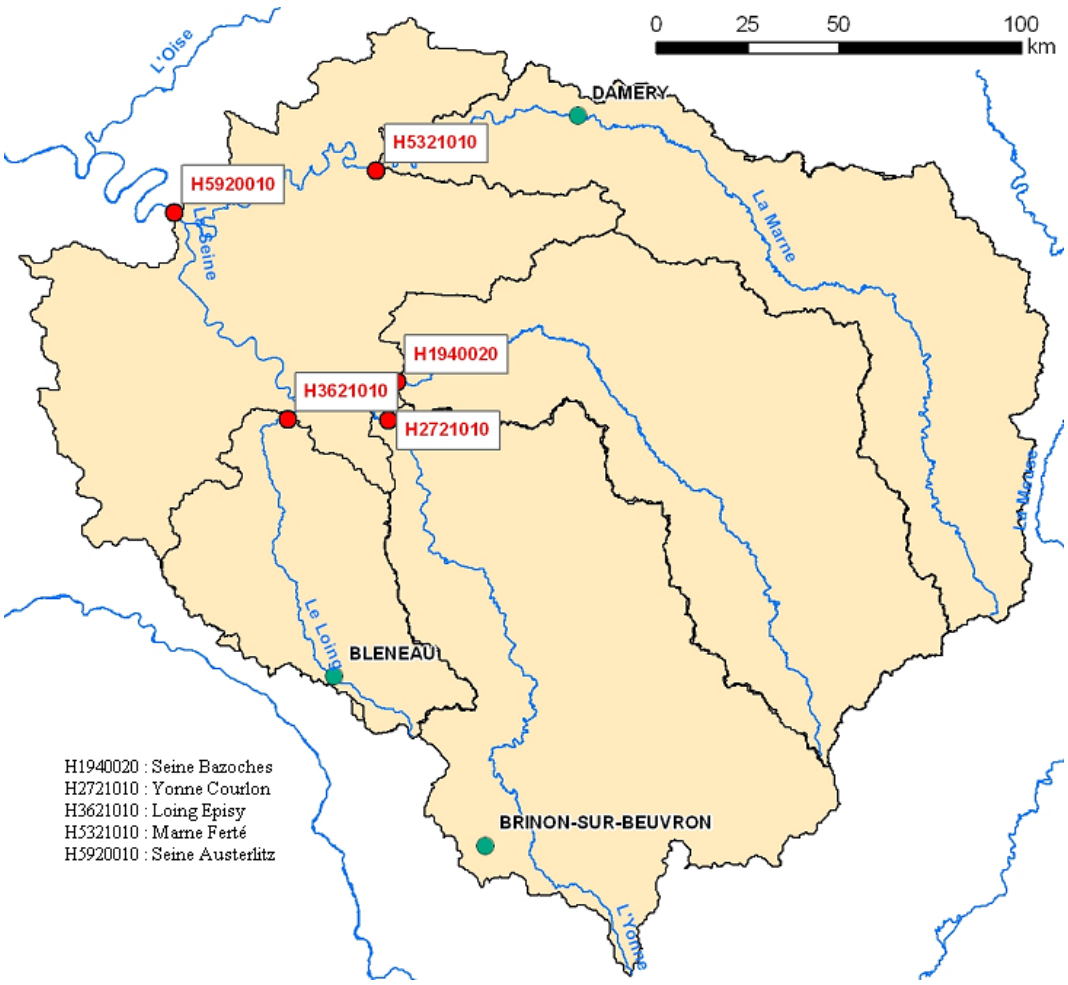

Fig. 4.1 the 4 sub-basins and the Paris Austerlitz basin.

4.2 Loing at Episy

4.2.1 Results

The model calibration on the period 1970-2006 gave the parameters values presented in table 4.2

When using those parameters on the 1909 – 1910 period the efficiency results given in table 4.3 were obtained. Finally, the observed and simulated flow values are shown on figure 4.2.

By simple integration of the curve presented on figure 4.2, the observed and simulated volumes of water in the Loing river that flowed at Episy between 14/01/1910 and 03/02/1910 are calculated. They are presented in table 4.4.

4.2.2 Discussion

The efficiency criteria obtained in validation on 1909-1910, that are presented in table 4.3 seem just acceptable but better than those obtained on the whole Paris Austerlitz basin (Tables 2.2, 2.6 and 2.8) with an NSE criterion that is higher than 0,70 for NSE calibration. Surprisingly, the calibration using the NSE criterion obtains better results – higher NSE(Q), NSE(VQ) and NSE(lnQ) - than calibrations with KGE and KGEmod criteria in validation on the 1910 flood.

Table 4.1 data used for the tests on the sub-basins

Basin	Surface used for conversion of volumetric values (km²)	Calibration			Validation		
		Data	Period	Source of the data	Data	Period	Source of the data
Loing at Episy	3 900	Observed Flow (mm/day)	August, 1st, 1970 to July, 31st 2006	*CEMAGREF*	Observed Flow (l/s)	January, 14th 1910 to February, 3rd 1910	*DIREN*
		Precipitation (mm)			Precipitation (mm)	January, 1st 1909 to February, 28th 1910	*Meteo France*
		Evapotranspiration (mm)			Evapotranspiration (mm)		*DIREN*
Marne at Ferté	8 800	Observed Flow (mm/day)	January, 1st, 1994 to December, 31st 2002	*CEMAGREF*	Observed Flow (l/s)	January, 14th 1910 to February, 15th 1910	*DIREN*
		Precipitation (mm)			Precipitation (mm)	January, 1st 1909 to February, 28th 1910	*Meteo France*
		Evapotranspiration (mm)			Evapotranspiration (mm)		*DIREN*
		Daily storage of the Marne reservoir (millions of m^3)		*Grands Lacs de Seine*			
Seine at Bazoches	10 100	Observed Flow (mm/day)	January, 1st, 1999 to December, 31st 2002	*DIREN*	Observed Flow (l/s)	January, 14th 1910 to February, 15th 1910	*DIREN*
		Precipitation (mm)	January, 1st, 1998 to December, 31st 2002		Precipitation (mm)	January, 1st 1909 to February, 28th 1910	*Meteo France*
		Evapotranspiration (mm)			Evapotranspiration (mm)		*DIREN*
		Daily storages of the Aube and Seine reservoirs (millions of m^3)		*Grands Lacs de Seine*			
Yonne at Courlon	10 700	Observed Flow (mm/day)	January, 1st, 1981 to December, 31st 1988	*CEMAGREF*	Observed Flow (l/s)	January, 14th 1910 to February, 15th 1910	*DIREN*
		Precipitation (mm)			Precipitation (mm)	January, 1st 1909 to February, 28th 1910	*Meteo France*
		Evapotranspiration (mm)			Evapotranspiration (mm)		*DIREN*
		Daily storage of the Panneciere dam (millions of m^3)		*Grands Lacs de Seine*			

Table 4.2 Loing at Episy : parameters values after calibration on 1970 2006

Parameter	Unit	Value after NSE calibration	Value after KGE calibration	Value after KGEmod calibration
Production store capacity : X_1	mm	478	589	549
Exchange coefficient : X_2	mm	-1,04	-0,66	-0,68
Routing store capacity : X_3	mm	43	44	44
Time basis for UH1: X_4	days	3,7	3,7	3,7
NSE obtained	.	0,877	0,872	0,873
KGE obtained	.	0,908	0,936	0,931
KGEmod obtained	.	0,919	0,942	0,955

Table 4.3 :Loing at Episy : efficiency results obtained on the 1910 flood with calibrat i0on on 1970 2006

Criterion	Result of simulation with NSE calibration	Result of simulation with KGE calibration	Result of simulation with KGEmod calibration
NSE calculated on flow values	0,733	0,687	0,695
NSE calculated on the square-root of flow values	0,668	0,648	0,638
NSE calculated on the logarithm of flow values	0,542	0,54	0,515

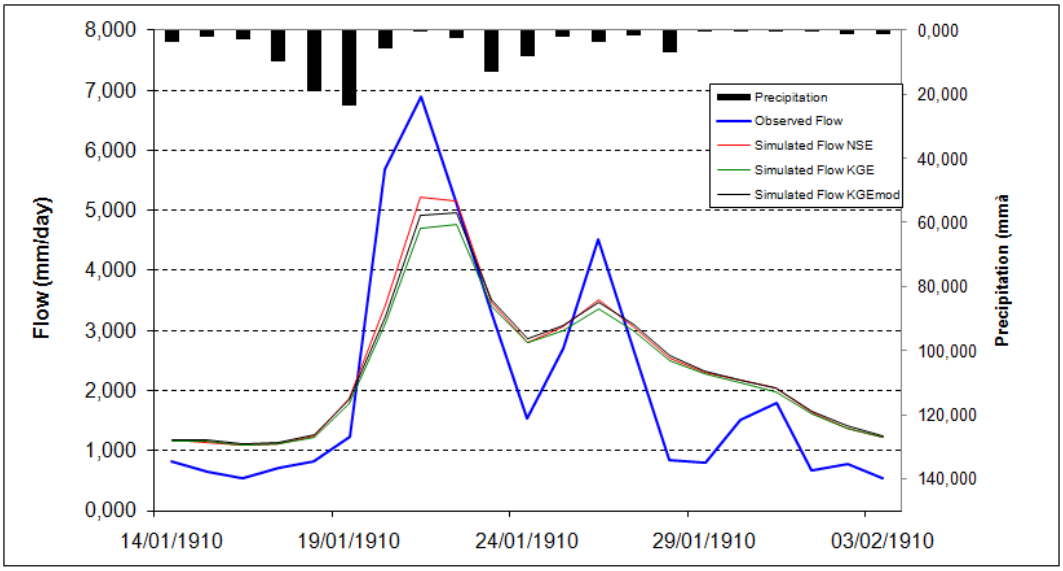

Fig. 4.2 Loing at Episy : precipitations, observed and simulated flows from 14/01/1910 to 03/02/1910 with calibration on 1970-2006

Table 4.4 :Loing at Episy : Observed and simulated discharge from 14/01/1910 to 03/02/1910

	Volume (m^3)	Difference of volume (Vsim-Vobs) in percentage of the observed volume
observed	$1,7.10^8$	.
Simulated NSE	$2.0.10^8$	14,86%
Simulated KGE	$1,9.10^8$	10,58%
Simulated KGEmod	$2.0.10^8$	14,20%

However, it can be seen on figure 4.2 that none of the simulations could actually replicate the peak flows of the flood and all of them are underestimating it. The simulated flow curves are flattened related to the observed flow curve which is much more irregular with very marked peak flows. Thus, despite the acceptable NSE obtained in validation, those simulations cannot be considered satisfactory as they are unable to replicate the most important part of the flood.

Surprisingly, the simulations give higher volumes of water than what was actually observed as it can be seen in table 4.4. However, these results do not contradict with the fact that water is missing in Paris Austeriltz : the difference in volumes at Episy (around 10^7 m^3) is very small related to the difference obtained at Paris Austerlitz (around 10^9 m^3).

4.3 Marne at la-Ferté-sous-Jouarre

4.3.1 Results

The model calibration on the period 1994-2002 gave the parameters values presented in table 4.5.

When using those parameters on the 1909 – 1910 period the efficiency results given in table 4.6 were obtained. Finally, the observed and simulated flow values are shown on figure 4.3.

By simple integration of the curve presented on figure 4.3, the observed and simulated volumes of water in the Marne river that flowed at Ferté-sous-Jouarre between 14/01/1910 and 15/02/1910 are calculated. They are presented in table 4.7.

Table 4.5 Marne at Ferté : parameters values after calibration on 1994 2002

Parameter	Unit	Value after NSE calibration not accounting for the upstream reservoir	Value after NSE calibration accounting for the upstream reservoir	Value after KGE calibration accounting for the upstream reservoir	Value after KGEmod calibration accounting for the upstream reservoir
Production store capacity : X_1	mm	14	452	417	381
Exchange coefficient : X_2	mm	-11,99	-0,64	-0,64	-0,69
Routing store capacity : X_3	mm	617	117	117	118
Time basis for UH1 : X_4	days	5,5	7,4	7,5	7,5
NSE obtained	.	0,854	0,891	0,89	0,887
KGE obtained	.	0,889	0,938	0,945	0,939
KGEmod obtained	.	0,828	0,915	0,946	0,96

Table 4.6 Marne at Ferté : efficiency results obtained on the 1910 flood with calibration on 1994-2002

Criterion	Result of simulation with NSE calibration without the water reservoir	Result of simulation with NSE calibration accounting for the water reservoir	Result of simulation with KGE calibration accounting for the water reservoir	Result of simulation with KGEmod calibration accounting for the water reservoir
NSE(Q)	-0,853	-0,431	-0,283	-0,154
NSE(VQ)	-0,945	-0,609	-0,431	-0,282
NSE(lnQ)	-1,029	-0,877	-0,657	-0,48

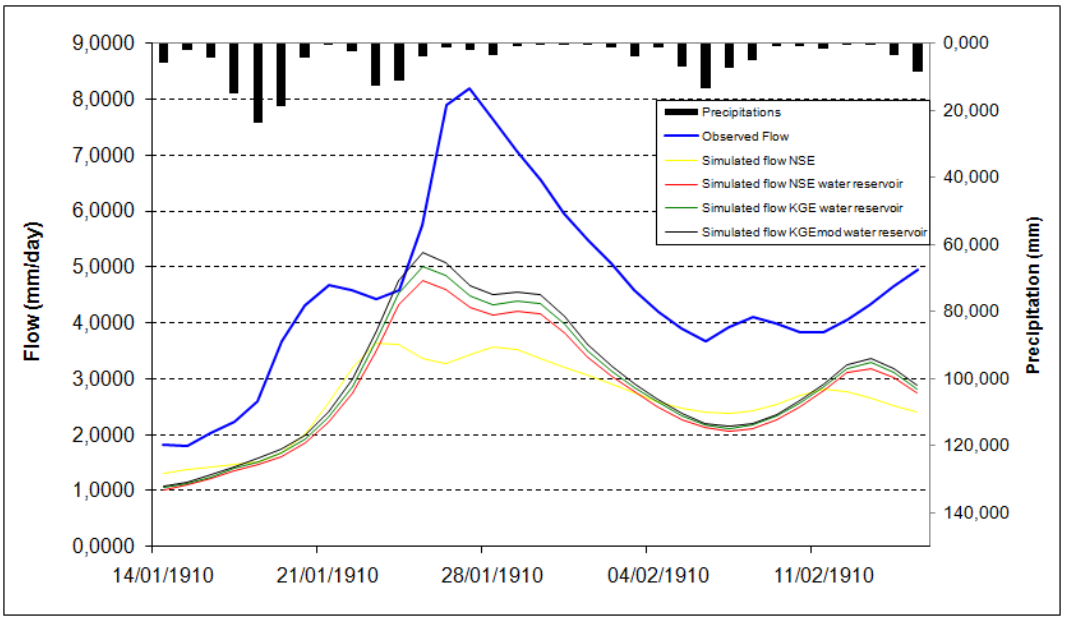

Fig. 4.3 Marne at Ferté : precipitations, observed and simulated flows from 14/01/1910 to 15/02/1910 with calibration on 1994 2002

Table 4.7 Marne Ferté : Observed and simulated discharge from 14/01/1910 to 15/02/1910

	Volume (m^3)	Difference of volume (Vobs-Vsim) in percentage of the observed volume
observed	$1,3.10^9$	.
Simulated NSE without the water reservoir	$7,7.10^8$	42,22%
Simulated NSE including the water reservoir	$8,1.10^8$	38,66%
Simulated KGE including the water reservoir	$8,4.10^8$	36,39%
Simulated KGEmod including the water reservoir	$8,7.10^8$	34,29%

4.3.2 Discussion

The NSE calibration that does not take the upstream reservoir into account results in unusual parameters values (Table 4.5) with a very large routing store capacity X_3 higher than the production store capacity X_1 which is particularly small. The exchange coefficient X_2 is also unusually high. However the NSE obtained in calibration is not too low.

The results obtained in validation are exceptionally bad with a Nash Sutcliffe Efficiency that is negative in all cases (Table 4.6). As for the Paris Austerlitz basin, the "less worse" result is obtained with parameters calibrated by the KGEmod criterion maximisation with the upstream reservoir accounted for. This analysis is confirmed by the hydrographs (Fig. 4.3) on which it can be seen that all the simulations are largely underestimating the flow and particularly its peak in late January. This underestimation can also be seen in table 4.7 with the volumes of water : from January 14th to February 15th, the best simulation is missing more than one third of the observed water volume.

Many attempts to improve those results were undertaken, for example by using different calibration periods. The parameters calibrated at the Châlons and Gournay stations – 2 other Stations on the Marne river, close to la-Ferté-sous-Jouarre, were also used in validation on the 1910 flood on the Marne basin at Ferté-sous-Jouarre. None of those attempts

could give significantly improved results, with an NSE criterion in validation that remained negative in all cases.

4.4 Seine at Bazoches-lès-Bray

4.4.1 Results

The model calibration on the period 1998-2002 gave the parameters values presented in table 4.8.

When using those parameters on the 1909 – 1910 period the efficiency results given in table 4.9 were obtained. Finally, the observed and simulated flow values are shown on figure 4.4.

By simple integration of the curve presented on figure 4.4, the observed and simulated volumes of water in the Seine river that flowed at Bazoches-lès-Bray between 14/01/1910 and 15/02/1910 are calculated. They are presented in table 4.10.

4.4.2 Discussion

For all the different calibrations, the time basis for UH1 X_4 is the same and has a high value (Table 4.8). This high value of the parameter can explain the delay which can be observed on figure 4.4 between the observed and the simulated peak flows. It can also be seen in table 4.8 that the production store capacity is significantly reduced when the water reservoirs are taken into account in the calibration as already observed in chapter 3.2.

The results obtained in validation on the 1910 flood are far from being satisfactory with NSE criteria hardly exceeding 0,5 (Table 4.9). Like for the Marne river and the Seine at Paris Austerlitz, the best results are obtained with KGEmod calibration taking the water reservoirs into account. This analysis is confirmed by figure 4.4 where it can be seen a clear underestimation of the peak flow for all calibration methods.

Table 4.8 Seine at Bazoches : parameters values after calibration on 1998 2002

Parameter	Unit	Value after NSE calibration without the water reservoirs	Value after NSE calibration including the water reservoirs	Value after KGE calibration including the water reservoirs	Value after KGEmod calibration including the water reservoirs
Production store capacity : X_1	mm	721	433	376	341
Exchange coefficient : X_2	mm	-0,16	-0,36	-0,41	-0,47
Routing store capacity : X_3	mm	100	134	137	138
Time basis for UH1 : X_4	days	10	10	10	10
NSE obtained	.	0,797	0,882	0,879	0,872
KGE obtained	.	0,884	0,921	0,939	0,931
KGEmod obtained	.	0,848	0,881	0,938	0,954

Table 4.9 Seine at Bazoches : efficiency results obtained on the 1910 flood with calibration on 1998-2002

Criterion	Result of simulation with NSE calibration without the water reservoirs	Result of simulation with NSE calibration including the water reservoirs	Result of simulation with KGE calibration including the water reservoirs	Result of simulation with KGEmod calibration including the water reservoirs
NSE(Q)	0,057	0,427	0,49	0,506
NSE(VQ)	-0,098	0,381	0,47	0,502
NSE(lnQ)	-0,478	0,206	0,348	0,41

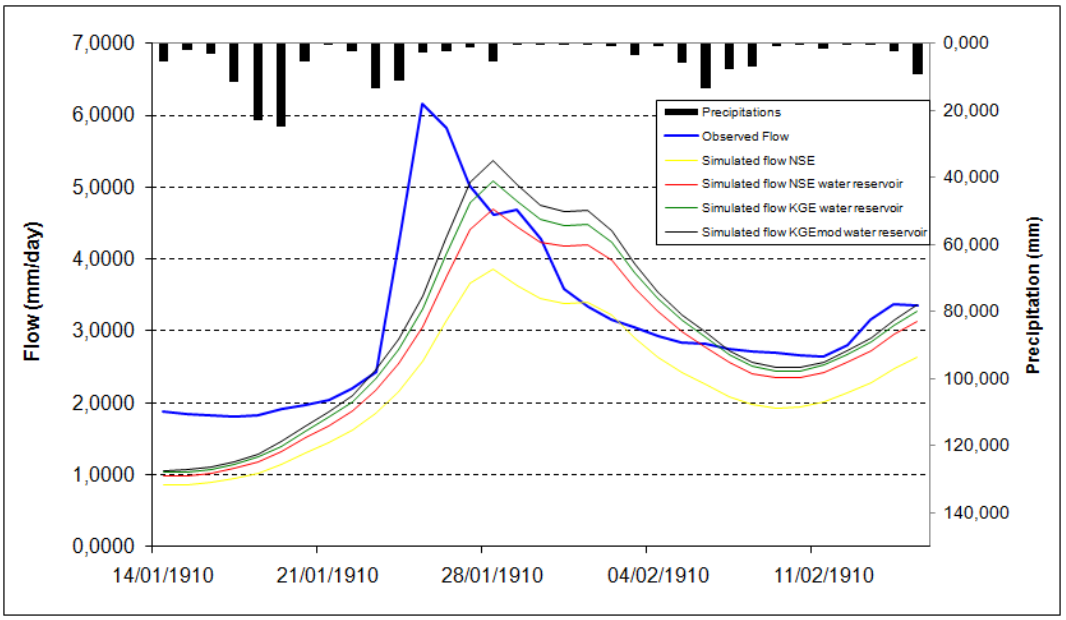

Fig. 4.4 Seine at Bazoches : precipitations, observed and simulated flows from 14/01/1910 to 15/02/1910 with calibration on 1998 2002

Table 4.10 Seine at Bazoches : Observed and simulated discharge from 14/01/1910 to 15/02/1910

	Volume (m^3)	Difference of volume (Vobs-Vsim) in percentage of the observed volume
observed	$1{,}0.10^9$	.
Simulated NSE without the water reservoir	$7{,}5.10^8$	27,70%
Simulated NSE including the water reservoir	$9{,}0.10^8$	12,75%
Simulated KGE including the water reservoir	$9{,}6.10^8$	7,30%
Simulated KGEmod including the water reservoir	$1.0.10^9$	3,73%

However the volume differences between observed and simulated flows are not so large (Table 4.10) and the missing water quantity for KGEmod calibration including the water reservoirs (around 10^7 m^3) can be neglected related to the missing water volume on the whole Paris Austerlitz basin. Indeed the observed hydrograph is more peaky than the simulated hydrographs. Thus in late January and early February, an overestimation of the flow can be observed for every calibration method taking the water reservoirs into account (Fig. 4.4).

4.5 Yonne at Courlon-sur-Yonne

4.5.1 Results

The model calibration on the period 1981-1988 gave the parameters values presented in table 4.11.

When using those parameters on the 1909 – 1910 period the efficiency results given in table 4.12 were obtained. Finally, the observed and simulated flow values are shown on figure 4.5.

By simple integration of the curve presented on figure 4.5, the observed and simulated volumes of water in the Yonne river that flowed at Courlon-sur-Yonne between 14/01/1910 and 15/02/1910 are calculated. They are presented in table 4.13.

Table 4.11 Yonne at Courlon : parameters values after calibration on 1981-1988

Parameter	Unit	Value after NSE calibration without the water reservoirs	Value after NSE calibration including the water reservoirs	Value after KGE calibration including the water reservoirs	Value after KGEmod calibration including the water reservoirs
Production store capacity : X_1	mm	558	515	517	481
Exchange coefficient : X_2	mm	0,74	0,74	0,82	0,81
Routing store capacity : X_3	mm	71	74	73	74
Time basis for UH1 : X_4	days	4,3	4,3	4,3	4,3
NSE obtained	.	0,873	0,876	0,875	0,874
KGE obtained	.	0,931	0,934	0,937	0,931
KGEmod obtained	.	0,933	0,928	0,941	0,955

Table 4.12 Yonne at Courlon : efficiency results obtained on the 1910 flood with calibration on 1981 1988

Criterion	Result of simulation with NSE calibration without the water reservoirs	Result of simulation with NSE calibration including the water reservoirs	Result of simulation with KGE calibration including the water reservoirs	Result of simulation with KGEmod calibration including the water reservoirs
NSE(Q)	0,883	0,917	0,926	0,943
NSE(VQ)	0,87	0,906	0,917	0,938
NSE(lnQ)	0,846	0,887	0,902	0,927

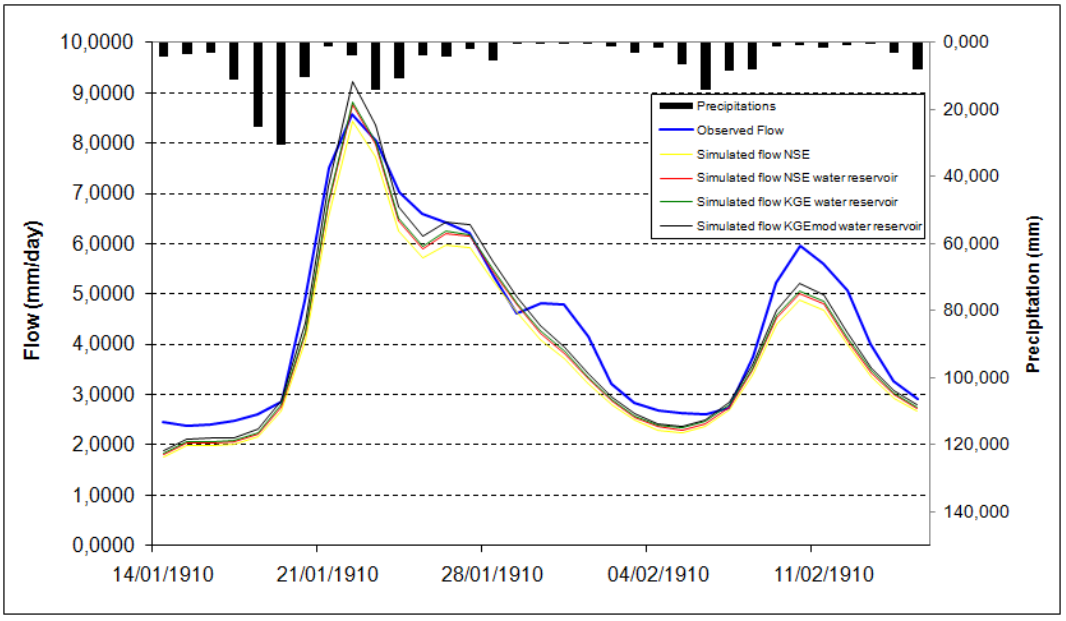

Fig. 4.5 Yonne at Courlon :precipitations, observed and simulated flows from 14/01/1910 to 15/02/1910 with calibration on 1981 1988

Table 4.13 Yonne at Courlon : Observed and simulated discharge from 14/01/1910 to 15/02/1910

	Volume (m^3)	Difference of volume (Vobs-Vsim) in percentage of the observed volume
observed	$1,6.10^9$	.
Simulated NSE without the water reservoir	$1,4.10^9$	11,80%
Simulated NSE including the water reservoir	$1,4.10^9$	9,15%
Simulated KGE including the water reservoir	$1,4.10^9$	8,24%
Simulated KGEmod including the water reservoir	$1,5.10^9$	5,59%

4.5.2 Discussion

The results of the validation on the 1910 flood are particularly good with a NSE(Q) and NSE(VQ) higher than 0,90 for all calibrations including the water reservoirs, with the best results obtained, once again, with KGEmod calibration (Table 4.12). The hydrographs presented on figure 4.5 confirm this analysis : the main peak flow – around January, 22nd – is very well reproduced and is even a bit overestimated by simulations with calibration including the water reservoirs. The second peak flow – around February, 11th – is rather underestimated by the model but the tendency is well respected.

The missing volumes of water are thus relatively small – less than 10% of the observed volume for all calibrations including the water reservoirs (Table 4.13). With KGEmod calibration including the water reservoirs, the missing volume of water (around 10^7 m^3) is negligible related to the overall missing volume on the Paris Austerltz basin.

4.6 Simplified propagation model

The GR4J model validation on the 1910 flood after calibrations on the recent years is thus giving very different results for the different sub-basins :

On the Yonne at Courlon basin the results are very satisfactory in terms of efficiencies, hydrographs and water volumes. Results are less satisfactory on the Loing at Episy basin with simulated hydrographs showing a clear underestimation of the peak flow. Results are bad on the Seine at Bazoches basin and very bad on the Marne at Ferté basin.

The above-listed differences suggest the existence of a localized phenomenon that took place in 1910, during or just before the flood, in some parts of the Seine basin - like in the Marne at Ferté and the Seine at Bazoches basins - but not in the Yonne at Courlon basin for example. This phenomenon could explain the bad results obtained in the model validation on the 1910 flood on the Paris Austerlitz basin, as it prevents a good simulation of the flow on some of its sub-basins.

To test this hypothesis, a simplified model of propagation was designed. This model simulates the flow at Paris Austerlitz from the measured flows at the gauging stations of Episy, Ferté-sous-Jouarre, Bazoches-lès-Bray and Courlon-sur-Yonne. The goal is not to replace the rainfall-runoff (hydrologic) simulation by a runoff-runoff (hydraulic) simulation but simply to test the consistence of the 4 upstream measurements with the Paris Austerlitz measurement in order to validate the overall quality of the measurement. If this consistency is proven, the other goal will be to determine how the errors in simulation on the 4 sub-basins – and particularly the Marne Ferté and Seine Bazoches basins - are propagated to affect the simulation of the flow in Paris Austerlitz and if the GR4J

error of simulation at Paris Austerlitz corresponds to the propagation of those errors on the sub-basins.

After a brief presentation of this very simplified propagation model, its results will be presented and discussed.

4.6.1 presentation of the model

In this very simplified model, the Seine flow at Austerlitz at day d, $Q_{SA}(d)$ is given by the equation :

$$Q_{SA}(d) = X \times \left[\begin{array}{l} Q_{LE}\left(d - \frac{D_{LE}}{c_{LE}}\right) + Q_{MF}\left(d - \frac{D_{MF}}{c_{MF}}\right) \\ + Q_{SB}\left(d - \frac{D_{SB}}{c_{SB}}\right) + Q_{YC}\left(d - \frac{D_{YC}}{c_{YC}}\right) \end{array} \right] \qquad \text{(Eq. 4.1)}$$

Where :

- X is a dimensionless multiplicative factor that accounts for the contribution of the Seine catchment downstream of the 4 gauging stations (see figure 4.1).
- $Q_s(d)$ is the water flow (in l/s) at the outlet of the sub-basin *s* at day *d*
- D_s is the distance (in km) between the outlet of sub-basin *s* and the outlet of the Paris Austerlitz basin.
- c_s is the average water celerity (in km/day) between the outlet of sub-basin *s* and the outlet of the Paris Austerlitz basin.
- The suffix LE stands for Loing Episy, MF for Marne Ferté, SB for Seine Bazoches and YC for Yonne Courlon.

The distances from the outlets of the sub-basins to the outlet of the Paris Austerlitz basin have been calculated using the Arc GIS software. They are given in table 4.14 below :

Table 4.14 distances from the outlets of the 4 sub-basins to the Paris Austerlitz gauging station

Sub-basin	Distance to the outlet of the Paris Austerlitz basin (km)
Loing Episy	96,3
Marne Ferté-sous-Jouarre	193,1
Seine Bazoches-lès-Bray	153,6
Yonne Courlon-sur-Yonne	133,4

The multiplicative factor X and the average celerities c_s have been taken as model parameters that need to be calibrated.

4 versions of the model have been tested. In the first two, the average celerities have been considered to be equal - $c_{LE} = c_{MF} = c_{SB} = c_{YC} = c$ – thus resulting in only 2 parameters (X, c) to calibrate.

In the first version of the model, the ratios $\frac{D_s}{c} = d_s$ were set equal to their nearest integer value and the values $Q_s(d\text{-}d_s)$ in equation 4.1 were thus the flow values (in l/s) at the outlet of the sub-basin *s* at day $d\text{-}d_s$ with d_s the delay in an integer number of days.

In the second version of the model, d_s was kept a float and the values of Q_s in equation 4.1 were given by a weighted average according to the equation :

$$Q_s\left(d-\frac{D_s}{c}\right)=\left[Int(d_s)+1-d_s\right]Q_s\left(d-Int(d_s)\right)+\left[d-Int(d_s)\right]Q_s\left(d-Int(d_s)-1\right) \quad \text{(Eq. 4.2)}$$

Where Int(d_s) is the integer part of d_s.

In the last 2 versions of the model, the average celerities were not considered equal anymore, thus resulting in 5 parameters to calibrate (X, c_{LE}, c_{MF}, c_{SB}, c_{YC}). In the third version, the delays d_s were taken as integers just like in the first version. In the fourth version, d_s was kept a float and equation 4.2 was applied just like in the second version.

4.6.2 Data

The data used for this simplified propagation model are summarized in table 4.15 below. For validation on the 1910 flows calculated with GR4J : Only the best results –i.e. the calculated flow with the highest NSE in validation on the 1910 flood – shown above were used as described in table 4.15.

4.6.3 Method

The model described in part 4.5.1 was written in Fortran. In calibration and validation, only the days when data were available on the 4 sub-basins – taking the delays into account - and on the Paris Austerlitz basin were used. The calibration was done by maximisation of the Nash-Sutcliffe Efficiency calculated by comparison of the observed and calculated – with the propagation model's equation 4.1 - flows at Paris Austerlitz. In validation, Nash-Sutcliffe Efficiencies were also calculated the same way.

4.6.4 Results

After calibration of the parameters, the delays d_s associated to each of the 4 sub-basins can be calculated and are shown in table 4.16.

Table 4.15 Data used to run the propagation model

	Observed flow values (converted in l/s) for Calibration		Observed flow values (converted in l/s) for Validation		GR4J-calculated flow values (converted in l/s) for Validation	
Basin	Period	Source of the data	Period	Source of the data	Period	Calculation of the data
Loing at Episy	January, 1st 1999 to July, 31st 2006	*DIREN*	January, 14th 1910 to February, 3rd 1910	*DIREN*	January, 14th 1910 to February, 3rd 1910	NSE calibration on 1970-2006
Marne at Ferté	January, 1st 1999 to July, 31st 2006	*DIREN*	January, 14th 1910 to February 15th 1910	*DIREN*	January, 14th 1910 to February 15th 1910	KGEmod calibration including the water reservoir on 1994-2002
Seine at Bazoches	January, 1st 1999 to July, 31st 2006	*DIREN*	January, 14th 1910 to February 15th 1910	*DIREN*	January, 14th 1910 to February 15th 1910	KGEmod calibration including the water reservoirs on 1998-2002
Yonne at Courlon	January, 1st 1999 to July, 31st 2006	*DIREN*	January, 14th 1910 to February 15th 1910	*DIREN*	January, 14th 1910 to February 15th 1910	KGEmod calibration including the water reservoir on 1981-1988
Seine at Paris Austerlitz	January, 1st 1999 to August, 31st 2006	*DIREN*	January, 1st 1910 to February, 28th 1910	*DIREN*	No data used	

Table 4.16 delays between the sub-basins outlet and Paris Austerlitz for each of the 4 versions of the propagation model

Sub-basin	Delay (in days) for version 1	Delay (in days) for version 2	Delay (in days) for version 3	Delay (in days) for version 4
Loing Episy	1	0	1	0
Marne Ferté	2	1	2	1
Seine Bazoches	2	1	3	1
Yonne Courlon	1	1	1	1

After calibration on the recent years, the propagation model was run in validation on the 1910 flood using the observed flow values of the sub-basins. The results are shown on figure 4.6 below. The Nash-Sutcliffe efficiencies obtained by comparison with the observed flow at Paris Austerlitz are shown in table 4.17.

The same calibrated parameters were then used a second time to run the propagation model on the 1910 flood using the GR4J-calculated flows of the sub-basins. The results are shown on figure 4.7 for comparison with the calculated flows on each sub-basin and on figure 4.8 for comparison with the GR4J-calculated flow at Paris-Austerlitz. The Nash-Sutcliffe efficiencies obtained by comparison with the observed flow at Paris Austerlitz are shown in table 4.18.

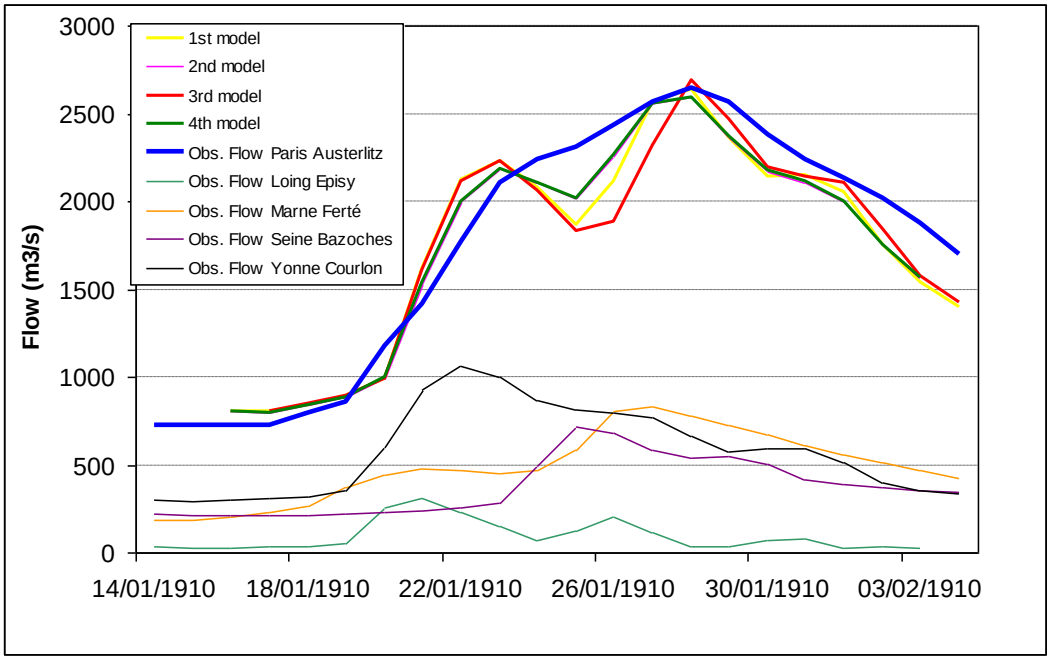

Fig. 4.6 results of the simplified propagation model using observed flows for the sub-basins and observed flows on the sub-basins

Table 4.17 NSE obtained for the 4 versions of the propagation model with observed flows on the sub-basins.

Version of the propagation model	NSE obtained when matching with the observed flow at Paris Austerlitz
1	0,886
2	0,933
3	0,843
4	0,935

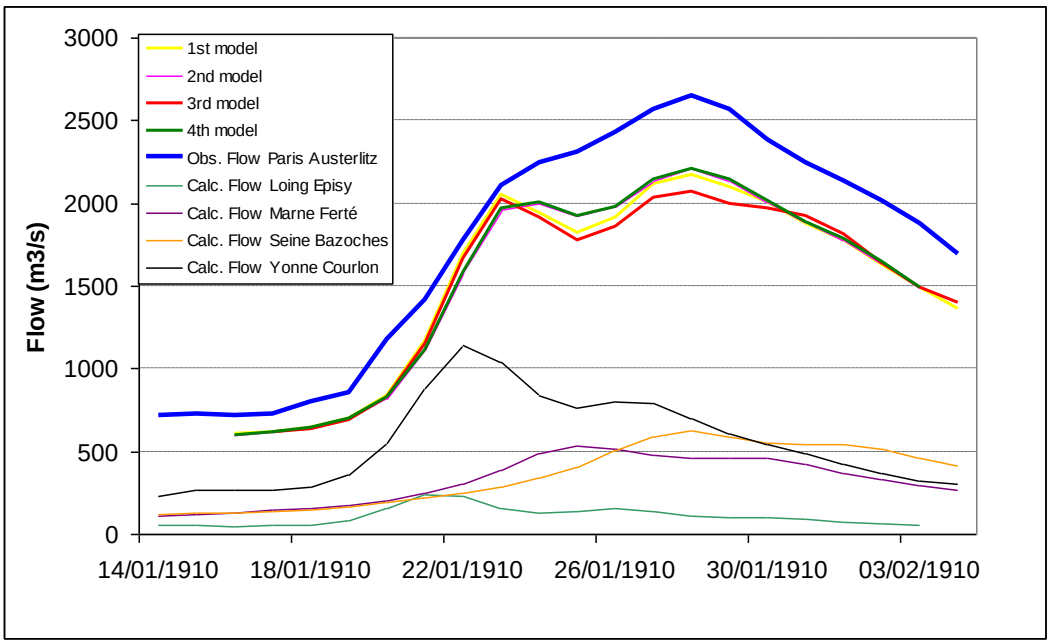

Fig. 4.7 results of the simplified propagation model using calculated flows for the sub-basins and GR4J-calculated flows on the sub-basins

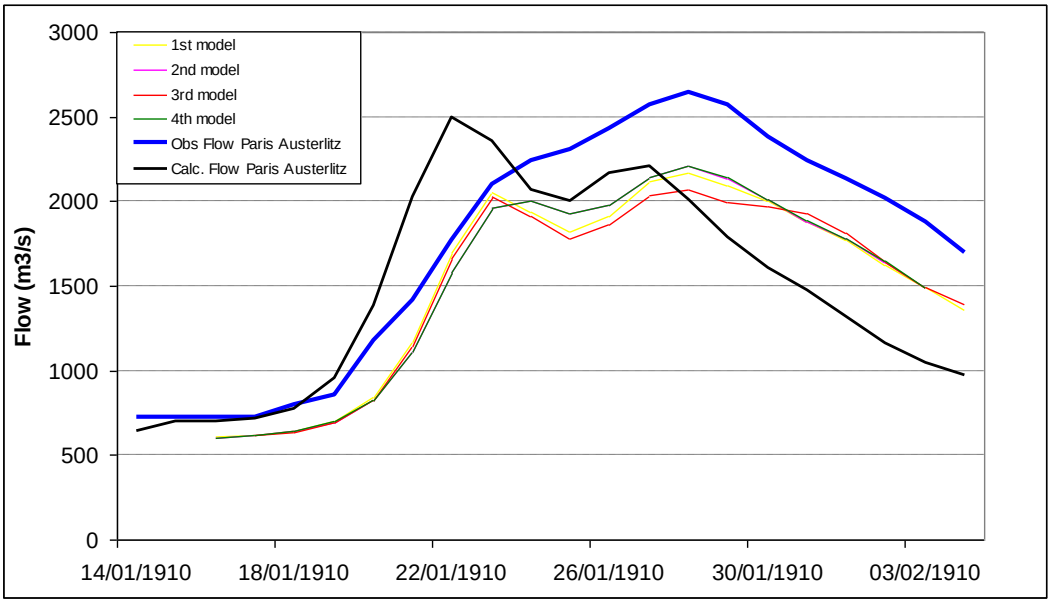

Fig. 4.8 results of the simplified propagation model using calculated flows on the sub-basins and GR4J-calculated flow at Paris Austerlitz

Table 4.18 NSE obtained for the 4 versions of the propagation model with calculated flows on the sub-basins

Version of the propagation model	NSE obtained when matching with the observed flow at Paris Austerlitz
1	0,719
2	0,756
3	0,613
4	0,76

4.6.5 Discussion

The propagation model gives good results in validation on the 1910 flood when using the observed sub-basins flows (Table 4.17). As it can be seen on figure 4.6, the peak flow is pretty well reproduced except for a gap around January, 25th that can be due to another tributary – like e.g. the Grand Morin river - not taken into account in the sub-basins studied, and with a peak flow reaching Paris Austerlitz at this very moment.

On figure 4.6, by comparing the simulated flow at Paris Austerlitz with the observed flows in each of the sub-basins and using the delays given in table 4.16, it can be seen that the first simulated peak flow – around January, 23rd, 24th – is mainly due to the arrival of the Yonne peak flow. The second simulated peak flow – around January, 28th – which is the main peak flow of the 1910 flood at Paris Austerlitz is mainly due to the arrival of the Marne and the little Seine (the Seine at Bazoches-lès-Bray) peak flows. The Loing influence is however more negligible in those 2 simulated peak flows.

Figure 4.7 shows the propagation model results when using the calculated flow for the sub-basins. When comparing it with figure 4.6, it can be seen that the first simulated peak flow – January, 23rd, 24th – is still pretty well reproduced due to a good simulation of the Yonne flow (see part 4.5). However the second peak flow of figure 4.6 – January, 28th – has disappeared on figure 4.7 where it is largely underestimated due to GR4J inability to reproduce the flows of the Marne at Ferté and of the Seine at Bazoches (see parts 4.3 and 4.4). The Nash Sutcliffe efficiencies obtained by the propagation model with the simulated flows on the sub-basins are thus lower than those obtained with the observed flows (Tables 4.17 and 4.18).

Finally, the comparison with the simulated flow at Paris Austerlitz that is drawn on figure 4.8 shows a similar trend between the propagation of the simulated sub-basins' flows and the simulation of the Paris Austerlitz flow. A first peak, corresponding to the well-simulated Yonne river, is well reproduced but then the simulation is failing to reproduce the main peak flow of the flood. The GR4J simulation of the Paris Austerlitz basin gets worse results than the propagation model with simulated sub-basins' flows because those sub-basins flows are calibrated independently with different techniques and periods with each time the best results being retained for the propagation model, while the simulation of the Paris Austerlitz basin is using the same calibration technique on its whole surface – that includes the 4 sub-basins. This may be one of the limitations of the lumped model.

It can also be seen on figure 4.8 that the first peak in the GR4J-calculated flow at Paris Austerlitz is a bit in advance (1 or 2 days) related to the observed first peak flow. This advance is also visible on figure 4.6 with the flows calculated with the propagation model. As seen above, it seems that this first peak flow corresponds to the arrival of the Yonne peak. In fact since 1910 and the calibration period (1999-2006), 3 locks (one at Saint Mammès, one at Samois-sur-Seine and one at Saint-Fargeau-Pont-Thierry) have been removed from the river between Courlon-sur-Yonne and Paris without any new lock being built. Those removals have thus increased the celerity of the flow between Courlon-sur-Yonne and Paris. As the propagation and the GR4J models are calibrated on periods without those locks, the simulated flows on 1910 will have a higher celerity than the observed flow that were slowed by them.

In conclusion, the errors of simulation that occur on the Marne at Ferté and the Seine at Bazoches sub-basins are propagating so as to prevent the Paris Austerlitz flow's accurate simulation at the very moment when the GR4J model is also failing to reproduce this basin flow. It can thus be thought that those problems that are encountered on those 2 sub-basins are at the origin of the inability of GR4J to replicate the 1910 flood on the whole Paris-Austerlitz basin.

4.7 Conclusion

GR4J has thus shown disappointing results on the whole Paris Austerlitz basin when trying to replicate the 1910 flood. However, the Yonne Courlon's flow perfect replication proves that the problem encountered by GR4J on the Paris Austerlitz basin is not general and that the model is actually able to replicate those flood flow under normal conditions.

The propagation model has proven that the sub-basins measures were consistent with the downstream measures at Paris Austerlitz, and the problem thus seems location-specific. Furthermore, the similarities between the propagation of the errors of simulation on the Marne Ferté and Seine Bazoches sub-basins and the simulation of the Paris Austerlitz basin suggest that the problem could be localized within those 2 basins. In this case some events occurring on those 2 basins would be preventing the model to give accurate results on the whole Paris Austerlitz basin.

This localized problem could be a particular physical process that is not accounted for in the GR4J model and that occurred at some special spot in 1910 or some mistakes in the data related to those sub-basins that are thus replicated in the data of the whole Paris-Austerlitz basin. In any case, this study has reduced the field of research for this problem that now appears location specific.

5 THE FROST HYPOTHESIS

It has been shown in the previous chapters that the problem encountered by GR4J to replicate the 1910 flood is very likely to be caused by some unaccounted process that occured during this period and that GR4J is unable to reproduce. Furthermore, this process has been localized in upstream the stations of the Marne at Ferté and the Seine at Bazoches.

To determine the nature of this "unaccounted" process, many documents from 1910 and later were studied in order to find information about the meteorology and the physical conditions of the soil, the water and the atmosphere. During this study, a Marne water temperature chronicle was found (Fig. 5.1).

It can be seen on figure 5.1 that the drop in water temperature that is observed during the 1910 flood corresponds to the peak flow observed at the Austerlitz station and, more importantly, happens at the precise moment when the observed and simulated flow curves are starting to diverge i.e. when the model starts to encounter problems to replicate the flow.

It has thus been considered that frost could have played a role in the 1910 flood by preventing the water from infiltrating into the soil. The rain water would then have run on this frozen soil – thus getting colder which would explain the drop in water temperature – to reach directly the rivers. Since GR4J has no way to account for frozen soils, this could explain the underestimation of the flow and of the volume of water reaching the outlet of the basin.

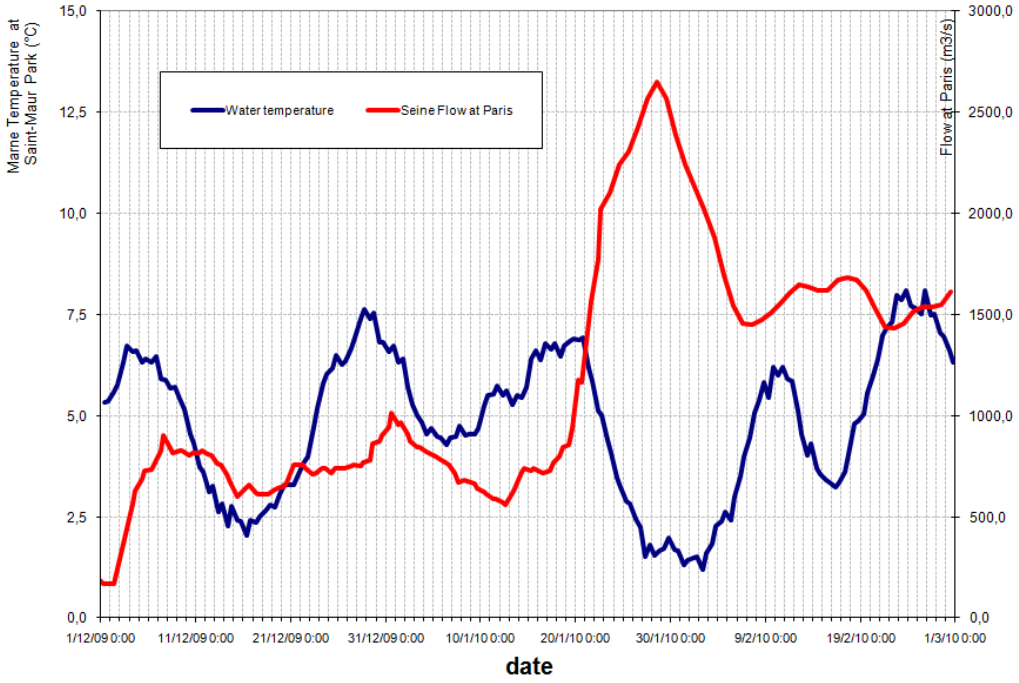

Fig. 5.1 Seine water temperature in 1910 displayed with observed and calculated water flow at Austerlitz

In 1910, on the Paris basin, rivers level and temperature measurements were performed by operators that were noting down the data on paper sheets. On those sheets a special column was dedicated to observations from the operators. If many of them left very few comments, indications about the meteorological conditions during the flood could be found on some of those sheets. Thanks to this, one can now be sure that soil had frozen during several days in December 1909 and January 1910 in at least 2 stations of the basin : Brinon-sur-Beuvron and Damery (see figure 5.1 for their localizations). This means that frost conditions were present during this period and it is thus very probable that soil had frozen on many other parts of the basin.

To test the frost influence on the 1910 flood hypothesis, first it is important to study more in details how frozen ground is formed and how it interact with the hydrological cycle. This chapter will thus give some theoretical background about frost conditions and behaviour. Then a frost module will be developed to be added on the GR4J model based on soil temperatures data. This module will then be tested on the different basins already studied.

5.1Theory of frozen ground

5.1.1 Frost definition and types

Dingman (1976) defines frozen soil as a soil the temperature of which is below 0°C but it does not necessarily mean that all the water contained in that soil is frozen. Indeed, "when soil water freezes, the water closest to soil particles remains in liquid form due to the absorptive and capillary forces exerted by soil particles. This supercooled soil water at subfreezing temperatures is equivalent to a depression of the freezing point." (Niu and Yang, 2006, p.939) where the freezing point is the temperature – normally set to 0°C – at which water is freezing.

Many parameters have an influence on this phenomenon like the water content (Dingman, 1976), the soil type with a freezing point slightly inferior for clayey or organic soils (Dingman, 1976, Zhang et al., 2010) or the soil pores radius : the smaller the pores, the more depressed (i.e. the lower) the freezing point (Roth, 2007).

It is thus possible to find liquid water co-existing with ice in the soil at temperatures well below 0°C. However, according to Lundin (1990) soil water vapour content can be neglected at temperatures below 0°C and the liquid content can be neglected at temperatures below -5°C.

The definition of frozen ground is thus very large and such a soil can have many different aspects – from all water being liquid to all water being solid – with different physical properties. Dingman (1976) suggests a classification between 4 types of frozen soils :

- The granular frost : the soil contains independent ice crystals.
- The honeycomb frost : the ice crystals become connected.
- The concrete frost : the soil is water saturated – and even sometimes oversaturated – and completely frozen. Sometimes ice lenses can be formed.
- The stalactite frost : the soil contains vertical ice needle crystals.
- Finally a 5th type can be added that is the porous concrete frost that is similar to the concrete frost but the soil is permeable to air.

5.1.2 factors influencing frost formation

Of course air temperature and sun radiation are important factors that directly affect the soil temperature and thus the frost formation.

However at the basin scale, other parameters can influence the spatial variation of frost types (Dingman, 1976) :

- The vegetative cover type : frost forms deeper and quicker in bare ground then in brush and fields, then in coniferous forests and finally has its shallowest and slowest formation in hardwood forests.
- The snow cover : it can prevent the frost formation in soil or reduce the frost depth because of its insulating effect. Air temperature influence is thus decreased while the soil is heated by an upward heat flow from the warmer deep soil that can lead to frost thawing.(see e.g. Dingman, 1976, Iwata et al., 2008, Lindstrom et al., 2002).
- Other factors like the soil grain size, its organic and water contents, the litter depth on top of it, the elevation of the water table or the human activities.

5.1.3 frost hydraulic and hydrologic effects

In the different models, water infiltration in the soil can be affected by frost in 3 different manners : it can be restricted (frost is preventing water infiltration, forming an impermeable layer), limited (frost is reducing water infiltration) and unlimited (large infiltration potential due to a large number of air-filled macropores) (Pomeroy et al., 2007, Zhang et al., 2010). In fact it could be observed that stalactite frost was absorbing water while concrete frost is virtually impermeable (equation criterion given by Bloomsberg and Wang, 1970). Other types of frost and especially granular frost will not have any particular effect or will increase infiltration (Dingman, 1976). In the 1910 flood case, the hypothesis is that, due to the frozen ground, rain infiltration was reduced. Thus, only concrete frost appears to be of interest in the new model that is to be developed.

In fact, the frozen ground hydraulic conductivity is dependant on many factors : the soil cover (Dingman, 1976), the soil type (Dingman, 1976, Zhang et al., 2010) or the unfrozen water content – the hydraulic conductivity being reduced by the reduction in liquid water content and an impedance factor related to the presence of ice (Lundin, 1990, Zhang et al., 2010). But other phenomena are taking place when the soil is freezing like the reduction of the water storage (Zhang et al., 2010). Furthermore, the water infiltrating in the soil will have a tendency to freeze causing a reduced infiltration and not being available in the hydrological cycle. But in return, the rain water infiltrating in the soil may cause the thaw of the frost (Dingman, 1976). Finally, frost can also change the structure of the soil – for example it can create cracks – thus changing its hydraulic properties (Lundin, 1990).

5.2 Presentation of the frost modules

The goal was to create a module that could be added to the GR4J model and that would take into account the reduced hydraulic conductivity and thus the reduced infiltration due to concrete frost in the soil. As a consequence of frozen soil definition, it was decided to base those modules on soil temperatures data that would have to be averaged on the whole basin because of the GR4J lumped characteristic. Finally this module should not require more than 2 parameters to calibrate in order to respect GR4J simplicity.

When exploring a new approach Andreassian et al. (2009) recommend that "several models for the same type of prediction" are developed. Two modules were thus created and tested. They are presented in this chapter.

5.2.1 The linear module

The linear module is the simplest choice when trying to represent the reduced infiltration and thus the increased runoff caused by frost conditions. It uses the daily mean soil temperature at a constant depth averaged on the basin surface as input data and modifies the recharge of the production store Ps (see part 2.1.2) according to the equation :

$$Ps = \begin{cases} 0 & if\ T(d) \le T_0 \\ Ps(Pn) & if\ T(d) \ge T_1 \\ Ps\left(Pn \times \left(1 - \frac{T_1 - T(d)}{T_1 - T_0} \right) \right) & if\ T_0 < T(d) < T_1 \end{cases} \quad \text{(Eq. 5.1)}$$

With ;

$$Ps(P) = \frac{X_1 \left[1 - \left(\frac{S_k}{X_1} \right)^2 \right] \tanh\left(\frac{P}{X_1} \right)}{1 + \frac{S_k}{X_1} \tanh\left(\frac{P}{X_1} \right)}$$

Where :

- Ps is the new calculated recharge of the production store on day d, in mm.
- Pn is the net precipitation on day d, in mm.
- T(d) is the mean soil temperature averaged on the basin surface on day d, in °C.
- T_0 is the surface-averaged soil temperature at which the whole basin is supposed to be frozen (soil temperature of total frost), in °C. This is the first parameter of the module.
- T_1 is the surface-averaged soil temperature at which the first particles of ice are being formed in soil (soil temperature of frost beginning), in °C. This is the second parameter of the module.
- The equation Ps(P) is already given in equation 2.1 in part 2.1.2 where the other quantities are described.

The production store recharge is thus reduced when the temperature is below T_1 where it is considered that frost is beginning to form. When temperature reaches T_0 the soil is supposed to be completely frozen and the production store is not recharged anymore. Between those 2 extremes, the quantity of net precipitation available for production store recharge is a linear function of the soil temperature.

All the water that does not get in the production store directly reaches the unit hydrographs and the routing store which is supposed to simulate a direct runoff without infiltration.

The other equations of the GR4J model are kept the same.

5.2.2 The Z&G module

This module is very similar to the linear module : it reduces the recharge of the production store when the daily mean soil temperature averaged on the basin surface is inferior to a temperature at which frost is supposed to begin : T_1. However the net precipitation fraction available for recharge is not a linear function of the soil temperature but its calculation is derived from Zhao and Gray (1997) that experimentally linked infiltration to soil temperature with a simple proportionality relation :

$$INF \propto \left(\frac{273{,}15 - T}{273{,}15} \right)^{-0{,}35} \qquad \text{(Eq. 5.2)}$$

Where :

- INF represents the infiltration capacity of the soil
- T represents the soil temperature, in °C.

This equation, with the power set equal to 0,35, is rather site specific but it could be adapted by adding one parameter. The production store recharge equation thus became :

$$Ps = \begin{cases} Ps(Pn) & if\ T(d) \geq T_1 \\ Ps\left(Pn \times \left(\dfrac{1 - \dfrac{T(d)}{273.15}}{1 - \dfrac{T_1}{273.15}} \right)^{\alpha} \right) & if\ T(d) < T_1 \end{cases} \qquad \text{(Eq. 5.3)}$$

Where :

- Ps is the new calculated recharge of the production store on day d, in mm.
- Pn is the net precipitation on day d, in mm.
- T(d) is the mean soil temperature averaged on the basin surface on day d, in °C.
- T_1 is the basin soil temperature of frost beginning, in °C. This is the first parameter of the module.
- α is the parameterized power in Zhao and Gray 's equation, without unit. This is the second parameter of the module. It is always negative.
- Ps(P) is given in equation 5.1

Here there is no temperature of total frost on the basin and the available water for production store recharge is a power function of the temperature. Otherwise, the Z&G module works exactly like the linear module.

5.3 Test of the new model including frost modules

The 2 modules presented in part 5.2 were tested on the 5 study basins already used in the previous chapters. Those tests routine and their results are presented in this chapter.

5.3.1 Data

All data used in those simulations are summarized in table 5.1.

Daily mean soil temperatures at 10cm depth were available on 11 stations only (data provided by *Meteo France*). For each of the 5 studied basins, those data were averaged on their surface using the inverse distance weighting method just as it was performed for precipitations in 1910 (see appendix 3.1). The only difference is that, in the inverse distance weighting equation (Eq. 3.10), the distances power was set to 1.123 instead of 2 after it was optimized.

5.3.2 Method

On each basin, the excel software was used to run GR4J alone, then GR4J with the linear frost module and finally GR4J with the Z&G frost module. The data were divided in 2 periods of approximately equal length (Period 1 and period 2 see table 5.1). For each one of those tests, GR4J with the frost module was calibrated on one period with validation on the other. The opposite test was then run. One year warm-up was used in each case, thus allowing for the first year of one period to overlap with the last year of the other as this year would not be used in the Efficiency calculation.

For each test, calibration was made by maximisation of the NSE, KGE and KGEmod criteria respectively. Water reservoirs were taken into account on the Marne at Ferté, the Yonne at Courlon and the Seine at Austerlitz basins but not on the Seine at Bazoches basin as data were lacking.

Thus 6 different calibrations were made for each of the models (3 criteria times 2 periods). 4 parameters were calibrated for GR4J (X_1, X_2, X_3 and X_4), 6 for GR4J + linear frost (same like GR4J + T_0 and T_1) and 6 for GR4J + Z&G frost (same like GR4J + α and T_1). For the 2 frost modules, the calibration was restricted by not allowing T_1 to be higher than 10°C as it was assumed that, at this averaged temperature on the basin, no spot could actually be frozen.

In validation, the NSE criterion was calculated first on all the data and then only on winter data i.e. data obtained from November, 16th to March, 15th (included). The goal of this last validation was of course to assess the frost modules effect without taking into account days when frost is very unlikely to happen.

Finally, on the Seine at Paris Austerlitz basin, the same tests were performed but instead of the average soil temperature data, the daily temperatures of the pixel with the coldest annual mean temperature were used as input to the frost modules both in calibration and validation.

5.3.3 Results

Loing at Episy basin :

The mean values of the parameters obtained after the different calibrations on the Loing at Episy basin are presented in table 5.2.

The NSE values obtained in validation on all the data after the different calibration are shown on figure 5.2 and the NSE values obtained in validation on the winter days (November, 16th to March, 15th) are shown on figure 5.3.

Table 5.1 data for frost module tests

Basin	Surface used for conversion of volumetric values (km²)	Data	Periods	Source of the data
Loing at Episy	3 900	Daily mean soil temperature at 10cm depth averaged on the basin surface (°C)	1st Period : from January, 1st 1984 to December, 31st 1996 2nd Period : from January 1st 1996 to July, 31st 2006	*Meteo France*
		Observed Flow (mm/day)		*CEMAGREF*
		Precipitation (mm)		
		Evapotranspiration (mm)		
Marne at Ferté	8 800	Daily mean soil temperature at 10cm depth averaged on the basin surface (°C)	1st Period : from January, 1st 1994 to December, 31st 1998 2nd Period : from January 1st 1998 to December, 31st 2002	*Meteo France*
		Observed Flow (mm/day)		*CEMAGREF*
		Precipitation (mm)		
		Evapotranspiration (mm)		
		Daily volume of the Marne reservoir (millions of m^3)		*Grands Lacs de Seine*
Seine at Bazoches	10 100	Daily mean soil temperature at 10cm depth averaged on the basin surface (°C)	1st Period : from January, 1st 1998 to December, 31st 2003 2nd Period : from January 1st 2003 to July, 31st 2009	*Meteo France*
		Evapotranspiration (mm)		*DIREN*
		Precipitation (mm)		
		Observed Flow (mm/day)	1st Period : from January, 1st 1999 to December, 31st 2003 2nd Period : from January 1st 2003 to July, 31st 2009 (some missing data in 2007 and 2008)	
Yonne at Courlon	10 700	Daily mean soil temperature at 10cm depth averaged on the basin surface (°C)	1st Period : from January, 1st 1984 to December, 31st 1986 2nd Period : from January, 1st 1986 to December, 31st 1988	*Meteo France*
		Observed Flow (mm/day)		*CEMAGREF*
		Precipitation (mm)		
		Evapotranspiration (mm)		
		Daily volume of the Panneciere dam (millions of m^3)		*Grands Lacs de Seine*
Seine at Paris Austerlitz	43 800	Daily mean soil temperature at 10cm depth averaged on the basin surface (°C)	1st Period : from January, 1st 1994 to December, 31st 1998 2nd Period : from January 1st 1998 to December, 31st 2002	*Meteo France*
		Precipitation (mm)		*CEMAGREF*
		Evapotranspiration (mm)		
		Daily volume of the 4 dams (millions of m^3)		*Grands Lacs de Seine*
		Observed Flow (mm/day)	1st Period : from January, 2nd 1995 to December, 31st 1998 2nd Period : from January, 1st 1998 to December, 31st 2002	*CEMAGREF*

Table 5.2 mean values of the different parameters obtained after calibration on the Loing at Episy basin

	GR4J	GR4J + linear frost	GR4J + Z&G frost
X1 (mm)	565	618	622
X2 (mm)	-0.82	-0.92	-0.92
X3 (mm)	43	50	50
X4 (d)	3.5	3.5	3.5
T0 (°C)		-26.7	
T1 (°C)		10.0	10.0
Alpha			-8.22

Marne at Ferté basin

The mean values of the parameters obtained after the different calibrations on the Marne at Ferté basin are presented in table 5.3.

The NSE values obtained in validation on all the data after the different calibration are shown on figure 5.4 and the NSE values obtained in validation on the winter days (November, 16th to March, 15th) are shown on figure 5.5.

Seine at Bazoches basin

The mean values of the parameters obtained after the different calibrations on the Seine at Bazoches basin are presented in table 5.4.

The NSE values obtained in validation on all the data after the different calibration are shown on figure 5.6 and the NSE values obtained in validation on the winter days (November, 16th to March, 15th) are shown on figure 5.7

Yonne at Courlon basin

The mean values of the parameters obtained after the different calibrations on the Yonne at Courlon basin are presented in table 5.5.

The NSE values obtained in validation on all the data after the different calibration are shown on figure 5.8 and as the results were practically the same for the 3 models – the 2 frost modules being inactive, no validation was made on the winter days.

Seine at Paris Austerlitz basin

The mean values of the parameters obtained after the different calibrations on the Seine at Paris Austerlitz basin are presented in table 5.6. The minimum soil temperature cases correspond to the tests that were performed using the temperature of the pixel with the coldest annual mean temperature instead of the temperature averaged on the basin surface in the 2 frost modules

The NSE values obtained in validation on all the data after the different calibration are shown on figure 5.9 and the NSE values obtained in validation on the winter days (November, 16th to March, 15th) are shown on figure 5.10.

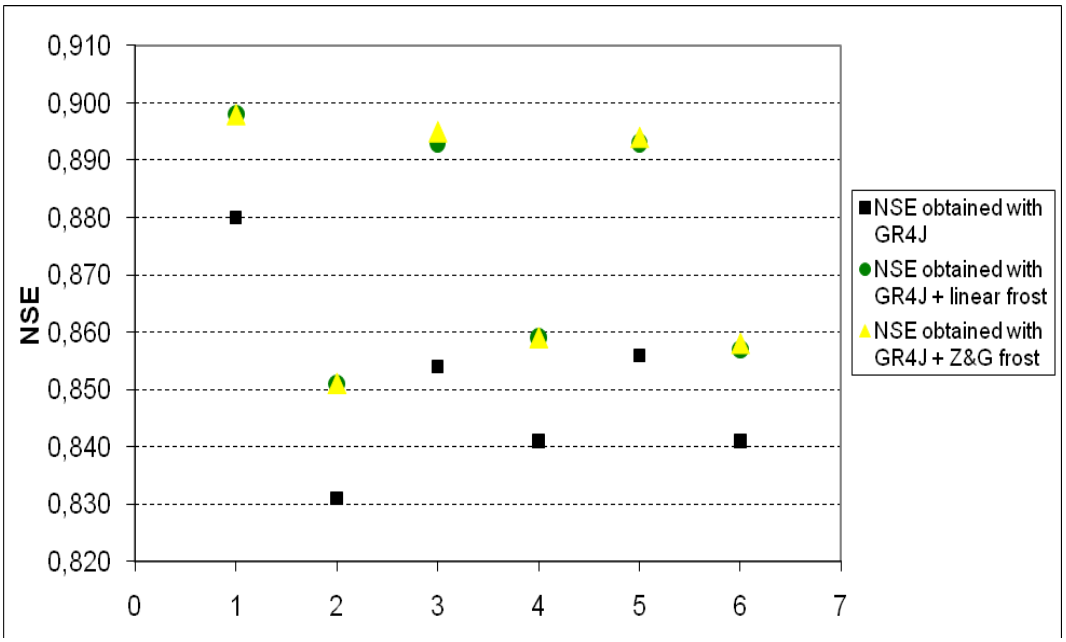

Fig. 5.2 NSE obtained in validation on all the data on the Loing at Episy basin. 1 : calibration NSE period 1 ; 2 :cal NSE per 2 ; 3 : cal KGE per 1 ; 4 : cal KGE per 2 ; 5 : cal KGEmod per 1 ; 6 : cal KGEmod per 2.

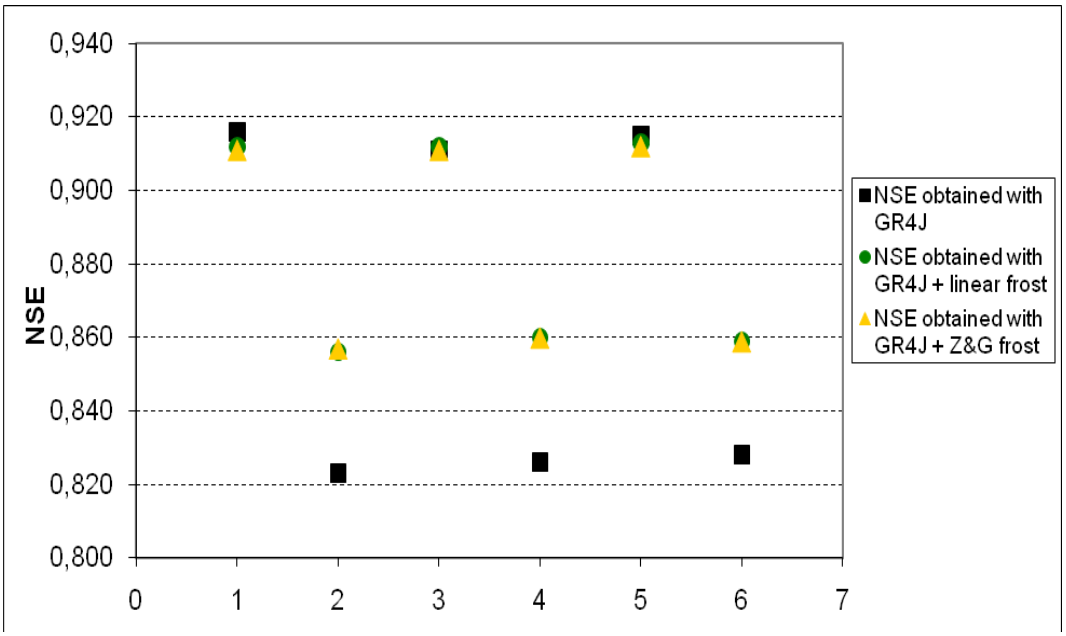

Fig. 5.3 NSE obtained in validation on the winter days on the Loing at Episy basin. 1 : calibration NSE period 1 ; 2 :cal NSE per 2 ; 3 : cal KGE per 1 ; 4 : cal KGE per 2 ; 5 : cal KGEmod per 1 ; 6 : cal KGEmod per 2.

Table 5.3 mean values of the different parameters obtained after calibration on the Marne at Ferté basin

	GR4J	GR4J + linear frost	GR4J + Z&G frost
X1 (mm)	393	444	446
X2 (mm)	-0.78	-0.70	-0.70
X3 (mm)	121	120	121
X4 (d)	7.5	7.5	7.5
T0 (°C)		-55	
T1 (°C)		10.0	10.0
Alpha			-5.11

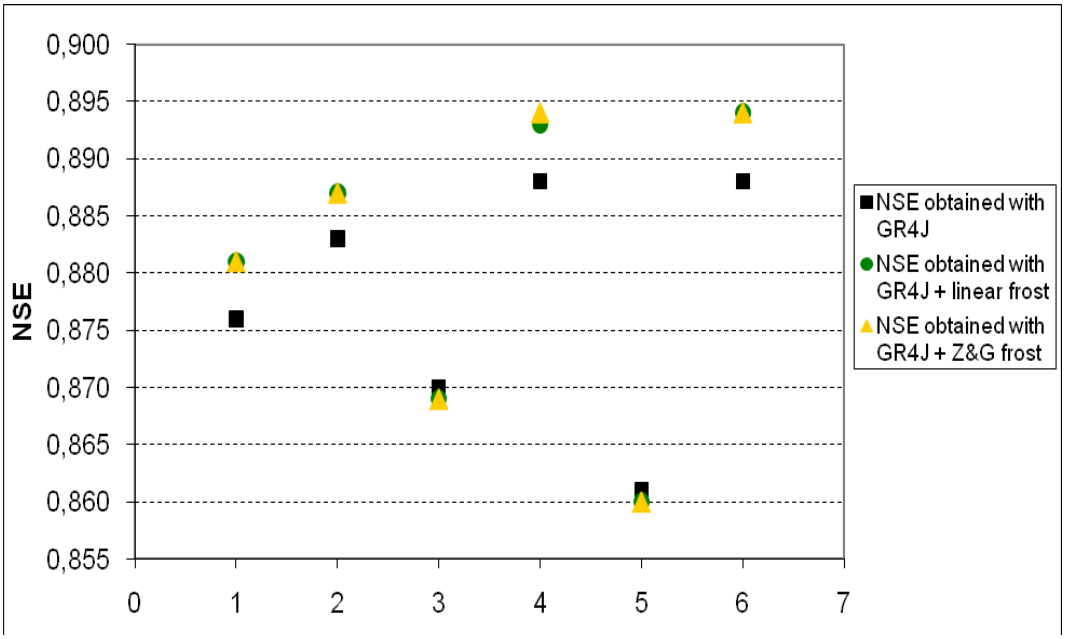

Fig. 5.4 NSE obtained in validation on all the data on the Marne at Ferté basin. 1 : calibration NSE period 1 ; 2 :cal NSE per 2 ; 3 : cal KGE per 1 ; 4 : cal KGE per 2 ; 5 : cal KGEmod per 1 ; 6 : cal KGEmod per 2.

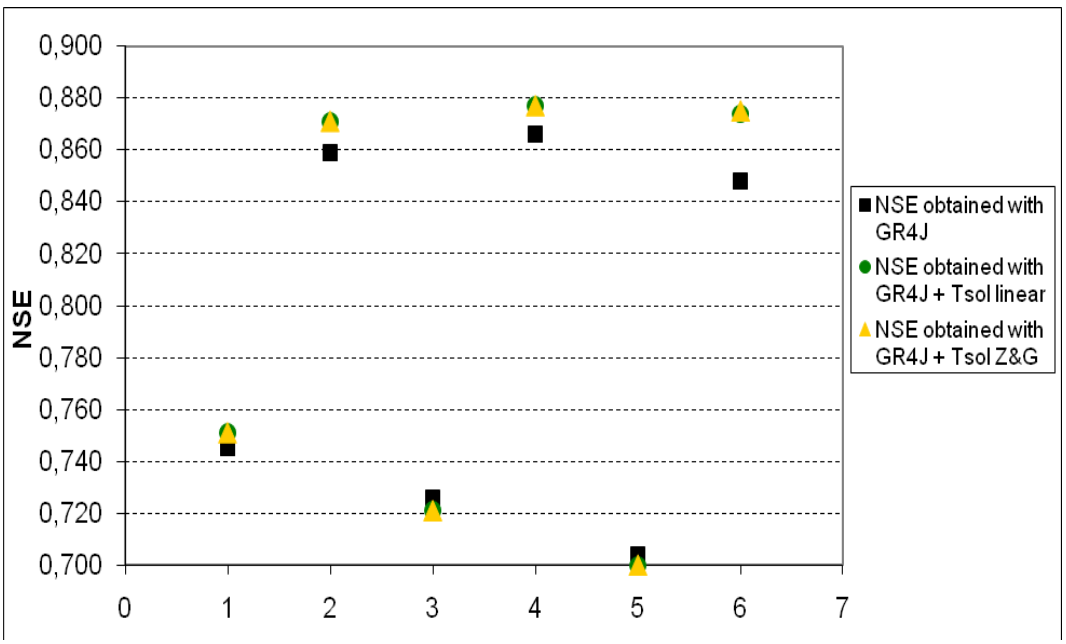

Fig. 5.5 NSE obtained in validation on the winter days on the Marne at Ferté basin. 1 : calibration NSE period 1 ; 2 :cal NSE per 2 ; 3 : cal KGE per 1 ; 4 : cal KGE per 2 ; 5 : cal KGEmod per 1 ; 6 : cal KGEmod per 2.

Table 5.4 mean values of the different parameters obtained after calibration on the Seine at Bazoches basin

	GR4J	GR4J + linear frost	GR4J + Z&G frost
X1 (mm)	475	582	336
X2 (mm)	-0.37	-0.41	-8.98
X3 (mm)	109	134	304
X4 (d)	9.7	9.8	9.4
T0 (°C)		-23.9	
T1 (°C)		10.0	5.1
Alpha			-14.44

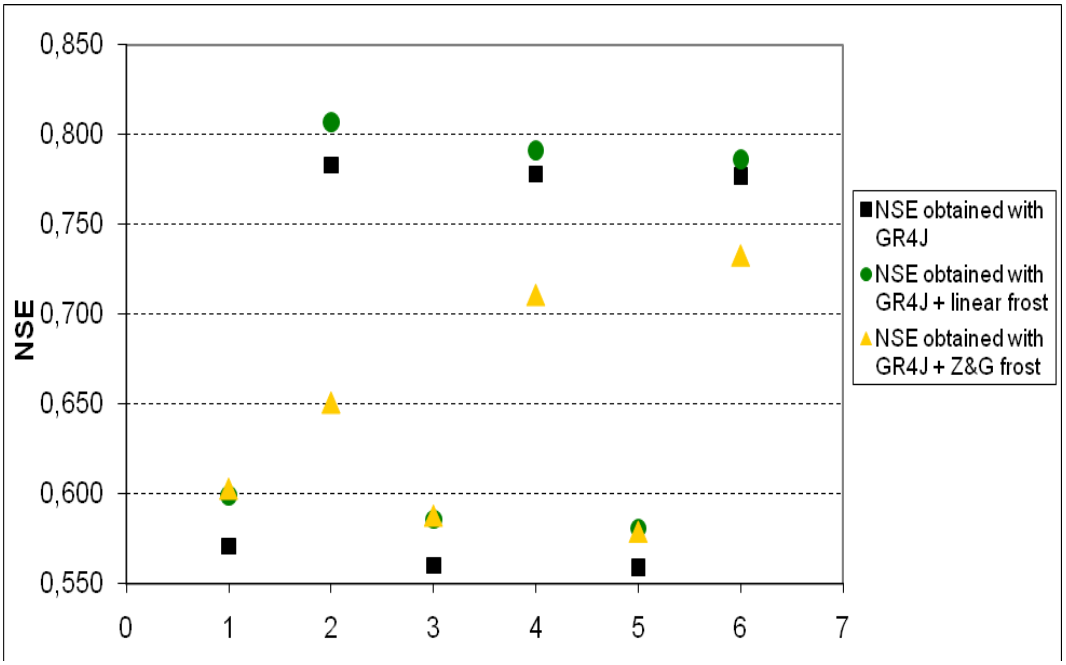

Fig. 5.6 NSE obtained in validation on all the data on the Seine at Bazoches basin. 1 : calibration NSE period 1 ; 2 :cal NSE per 2 ; 3 : cal KGE per 1 ; 4 : cal KGE per 2 ; 5 : cal KGEmod per 1 ; 6 : cal KGEmod per 2.

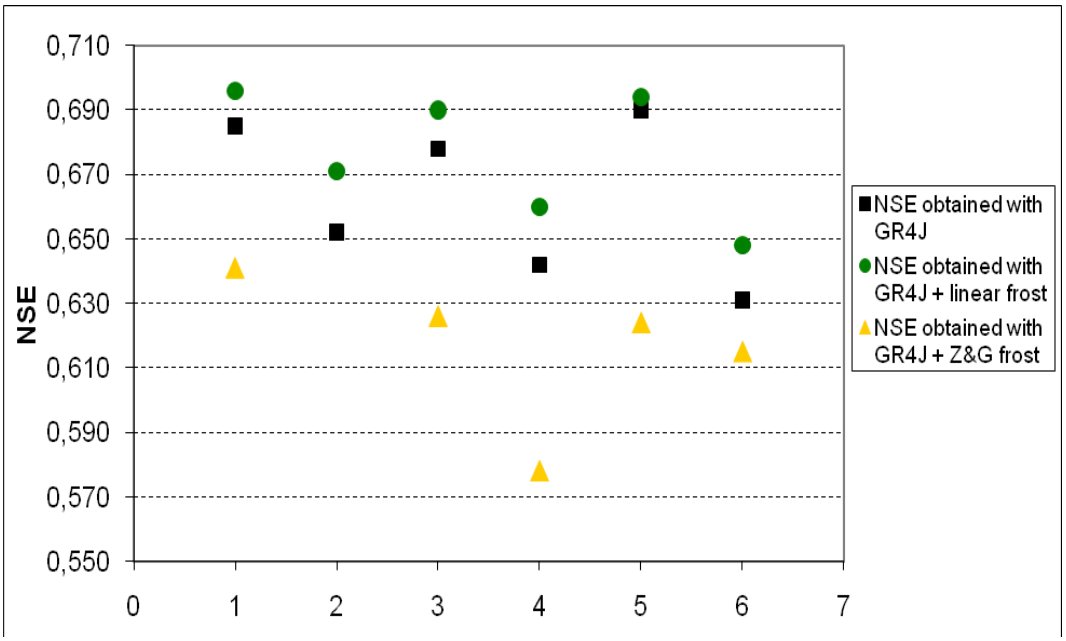

Fig. 5.7 NSE obtained in validation on the winter days on the Seine at Bazoches basin. 1 : calibration NSE period 1 ; 2 :cal NSE per 2 ; 3 : cal KGE per 1 ; 4 : cal KGE per 2 ; 5 : cal KGEmod per 1 ; 6 : cal KGEmod per 2.

Table 5.5 mean values of the different parameters obtained after calibration on the Yonne at Courlon basin

	GR4J	GR4J + linear frost	GR4J + Z&G frost
X1 (mm)	433	433	457
X2 (mm)	0.79	0.79	0.80
X3 (mm)	71	71	72
X4 (d)	4.2	4,2	4,2
T0 (°C)		-58.4	
T1 (°C)		-0.9	8.9
Alpha			-6.11

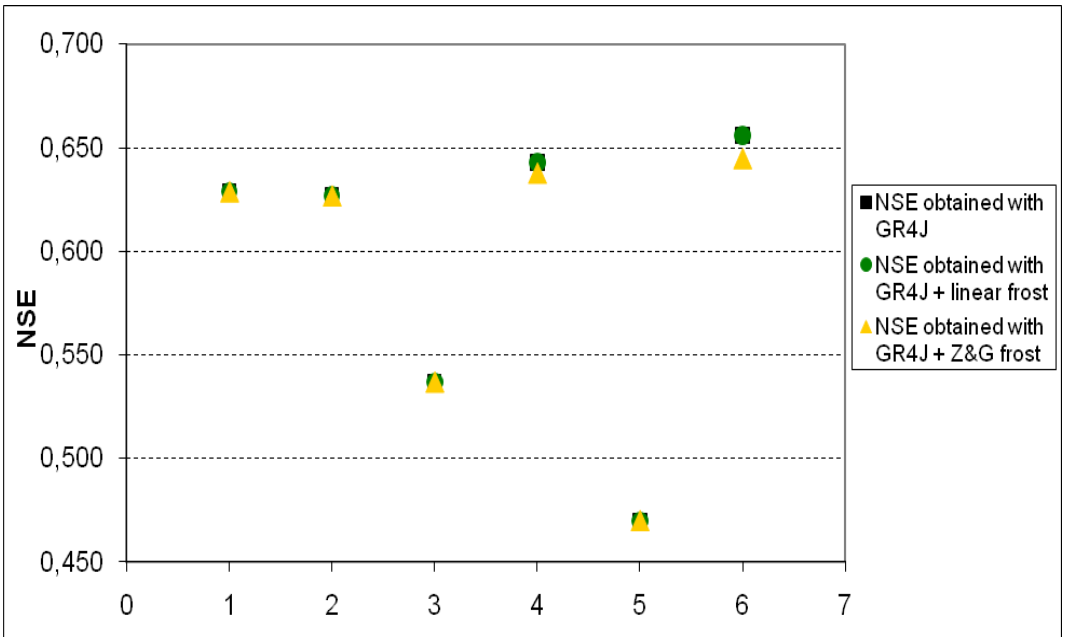

Fig. 5.8 NSE obtained in validation on all the data on the Yonne at Courlon basin. 1 : calibration NSE period 1 ; 2 :cal NSE per 2 ; 3 : cal KGE per 1 ; 4 : cal KGE per 2 ; 5 : cal KGEmod per 1 ; 6 : cal KGEmod per 2.

Table 5.6 mean values of the different parameters obtained after calibration on the Seine at Paris basin

	GR4J	GR4J + linear frost	GR4J + linear frost min soil t°	GR4J + Z&G frost	GR4J + Z&G frost min soil t°
X1 (mm)	553	594	590	587	583
X2 (mm)	0.18	0.16	0.16	0.17	0.16
X3 (mm)	93	101	101	106	106
X4 (d)	4.2	4.3	4.3	3.7	3.7
T0 (°C)		-46.8	-52.9		
T1 (°C)		10.0	10.0	10.0	10.0
Alpha				-4.81	-5.14

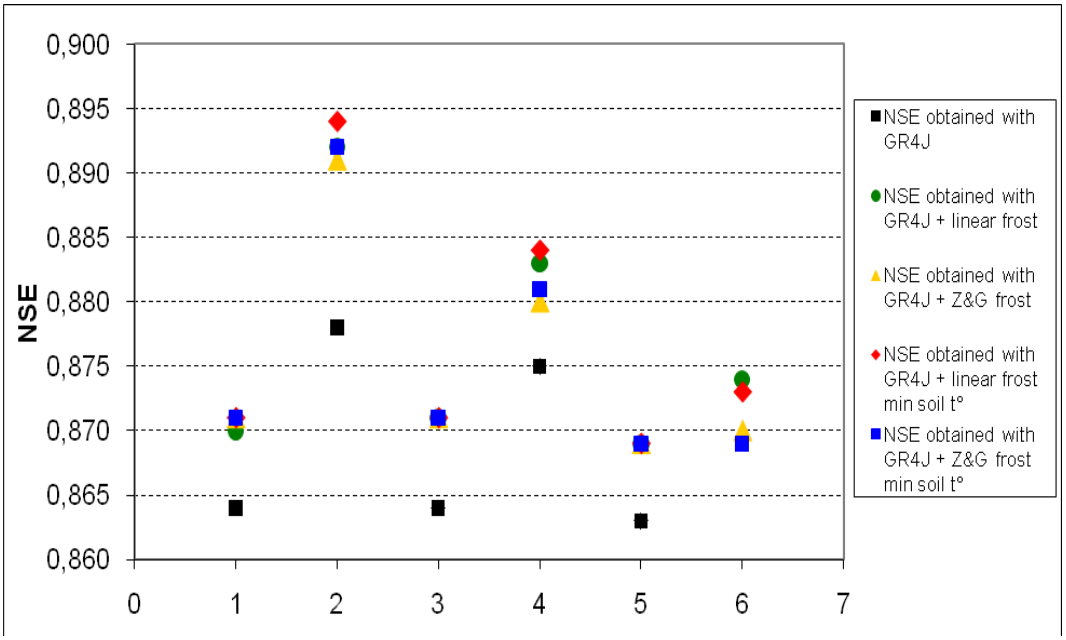

Fig. 5.9 NSE obtained in validation on all the data on the Seine at Paris basin. 1 : calibration NSE period 1 ; 2 :cal NSE per 2 ; 3 : cal KGE per 1 ; 4 : cal KGE per 2 ; 5 : cal KGEmod per 1 ; 6 : cal KGEmod per 2.

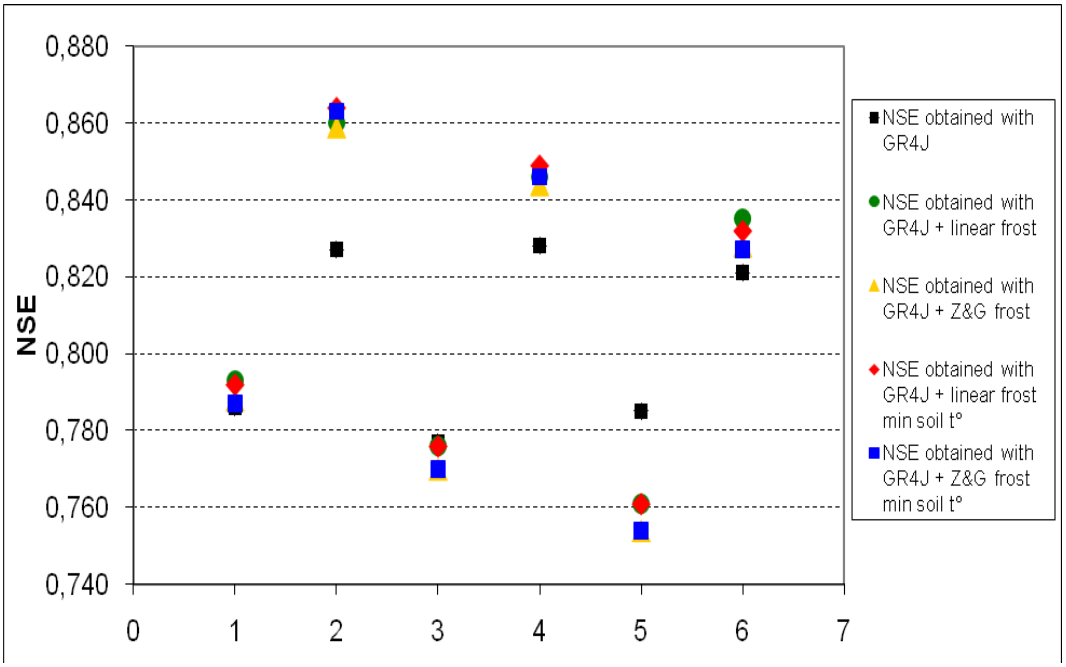

Fig. 5.10 NSE obtained in validation on the winter days on the Seine at Paris basin. 1 : calibration NSE period 1 ; 2 :cal NSE per 2 ; 3 : cal KGE per 1 ; 4 : cal KGE per 2 ; 5 : cal KGEmod per 1 ; 6 : cal KGEmod per 2.

5.3.4 Discussion

The Effects of the frost modules on the GR4J parameters can be seen in tables 5.2, 5.3, 5.4 and 5.6. The production store capacity (X_1) is increased in all those cases - except for the Z&G frost module on the Seine at Bazoches basin (Table 5.4) which is a particular case that will be discussed below. Thus more water will be taken from rain to be brought to this store which is a way for the model to counterbalance the frost modules that are preventing water to integrate this same store. The routing store capacity (X_3) is more stable but can be increased in some cases. No general trend can be drawn for the exchange coefficient (X_2) that is sometimes stable, sometimes increased and sometimes decreased. Finally the frost modules addition does not have any significant consequence on the time basis for UH1 (X_4).

On those same tables (Tables 5.2, 5.3, 5.4 and 5.6) the frost specific parameters behaviour can also be assessed. The frost beginning temperature T_1 is almost always set at its maximum value (10°C) for the 2 frost modules, meaning that the model is integrating as many days as possible within those modules (if the soil temperature is higher than T_1 on one day then the frost modules do not have any effect). Of course there is no ice within a soil at 10°C but this is an average value and it could still be considered that some spots of the basin have a soil temperature below 0°C. Thus this result is not completely artificial. However, in the linear module case, the total frost temperature T_0 is always very low (from – 23°C to – 58°C) : there is of course nothing physical there, it just means that the model attempts to flatten the curve [infiltration/soil temperature] thus not allowing a too harsh variation of the rain fraction available for the capacity store recharge. This is coherent with a very high T_1 value. For the Z&G module, the alpha parameter always gets a very high absolute value compared to Zhao and Gray (1997) empirical result (Eq. 5.2).

One special case is the Z&G module results on the Seine at Bazoches basin (Table 5.4). When the calibration is made on the 2nd period (see table 5.1), the parameters get very unusual values with a production store capacity inferior to 18mm, an exchange coefficient inferior to -13mm and a routing store capacity higher than 420mm (thus far higher than the production store capacity). The temperature of frost beginning T_1 is also very low (inferior to 0.3°C). The results obtained in validation are relatively bad compared to the other models (Fig. 5.6 and 5.7). The reason could be that the software identified a secondary optimum instead of the right optimum. But in any case, it is a clue that the Z&G module can lead to very false results.

But another, more interesting, special case is the Yonne at Courlon basin (Table 5.5 and Fig. 5.8). Here the model has completely cancelled the frost modules effect by putting a low value on the T_1 parameter thus excluding all the data – except for 2 Z&G calibration that did not give better results in validation than GR4J alone (Fig. 5.8). Thus in this basin, the frost modules are completely useless.

The results obtained in validation on all the data are displayed on figures 5.2, 5.4, 5.6 and 5.9. Globally the frost modules are bringing a small increase in the efficiencies obtained, with a maximum raise of the NSE values of 0.02 in the Loing at Episy basin (Fig. 5.2). But in some cases, the results obtained by the 2 modules are very comparable to those obtained by GR4J alone or even worse like for the Marne at Ferté (Fig. 5.4). It can also be seen that the 2 modules are getting very similar results except on the Seine at Bazoches (Fig. 5.6) for the reasons

explained above. Finally, as shown on figure 5.9 the temperature of the coldest pixel is not bringing a significant increase in the model efficiency in validation.

Surprisingly, the validation on winter days (from November, 16th to March, 15th) is not favourable to the frost modules (Fig. 5.3, 5.5, 5.7 and 5.10). The increase in NSE obtained with those modules is less significant for every basin than when the validation is done on every data. There are also more cases of comparable results between the 3 models (GR4J alone, GR4J + linear frost, GR4J + Z&G frost) and in some cases, GR4J alone is even getting better results (see for example figure 5.10). On the Seine at Bazoches basin (Fig. 5.7) it can be seen that the Z&G frost module is giving results far less satisfactory than GR4J alone or the linear module even when calibrated on the 1st period – where the parameters obtained are "normal".

In every case, even the maximum raise of 0.02 in the NSE obtained in validation is not significant enough to justify the addition of 2 parameters to GR4J. Those very poor results may however be coming from the fact that frost is actually very rare in the Seine basin and that too few episodes were happening during the test periods for the modules to be calibrated correctly and to show a real difference in validation. As an example, on the Seine at Austerlitz basin, 3 periods only were identified with a significant number of days with a soil temperature inferior to 2°C in a row. The hydrographs obtained by the 3 models in NSE calibration and the observed rain on those 3 time periods are shown on figures 5.11, 5.12 and 5.13.

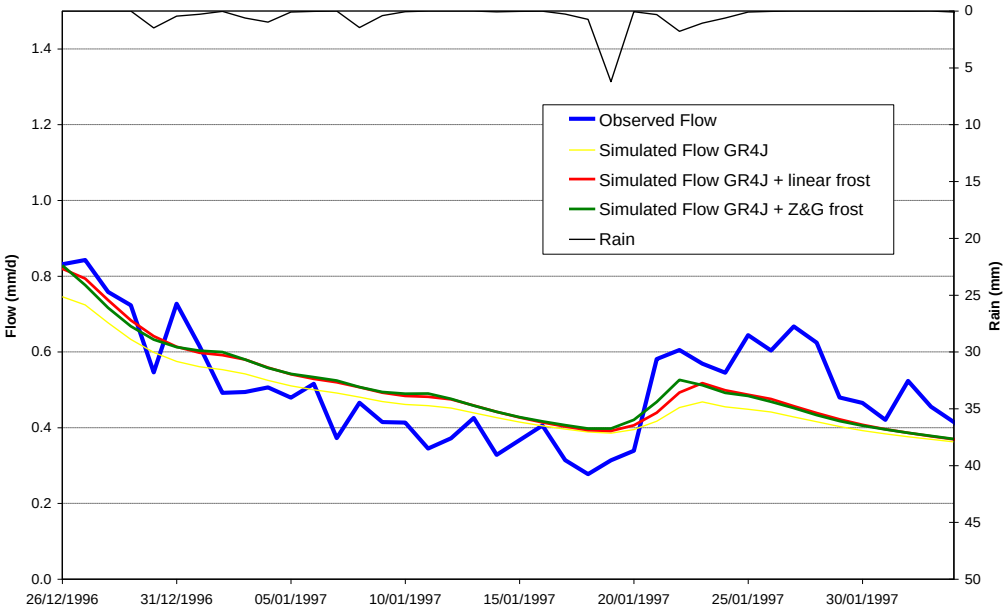

Fig. 5.11 Observed rain and observed and simulated flows with the 3 models in NSE calibration from 26/12/1996 to 03/02/1997.

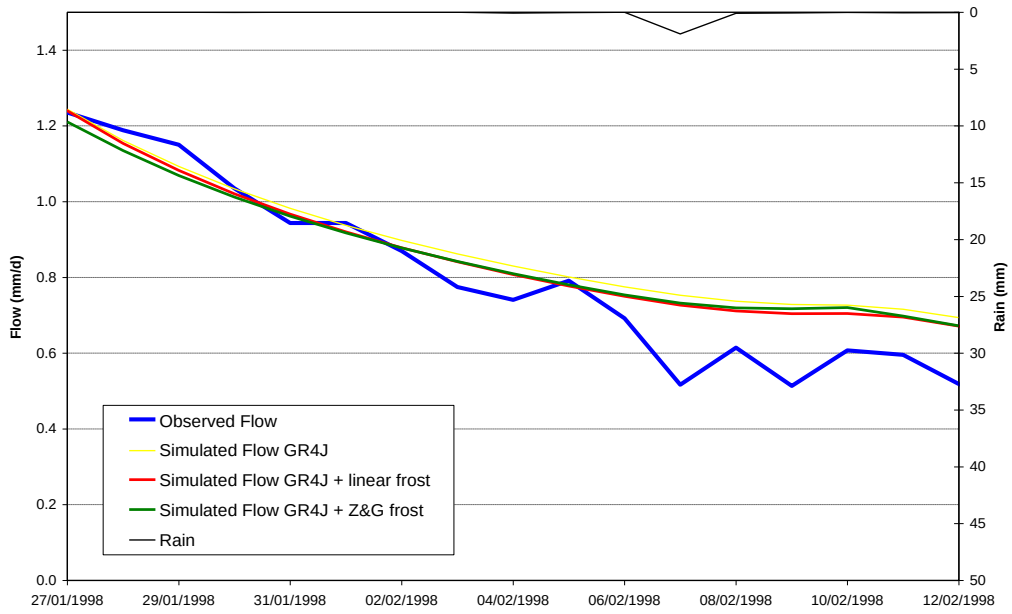

Fig. 5.12 Observed rain and observed and simulated flows with the 3 models in NSE calibration from 27/01/1998 to 12/02/1998

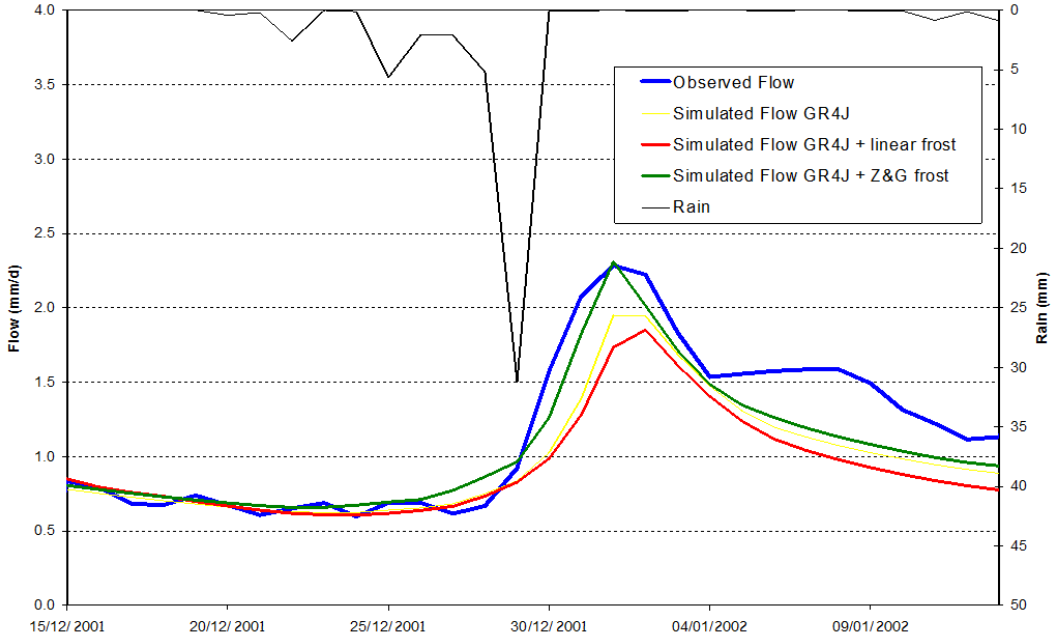

Fig. 5.13 Observed rain and observed and simulated flows with the 3 models in NSE calibration from 15/12/2001 to 13/01/2002

It can thus be seen that on those 3 periods that are the only ones where frost is likely to have formed on a significant part of the basin, it is only during the last one (from December, 15th 2001 to January, 13th 2002, Fig. 5.13) that a significant amount of rain was observed. On the two other periods (Fig. 5.11 and 5.12), even if the soil was frozen, there were no significant rain and thus those data are useless for the frost modules.

Thus on all the data available, only one month in December 2001 – January 2002 is actually of interest for the frost modules which is not enough for them to get calibrated or show a real difference in validation.

So, in the absence of other, more relevant data, it is not possible to conclude on their relative efficiency.

5.4 Conclusion

According to the literature review, frost, and especially concrete frost, could have an impact on the soil infiltration potential, thus increasing the rainwater runoff into the rivers. This phenomenon could have taken place during the 1910 flood and as it is not taken into account in GR4J, it could explain the large difference obtained between observed and simulated flood during this event.

Two soil frost modules were thus presented. They use daily mean temperatures averaged on the surface basin and remove a fraction of the net precipitation from the available water for the production store recharge when the soil is supposed to be frozen in some part of the basin.

Unfortunately, on the Seine basin upstream Paris, frost is a too rare phenomenon for the models to be tested effectively and no definitive conclusion would be drawn after the tests on their efficiency compared to GR4J alone. However, as they are the only tools available, those modules should now be used on the 1910 flood in order to see if they could improve its simulation. The Z&G module was shown to present dangerous interactions during calibration, thus the linear module, which is also simpler and seems to give better results shall be preferred in the next steps.

References

ANDREASSIAN, V., LE MOINE, N., MATHEVET, T., LERAT, J., BERTHET, L. & PERRIN, C. (2009) The hunting of the hydrological snark. *Hydrological Processes,* 23**,** 651-654.

BLOOMSBERG, O. L. & WANG, S. J. (1970) Effect of moisture content on permeability of frozen soils. *Eos: Transactions American Geophysical Union,* 51**,** 205.

DINGMAN, S. L. (1976) HYDROLOGIC EFFECTS OF FROZEN GROUND, Literature Review and Synthesis. *CRREL Special Report (US Army Cold Regions Research and Engineering Laboratory).*

IWATA, Y., HAYASHI, M. & HIROTA, T. (2008) Comparison of snowmelt infiltration under different soil-freezing conditions influenced by snow cover. *Vadose Zone Journal,* 7**,** 79-86.

LINDSTROM, G., BISHOP, K. & LOFVENIUS, M. O. (2002) Soil frost and runoff at Svartberget, northern Sweden - measurements and model analysis. *Hydrological Processes,* 16**,** 3379-3392.

LUNDIN, L. C. (1990) Hydraulic-Properties in an Operational Model of Frozen Soil. *Journal of Hydrology,* 118**,** 289-310.

NIU, G. Y. & YANG, Z. L. (2006) Effects of frozen soil on snowmelt runoff and soil water storage at a continental scale. *Journal of Hydrometeorology,* 7**,** 937-952.

POMEROY, J. W., GRAY, D. M., BROWN, T., HEDSTROM, N. R., QUINTON, W. L., GRANGER, R. J. & CAREY, S. K. (2007) The cold regions hydrological process representation and model: a platform for basing model structure on physical evidence. *Hydrological Processes,* 21**,** 2650-2667.

ROTH, K. (2007) *Soil Physics, Lecture Notes*, Institute of Environmental Physics, University of Heidelberg.

ZHANG, Y., CAREY, S. K., QUINTON, W. L., JANOWICZ, J. R., POMEROY, J. W. & FLERCHINGER, G. N. (2010) Comparison of algorithms and parameterisations for infiltration into organic-covered permafrost soils. *Hydrology and Earth System Sciences,* 14**,** 729-750.

ZHAO, L. T. & GRAY, D. M. (1997) A parametric expression for estimating infiltration into frozen soils. *Hydrological Processes,* 11**,** 1761-1775.

6 SOIL TEMPERATURE MODELS

Knowledge of soil temperature is essential to predict frost formation. Indeed Dingman (1976) defines frozen ground as a soil which temperature is below 0°C – which does not necessarily mean that the water present in this soil has actually frozen (see for example Niu and Yang, 2006, Roth, 2007, Zhang et al., 2010). Soil temperature measurement has thus been at the basis of the modules developed in the previous chapters to simulate the frozen ground effects on the hydrological cycle. To test the frost hypothesis on the 1910 flood, reliable soil temperature data are thus needed.

However, soil temperature is not a routine measurement, and relatively few data exist in France. In particular, there is no measure of soil temperature during the 1910 flood. It has thus been decided to use a model that can reasonably estimate soil temperature from a more accessible input data : air temperature.

After a brief description of the different types of models found in the literature and the factors they use to derive soil temperature from air temperature, the 4 different models that were chosen to be used with GR4J will be described. Comparative tests between those 4 models have been performed on 11 stations, the results will be presented and discussed in a third part.

6.1 Modeling soil temperature

6.1.1 Factors influencing the soil temperature

Many factors have an influence on soil temperature. Williams and Gold (1977) have suggested a classification of those factors into three main categories :

- Meteorological variables, like sunshine, air temperature, wind and precipitation,… and particularly the changes in these conditions (see e.g. Bocock et al., 1977, Roth, 2007, Zhang et al., 2005). The sun (sunshine period duration, sun position) appears to be one of the most important factor (Williams and Gold, 1977). It is often represented in the models by terms in $\sin(\omega d)$ or $\cos(\omega d)$ with d the day of the year (from 0 to 365) and $\omega=2\pi/365$ (see e.g. Paul et al., 2004, Plauborg, 2002, Roodenburg, 1985). Those terms are also used to represent the annual cycles of air and soil temperatures (Hasfurther and Burman, 1974).
- Ground variables, like snow cover, soil type, vegetation,… In particular snow has a great influence on soil temperature and soil-atmosphere coupling because of its insulating effect (Isard and Schaetzl, 1995, Lindstrom et al., 2002, Zhang et al., 2005).
- Underground variables, like the deep soil temperature,…

It is not possible to measure all these variables, but they are often more or less linked together or can compensate each-other and a model taking only a few factors into account – like e.g. the air temperature - can get relatively good results (Hasfurther and Burman, 1974, Williams and Gold, 1977).

Finally, soil temperature has a larger variability toward soil surface with meteorological and ground variables having a highest influence. At deeper horizons, this influence diminishes (the atmosphere-soil coupling is weaker) and the soil temperature varies less (Williams and Gold, 1977). Some model thus take explicitly into account the depth at which the temperature is to be estimated with a propagation function and

distinguish soil surface temperatures –which are still different from air temperatures (Thunholm, 1990) – and temperatures at given depths (see e.g; Gupta et al., 1981, Li and Koike, 2003, Wang et al., 2010).

In this study, only the most accessible variables can be used, like precipitation, air temperature or the day of the year. The availability of the necessary data will thus constitute the limiting factor in the choice between the different models existing in the literature.

6.1.2 The different models

Isard and Schaetzl (1995) give a classification of the different soil temperature prediction models :

- Models based on physics (see e.g. Guaraglia et al., 2001, Li and Koike, 2003, Thunholm, 1990, Wang et al., 2010). They often use energy balance and mass and heat flows equations to model the soil temperature and its evolution. They use a lot of parameters like soil hydraulic conductivity, soil water and vapour content that are difficult to measure. Finally, they often divide the soil into different layers or the area into different parts. They are thus very site specific and not suited to get integrated in a daily lumped model like GR4J.
- Models based on statistics (see e.g. Bocock et al., 1977, Gupta et al., 1981, Gupta et al., 1982, Paul et al., 2004, Plauborg, 2002, Roodenburg, 1985). They are more general and can thus be applied to many different sites. They are not explicitly based on physics but on statistical correlations between soil temperatures and other simple factors like e.g. air temperature. They are also less data demanding but they use parameters that need to be calibrated. In the frame of this study, this kind of model seems more suited.

If a model is to be created, it has to be robust and to involve as few parameters to calibrate as possible just like GR4J. Despite their help in understanding the different processes involved in the soil temperature changes, no models based on physics could meet those requirements and all the selected models were based on statistics.

6.2 Selected models

6.2.1 Bocock model

This model was adapted from Bocock et al. (1977) who presented 6 different models for soil temperature estimation and compared their performance in calibration-validation tests run at different stations and for 2 different depths (0 cm and 50 cm). The 6 models were all based on statistical correlations between soil temperatures and other climatic variables, mostly air temperature.

The first model presented in Bocock et al. (1977) is a linear regression linking soil and air temperatures. The model appears to be very simple but obtains relatively poor results in validation and thus was not chosen for integration in GR4J.

The second model is a multiple regression based on 14 different factors taking into account the air temperature, the solar radiation, the day length, the wind, the precipitation and the humidity. Only some of those factors proved to be of some importance after calibration – but the important factors were not all the same for the 2 depths of investigation. Despite relatively good results, the important number of input data and of parameters to calibrate was preventing the use of this model for integration in GR4J.

The four last models were based on harmonics. In calibration, air and soil temperatures are approximated by harmonics. According to Bocock et al. (1974), 90% of the variability is taken into account with only the fundamental harmonic (1st harmonic). Only this first harmonic was thus used in order to reduce the number of parameters to calibrate. The formula is given by Bocock et al. (1974) :

$$T_{harmo,k}(d) = C_k + A_k \sin\left(\frac{2\pi d}{365} + \varphi_k\right) \quad \text{(Eq. 6.1)}$$

Where :

- $T_{harmo}(d)$ is the approximated temperature at day d (in °C)
- C is the constant, a parameter to calibrate (in °C)
- A is the amplitude of the harmonic, a parameter to calibrate (in °C)
- d is the day of the year (between 0 and 365)
- φ is the phase of the harmonic, a parameter to calibrate (in rad.)
- the suffix k stands for air or soil.

Thus there are two times 3 parameters to calibrate to get those harmonics for air and soil temperatures but the 2 calibrations are completely independent.

Then, still in calibration, the deviation between the observed and the harmonic values of the air and soil temperatures can be calculated as follow :

$$D_k(d) = T_{obs,k}(d) - T_{harmo,k}(d) \quad \text{(Eq. 6.2)}$$

Where :

- D(d) is the temperature deviation at day d (in °C)
- $T_{obs}(d)$ is the observed temperature at day d (in °C)
- $T_{harmo}(d)$ is the temperature approximated by harmonics at day d (in °C)
- the suffix k stands for air or soil

Finally, in calibration, a regression analysis of soil temperature deviation on air temperature deviation is performed. The four last models present different type of regression at this step. Only the 3rd and 6th models were chosen as they are the ones giving the best results.

In the 3rd model, the regression formula is given by equation 6.3 :

$$D_{soil}(d) = X_0 + X_! \times D_{air}(d) + X_2 \times D_{air}(d)^2 \quad \text{(Eq. 6.3)}$$

Where :

- $D_{soil}(d)$ and $D_{air}(d)$ are the temperature deviations at day d (in °C)
- X_0, X_1 and X_2 are parameters to calibrate.

In the 6th model, the air temperature of the previous day is taken into account and the regression formula is given by equation 6.4 :

$$D_{soil}(d) = Y_0 + Y_1 \times D_{air}(d) + Y_2 \times D_{air}(d-1) \quad \text{(Eq. 6.4)}$$

Where :

- $D_{soil}(d)$ and $D_{air}(d)$ are the temperature deviations at day d (in °C)
- Y_0, Y_1 and Y_2 are parameters to calibrate.

Whether it is the 3rd or the 6th model that is used, there are 3 more parameters to calibrate independently of the two times 3 parameters to calibrate for the harmonics (the 3 calibrations are done one after the other).

In validation, the same harmonic is taken for air temperatures (Eq. 6.1) with the parameters obtained in calibration but the deviation is calculated against the temperatures observed during the validation period.

Using equation 6.3 or equation 6.4 with the calibrated parameters, the soil temperature deviations during the validation period can be estimated. Then the soil temperature can be calculated by adding the estimated deviations to the harmonic obtained with the calibrated parameters as described in equation 6.5 below :

$$\begin{cases} T_{soil,calc}(d) = C_{soil} + A_{soil} \sin\left(\dfrac{2\pi d}{365} + \varphi_{soil}\right) \\ \qquad + \begin{cases} X_0 + X_! \times D_{air}(d) \\ \quad + X_2 \times D_{air}(d)^2 \quad (\text{mod}.3) \\ Y_0 + Y_1 \times D_{air}(d) \\ \quad + Y_2 \times D_{air}(d-1) \quad (\text{mod}.6) \end{cases} \\ D_{air}(d) = T_{obs,air}(d) - \left[C_{air} + A_{air} \sin\left(\dfrac{2\pi d}{365} + \varphi_{air}\right) \right] \end{cases} \quad \text{(Eq. 6.5)}$$

Where :

- $T_{soil,calc}(d)$ is the calculated soil temperature at day d (in °C)
- C_{soil}, A_{soil} and φ_{soil} are the parameters for the soil harmonic, calculated in calibration
- d is the day of the year
- X_0, X_1 and X_2 are the parameters for the regression of soil temperature deviation on air temperature deviation for model 3, and calculated in calibration
- Y_0, Y_1 and Y_2 are the parameters for the regression of soil temperature deviation on air temperature deviation for model 6, and calculated in calibration
- $T_{obs,air}(d)$ is the observed air temperature at day d (in °C)
- C_{air}, A_{air} and φ_{air} are the parameters for the air harmonic, calculated in calibration

6.2.2 Paul et al. model

This model is an adaptation of the much more complex model described by Paul et al. (2004). It is based on equation 6.6 that gives the soil temperature :

$$T_{soil}(d) = M_{soil} + A_{soil}\sin\left(\frac{2\pi(d - d_{ref})}{365}\right) - D_{soil}(d) \qquad \text{(Eq. 6.6)}$$

Where :

- $T_{soil}(d)$ is the soil temperature at day d (in °C)
- M_{soil} is the annual mean soil temperature (in °C)
- A_{soil} is the annual amplitude of the soil temperature (in °C)
- $D_{soil}(d)$ is the daily fluctuation of soil temperature at day d (in °C)
- d is the day of the year (from 0 to 365)
- d_{ref} is the reference day for the calculation of the harmonic

M_{soil}, A_{soil} and D_{soil} are calculated using the air temperature data. First, an harmonic form with fluctuations is applied to the air temperature as described in equation 6.7 :

$$T_{air}(d) = M_{air} + A_{air}\sin\left(\frac{2\pi(d - d_{ref})}{365}\right) - D_{air}(d) \qquad \text{(Eq. 6.7)}$$

Where :

- $T_{air}(d)$ is the air temperature at day d (in °C)
- M_{air} is the annual mean air temperature that is directly calculated (in °C)
- A_{air} is the annual amplitude of the air temperature that has to be calibrated (in °C)
- $D_{air}(d)$ is the daily fluctuation of air temperature at day d (in °C)
- d is the day of the year (from 0 to 365)
- d_{ref} is the reference day for the calculation of the harmonic that has to be calibrated and that is the same for soil temperature harmonic.

Then we have :

$$M_{soil} = M_{air} \times f_M \qquad \text{(Eq. 6.8)}$$

$$A_{soil} = A_{air} \times f_A \qquad \text{(Eq. 6.9)}$$

$$D_{soil} = D_{air} \times f_D \qquad \text{(Eq. 6.10)}$$

Where :

- f_M, f_A and f_D are parameters that are to be calibrated

In calibration, the mean air temperature is calculated and the air amplitude and reference day are then calibrated against the observed values. Then the daily air fluctuations can be calculated for every day.

Finally, f_M, f_A and f_D are calibrated in order to maximise the efficiency calculated on the soil temperature values.

In validation, the mean air temperature is re-calculated on the new time period, the air amplitude and reference day are re-calibrated and new fluctuations can then be calculated. Equations 6.6, 6.8, 6.9 and 6.10 are then used to estimate the soil temperature values using the calibrated values of f_M, f_A and f_D.

There are thus 2 parameters to calibrate for the air harmonics and then 3 parameters to calibrate to calculate the mean, the amplitude and the fluctuations of soil temperatures. Those 2 calibrations are performed separately.

Like the Bocock model, the Paul model is transforming the air and soil temperatures into harmonics. However, in the Bocock model, the link between the 2 harmonics is calibrated only on the deviations or fluctuations while in the Paul model, the mean, the amplitude and the fluctuations for the soil temperatures are functions of the mean, the amplitude and the fluctuations for air temperatures.

6.2.3 Plauborg model

This model excerpted from Plauborg (2002) is the simplest of the 4 presented in this study. It is based on a single equation giving the soil temperature function of the day of the year and of the air temperature :

$$\begin{aligned} T_{soil}(d) = {} & \alpha_0 + \alpha_1 T_{air}(d-2) + \alpha_2 T_{air}(d-1) + \alpha_3 T_{air}(d) \\ & + \beta_1 \sin\left(\frac{2\pi}{365} d\right) + \beta_2 \sin\left(2 \times \frac{2\pi}{365} d\right) \\ & + \delta_1 \cos\left(\frac{2\pi}{365} d\right) + \delta_2 \cos\left(2 \times \frac{2\pi}{365} d\right) \end{aligned} \qquad \text{(Eq. 6.11)}$$

Where :

- $T_{soil}(d)$ is the calculated soil temperature at day d (in °C)
- $T_{air}(d)$ is the observed air temperature at day d (in °C)
- d is the day of the year (from 0 to 365)
- α_0, α_1, α_2, α_3, β_1, β_2, δ_1 and δ_2 are parameters that must be calibrated

There are 8 parameters to calibrate for the complete model and this may seem too much in front of the 4 parameters used in GR4J. However, Plauborg (2002) notes that some of those parameters can be removed – i.e. set to 0 – resulting in a small loss of efficiency of the model.

In this study, the complete model will be called Plauborg 8 parameters. By removing the term in $T_{air}(d-2)$ in equation 6.11 – i.e. $\alpha_1 = 0$ – a new model is created with 7 parameters that will be called Plauborg 7 parameters. From Plauborg 8 parameters, by removing the 2 harmonic terms in $2 \times \frac{2\pi}{365} d$ - i.e. $\beta_2 = \delta_2 = 0$ - a new model is designed with 6 parameters that will be called Plauborg 6 parameters. Finally, from Plauborg 8 parameters, by removing those 3 terms – i.e. $\alpha_1 = \beta_2 = \delta_2 = 0$ – a new model with 5 parameters appears that will be called Plauborg 5 parameters.

6.2.4 Lindström et al. model

This last model is a simplification of the one presented in Lindstrom et al. (2002). It is the only one taking the snow cover depth into account. It is based on a single equation :

$$T_{soil}(d) = (1 - w_A - w_D)T_{soil}(d-1) + w_A T_{air}(d) + w_D T_D \quad \text{(Eq. 6.12)}$$

With :

$$w_A = \frac{1}{m + k_S d_S(d)} \quad \text{(Eq. 6.13)}$$

Where :

- $T_{soil}(d)$ is the calculated soil temperature at day d (in °C)
- $T_{air}(d)$ is the observed air temperature at day d (in °C)
- $d_S(d)$ is the observed snow depth at day d (in cm.)
- T_D is the deep soil temperature. This constant can be measured but in this study it has been considered a parameter to calibrate (in °C)
- w_D is the deep soil temperature weight, a parameter to calibrate
- m and k_S are parameters to calibrate

This model is thus using 4 parameters that are to be calibrated. It is very different from the other models, as it is not taking into account the sunshine nor the sinusoidal shape of the soil temperature evolution during the year (no term in $\sin\left(\frac{2\pi}{365}d\right)$). However, it is the only model taking into account the snow depth – that can have a large influence as seen in part 6.1.1 – the deep soil temperature and the previous day's soil temperature. Of course, the use of the previous day's temperature necessitates a small warm-up period at the beginning as the first day's temperature will be set arbitrarily. For this day –and every day after a gap in the data preventing calculation of the previous day's temperature – the temperature was calculated as follow :

$$T_{soil}(d) = (1 - w_A - w_D)\frac{T_{air}(d) + T_D}{2} + w_A T_{air}(d) + w_D T_D \quad \text{(Eq. 6.14)}$$

Where the terms of the equation are the same as in equations 6.12 and 6.13.

6.3 Testing the models

Tests have been run on different stations to evaluate the accuracy of the different models. As the main goal is to model low temperatures, some tests were specifically calculating models' efficiencies on days when the observed soil temperatures were strictly inferior to 1°C.

6.3.1 Data

All the data were provided by *Meteo France*.

Air temperatures and soil temperatures at 10 cm depth were available on 11 stations of the Seine basin. On each one of those stations, two periods of time have been identified where enough data were available – i.e. no more than 1 missing value for air and soil temperatures per month. On each of those periods, the number of days with available soil temperatures and the number of days with available soil temperatures

strictly inferior to 1°C have been counted. The results are presented in table 6.1.

In table 6.1, the stations with at least one period with less than 50 days of observed soil temperature inferior to 1°C (that will be called days with Tobs<1°C) have been coloured in grey. Those stations will not be used for any test calibrating or calculating efficiencies (in validation) on days with Tobs<1°C because there is not enough data for the test to be reliable.

Table 6.1 Periods of data used for each station, with number of soil temperatures and soil temperatures <1°C

Station code	Period	Number of days with soil temperature data at 10cm depth	Number of days with soil temperatures at 10cm depth < 1°C
2320001	1984-1992	3288	174
2320001	1993-2000	2919	60
10030001	1988-1992	1827	53
10030001	1993-1997	1823	4
21473001	1984-1988	1827	132
21473001	1989-1992	1459	80
51183001	1989-1994	2190	70
51183001	1995-2000	2183	56
52448001	1991-1993	1093	74
52448001	1994-1996	1096	19
58062001	1995-1999	1824	36
58062001	2000-2003	1460	44
58160001	1996-2000	1826	27
58160001	2001-2005	1825	7
75114001	1984-1986	1096	55
75114001	1987-1988	731	25
77306001	1989-1997	3278	116
77306001	1998-2006	3280	102
78621001	1996-2002	2552	42
78621001	2003-2009	2553	13
89346001	1996-1998	1095	33
89346001	1999-2001	1095	9

Snow depth data were available on the same 11 stations. However, there were lots of missing data that have been replaced by a value of 0 cm of snow. Even without taking those missing data into consideration, for each one of the stations, it could be noticed that there were very few days where a snow cover was reported which could be a problem for the Lindström model to which snow depth was a major input data. This is due to the fact that snow is not a current phenomenon in this part of France.

6.3.2 Method

The Fortran software was used to run the different tests. For every model, all the parameters were calibrated using the NSE criterion.

In the first test, the calibration was made by calculation of the Nash-Sutcliffe Efficiency on all the available data. In validation, 8 indicators were calculated :

- NSE on all the available data
- Maximum difference – in absolute value - between observed and calculated soil temperatures using all the data.
- Mean difference – in absolute value – between observed and calculated soil temperatures using all the data.
- NSE calculated only on days with Tobs<1°C (i.e. with an observed soil temperature strictly inferior to 1°C).
- Maximum difference – in absolute value - between observed and calculated soil temperatures using only data from days with Tobs<1°C.
- Mean difference – in absolute value – between observed and calculated soil temperatures using only data from days with Tobs<1°C.
- Maximum difference – in absolute value - between observed and calculated soil temperatures using only data from days with Tcalc<1°C (i.e. with a calculated soil temperature inferior to 1°C)..
- Mean difference – in absolute value – between observed and calculated soil temperatures using only data from days with Tcalc<1°C.

The 3 indicators calculated on days with Tobs<1°C are particularly useful because those days are the ones of particular interest as frost is likely to be formed. It is thus important to have an error as small as possible on the calculated temperature because this temperature will be at the basis of the frost module that will be added to GR4J. Those indicators were calculated only on the stations appearing in white in table 6.1 as there were not enough data on the others for the calculation to be reliable.

The 2 last indicators are calculated on days with Tcalc<1°C. They are also of interest because, on those days, it is likely that the model will predict frost that may not happen in the reality if there is a too large error between observed and calculated temperatures.

In a second test, the calibration was made by maximisation of the NSE criterion calculated only on the days with Tobs<1°C. The aim was to allow for a better efficiency of the models on those days that are the only ones of interest. However in Bocock and Paul models, the calibrations of the harmonic were still made using all the data. The same 8 indicators were calculated in validation.

6.3.3 Results

As a first example, a graph showing the observed temperatures and the calculated temperatures in validation with the different models on station 77306001 with calibration on all the data on the period from January, 1st 1989 to December, 31st 1997 is displayed on figure 6.1.

Similarly, on figure 6.2 is displayed the graph showing observed and calculated soil temperatures on station 77306001 with calibration only on days with Tobs<1°C on the period from January, 1st 1989 to December, 31st 1997.

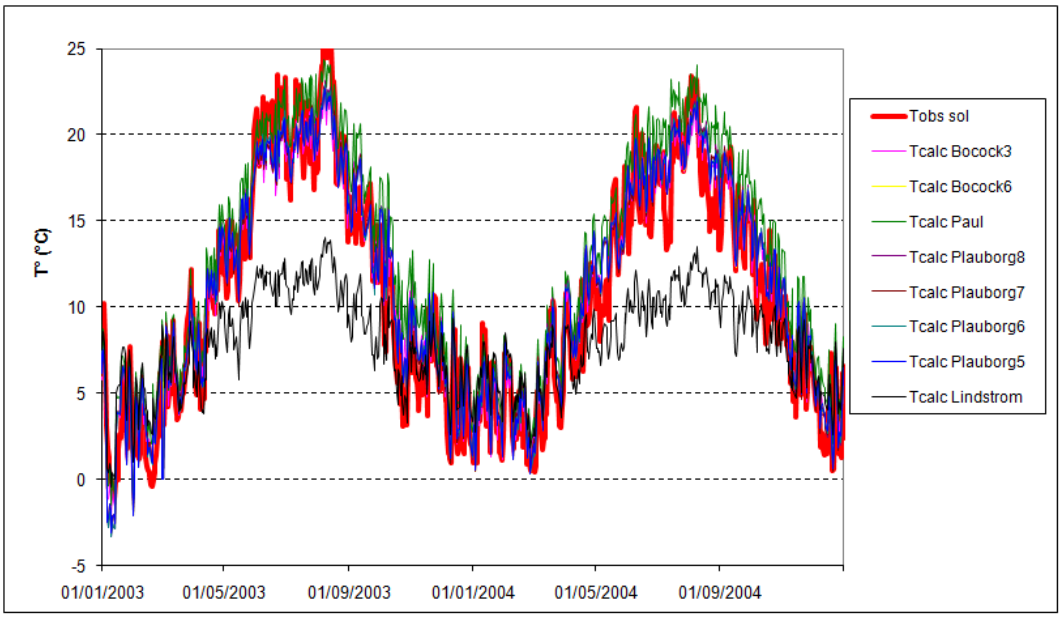

Fig. 6.1 observed and calculated soil temperatures at station 77306001 with calibration on all the data on the period 1989-1997

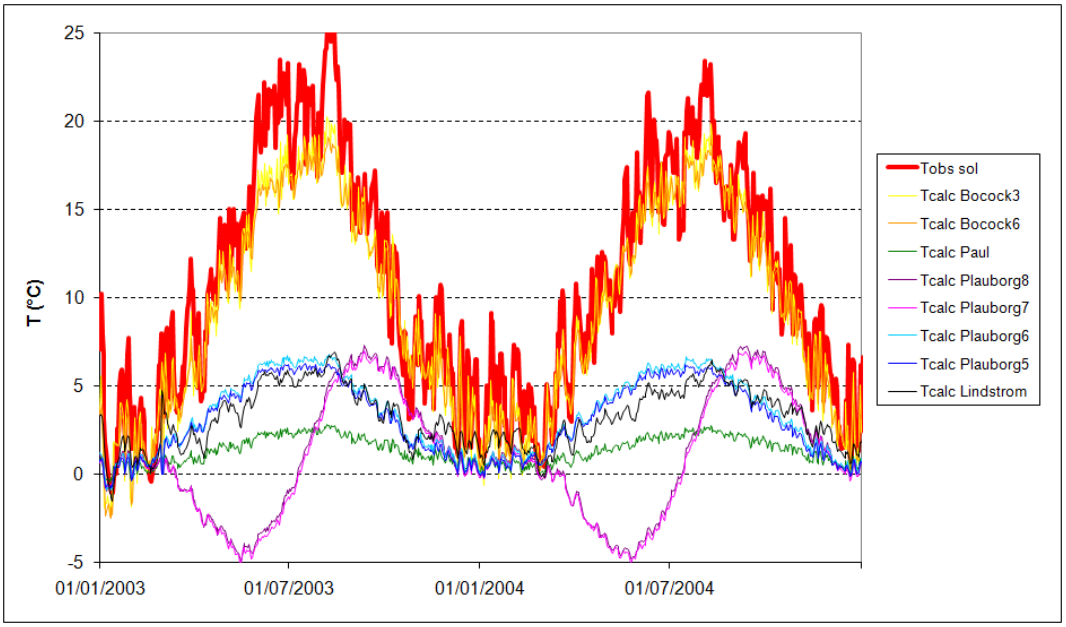

Fig. 6.2 observed and calculated soil temperatures at station 77306001 with calibration on days with Tobs<1°C on the period 1989-1997

NSE calculated on all the data

The NSE calculated on all the data obtained on the different stations by the different models with calibration on all the data are shown on figure 6.3 below. To allow for a better reading of the graph, some NSE values inferior to -0.2 obtained by the Lindström model on some stations are not represented.

On figure 6.4 are displayed the NSE calculated on all the data obtained with calibration on days with Tobs<1°C. One Paul et al value was excluded as it was equal to -12,4.

Maximum difference calculated on all the data

The maximum differences between observed and calculated soil temperatures in absolute value obtained after calibration on every data are shown on figure 6.5 below. 3 values of the maximum differences are not shown on this graph for the Lindström model as they are superior to 30°C.

Similarly, on figure 6.6 are shown the maximum differences obtained after calibration on days with Tobs<1°C.

Mean difference calculated on all the data

The mean differences (in absolute value) between observed and calculated soil temperatures obtained after calibration on every data are shown on figure 6.7 below. 17 values of the mean differences are not shown on this graph for the Lindström model as they are superior to 4°C.

Similarly, on figure 6.8 are shown the mean differences obtained after calibration on days with Tobs<1°C.

NSE calculated on days with Tobs<1°C

The NSE calculated on days with Tobs<1°C with calibration on all the data are shown on figure 6.9 below. 5 values are missing for the Lindström model as they were all inferior to -60.

On figure 6.10 are displayed the NSE calculated on days with Tobs<1°C obtained with calibration on days with Tobs<1°C.

Maximum difference calculated on days with Tobs<1°C

The maximum differences (in absolute value) between observed and calculated soil temperatures on days with Tobs<1°C obtained after calibration on every data are shown on figure 6.11 below. One value of the maximum differences is not shown on this graph for the Lindström model as it is superior to 1000°C.

Similarly, on figure 6.12 are shown the maximum differences calculated on days with Tobs<1°C and obtained after calibration on days with Tobs<1°C. One Bocock 3 and one Lindstöm values are missing as they were superior to 8°C.

Mean difference calculated on days with Tobs<1°C

The mean differences (in absolute value) between observed and calculated soil temperatures calculated on days with Tobs<1°C and obtained after calibration on every data are shown on figure 6.13 below. 1 value of the mean differences is not shown on this graph for the Lindström model as it is superior to 60°C.

Similarly, on figure 6.14 are shown the mean differences calculated on days with Tobs<1°C and obtained after calibration on days with Tobs<1°C.

Maximum difference calculated on days with Tcalc<1°C

The maximum differences (in absolute value) between observed and calculated soil temperatures on days with Tcalc<1°C obtained after calibration on every data are shown on figure 6.15 below. 3 values of the maximum differences are not shown on this graph for the Lindström model as they are superior to 15°C.

Similarly, on figure 6.16 are shown the maximum differences calculated on days with Tcalc<1°C and obtained after calibration on days with Tobs<1°C. One Paul et al value was excluded as it was equal to 39,8°C.

Mean difference calculated on days with Tcalc<1°C

The mean differences (in absolute value) between observed and calculated soil temperatures calculated on days with Tcalc<1°C and obtained after calibration on every data are shown on figure 6.17 below. 3 values of the mean differences are not shown on this graph for the Lindström model as they are superior to 5°C.

Similarly, on figure 6.18 are shown the mean differences calculated on days with Tcalc<1°C and obtained after calibration on days with Tobs<1°C.

Summary of the previous results

The previous results are summarized in table 6.2 that for each model and each criterion, gives the mean of the results obtained on the different stations.

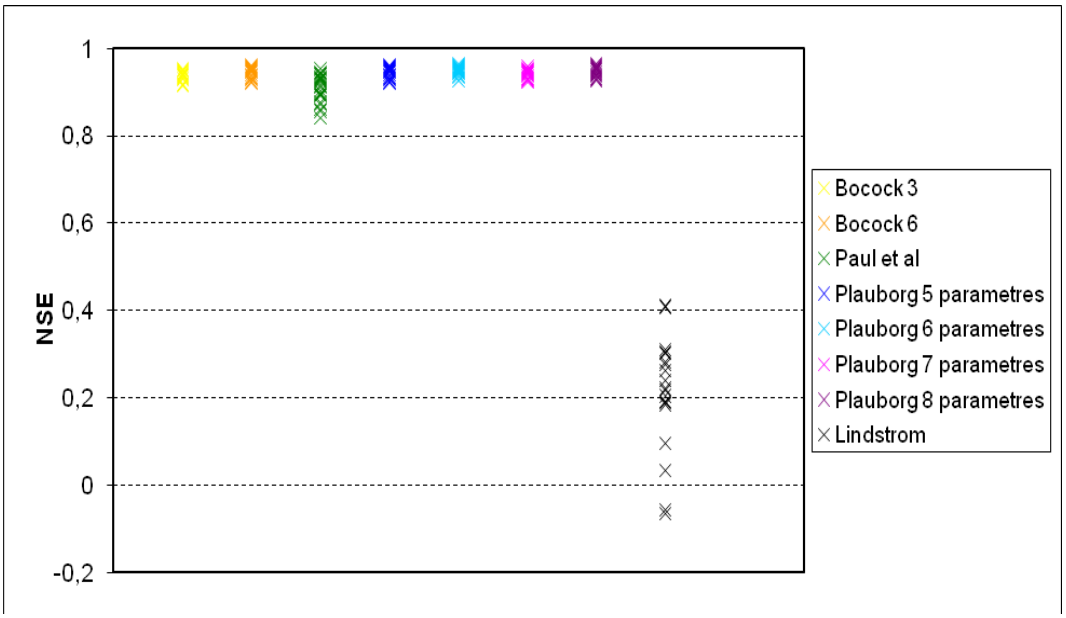

Fig. 6.3 NSE calculated on all the data obtained by the different models with calibration on all the data. 2 NSE values obtained by Lindström and inferior to -0.2 were excluded.

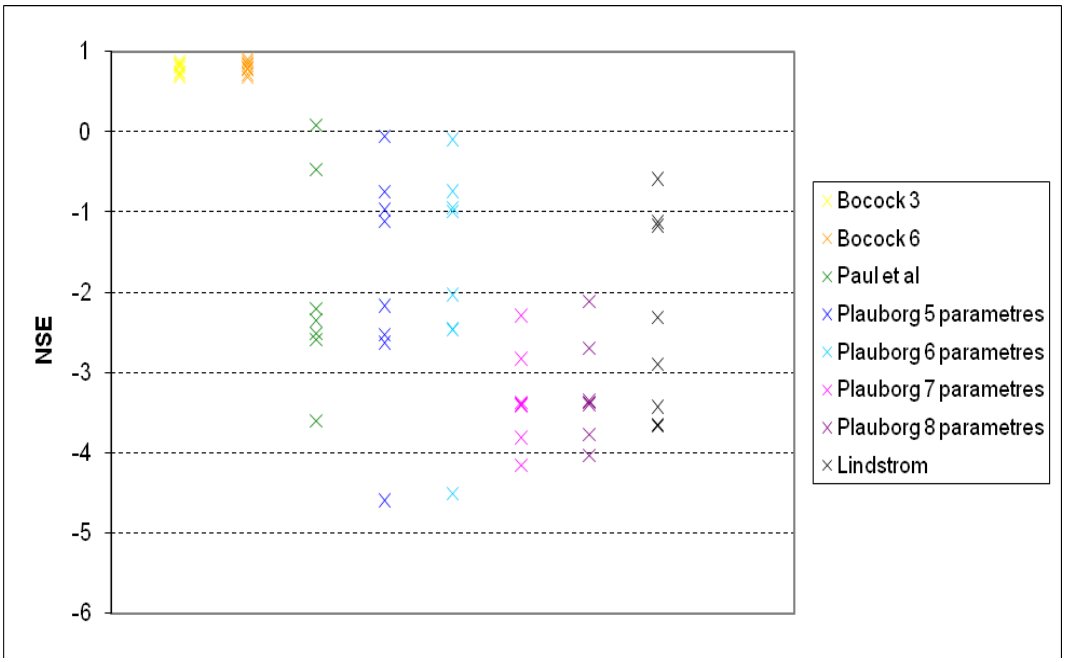

Fig. 6.4 NSE calculated on all the data obtained by the different models with calibration on days with Tobs<1°C. 1 NSE valus obtained by Paul et al and equal to -12,4 was excluded

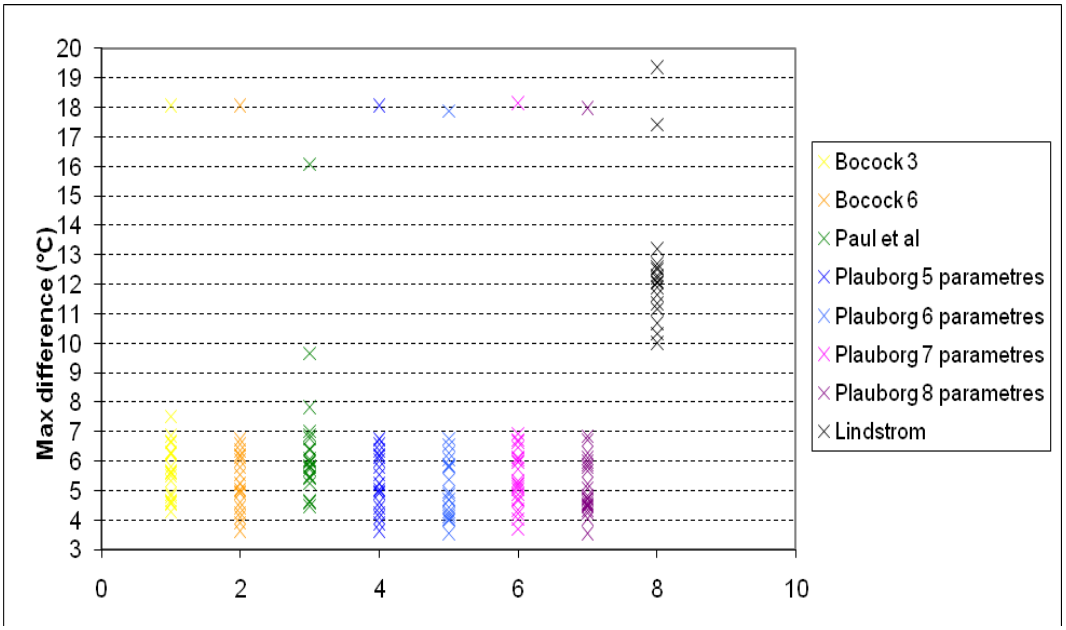

Fig. 6.5 Maximum differences calculated on all the data obtained by the different models with calibration on all the data. 3 values obtained by Lindström and superior to 30°C. were excluded.

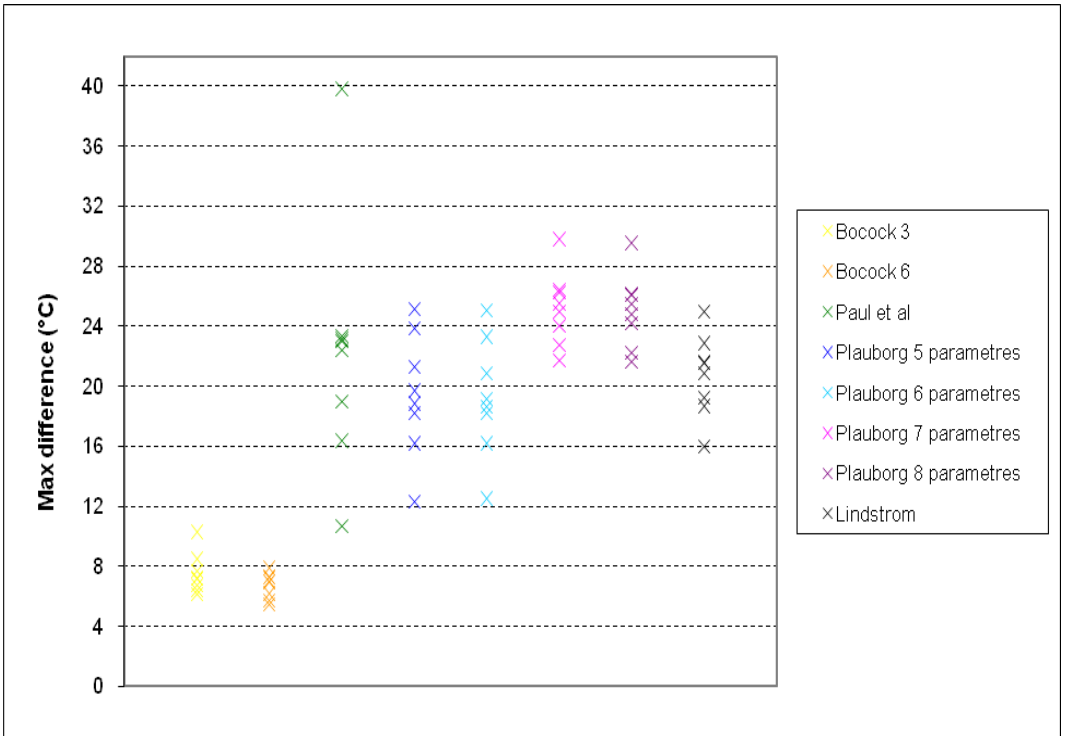

Fig. 6.6 Maximum differences calculated on all the data obtained by the different models with calibration on days with Tobs<1°C.

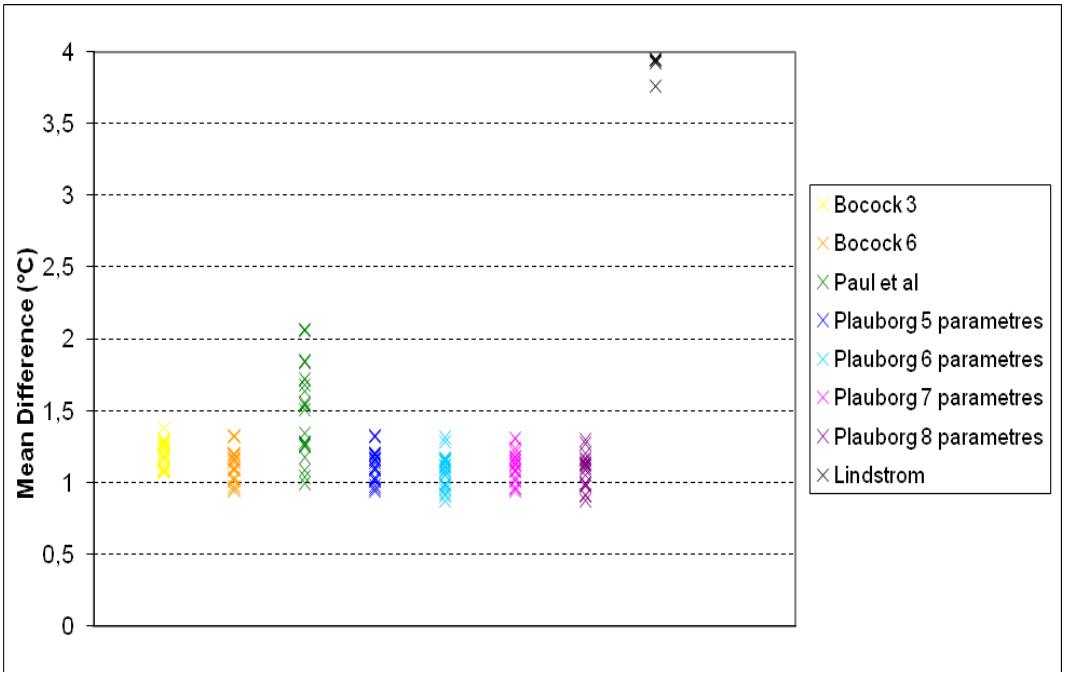

Fig. 6.7 Mean differences calculated on all the data obtained by the different models with calibration on all the data. 17 values obtained by Lindström and superior to 4°C. were excluded

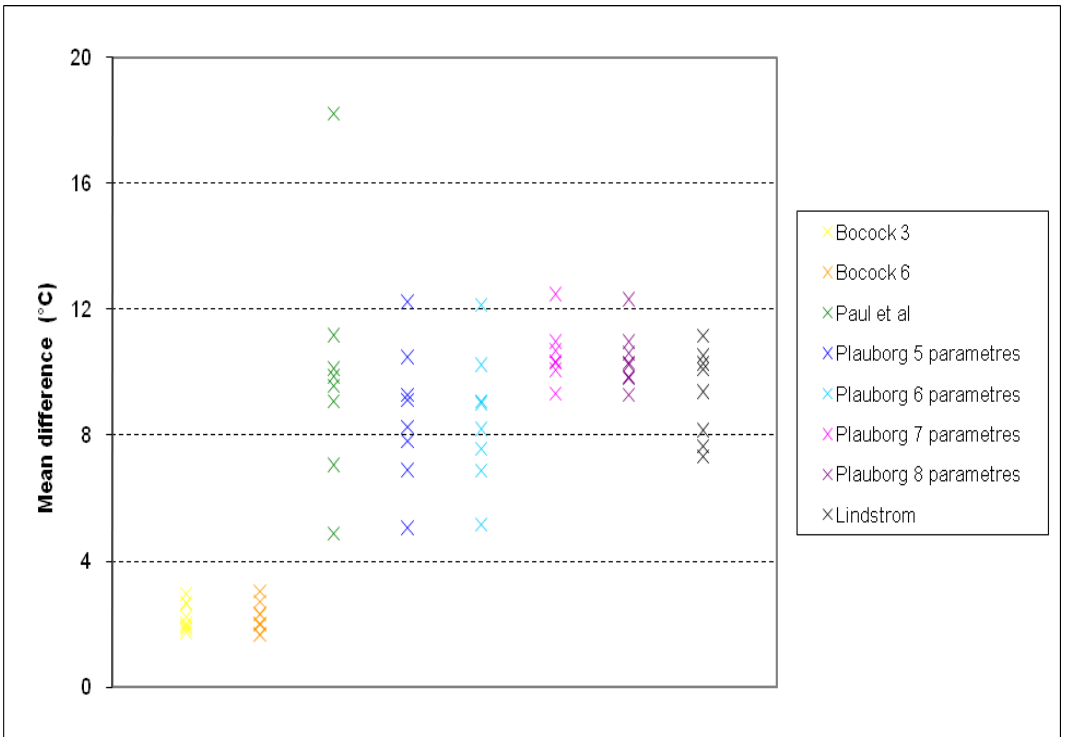

Fig. 6.8 Mean differences calculated on all the data obtained by the different models with calibration on days with Tobs<1°C.

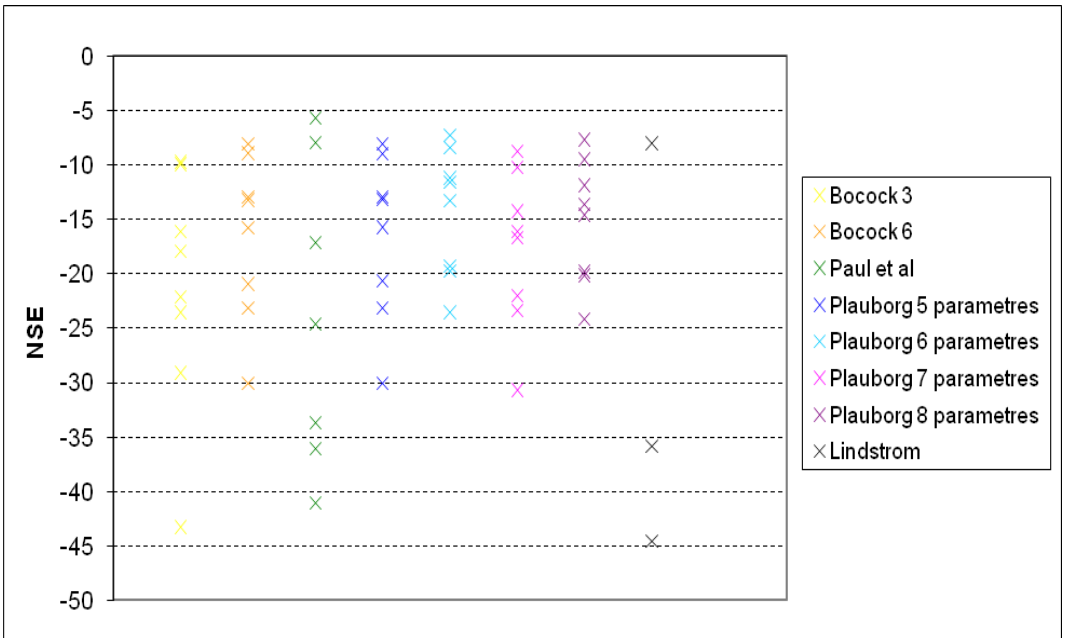

Fig. 6.9 NSE calculated on days with Tobs<1°C obtained by the different models with calibration on all the daya. 5 NSE values obtained by Lindström and inferior to -60 were excluded.

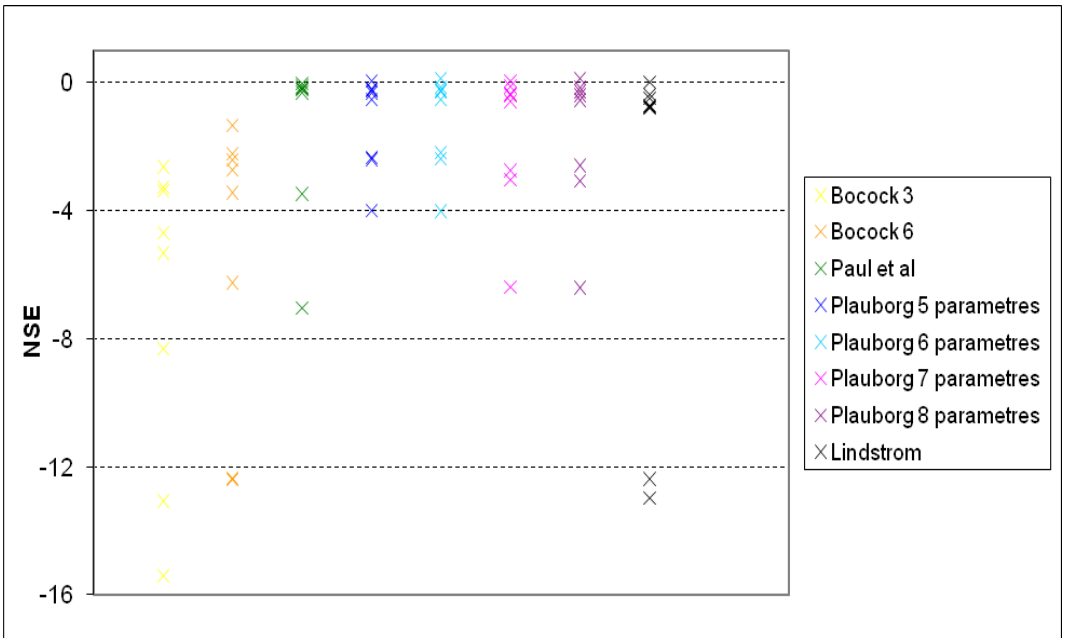

Fig. 6.10 NSE calculated on days with Tobs<1°C obtained by the different models with calibration on days with Tobs<1°C.

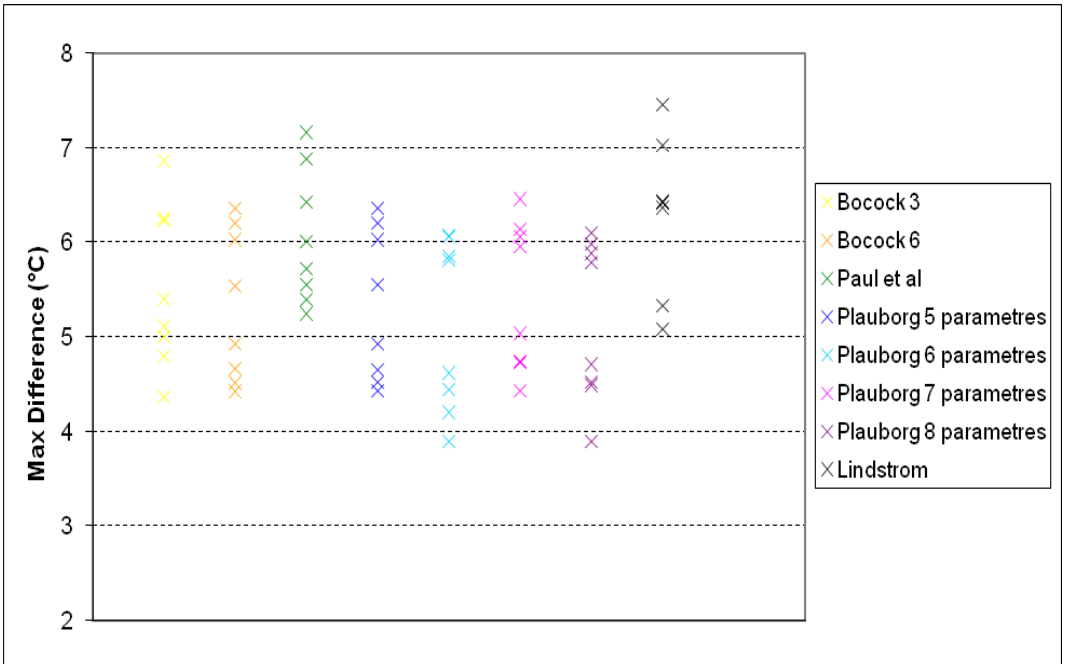

Fig. 6.11 Maximum differences calculated on days with Tobs<1°C obtained by the different models with calibration on all the data. 1 value obtained by Lindström and superior to 1000°C. was excluded.

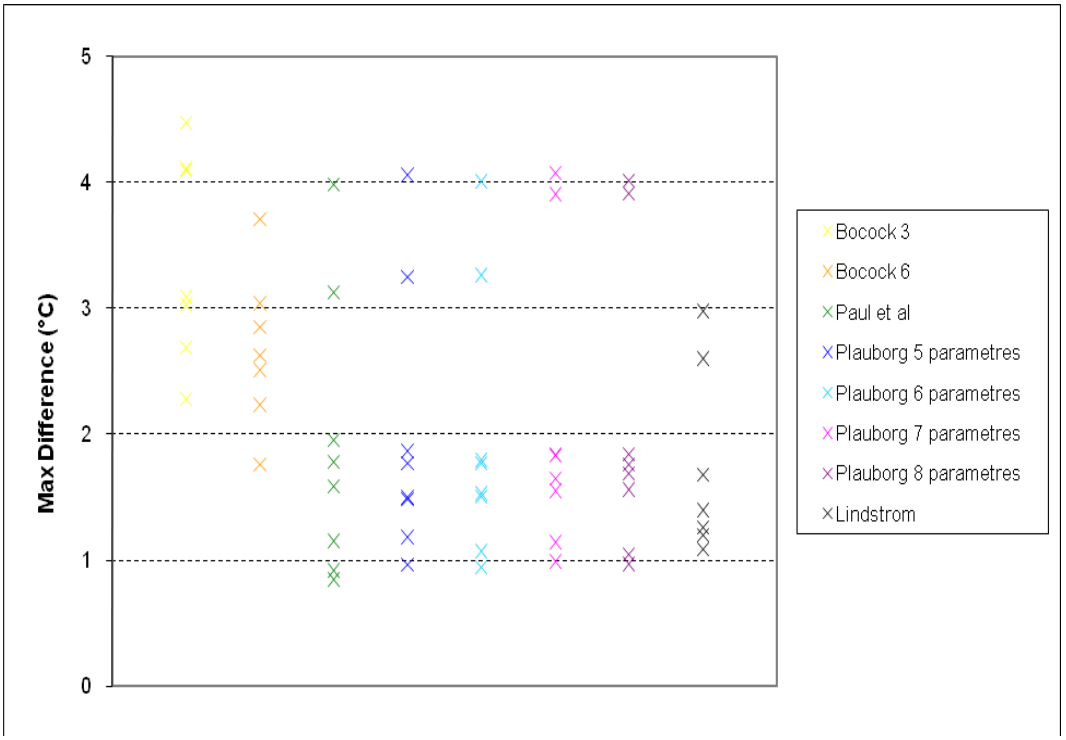

Fig. 6.12 Maximum differences calculated on days with Tobs<1°C obtained by the different models with calibration on days with Tobs<1°C. 1 Bocok 3 and 1 Lindström values are excluded as they are higher than 8°C.

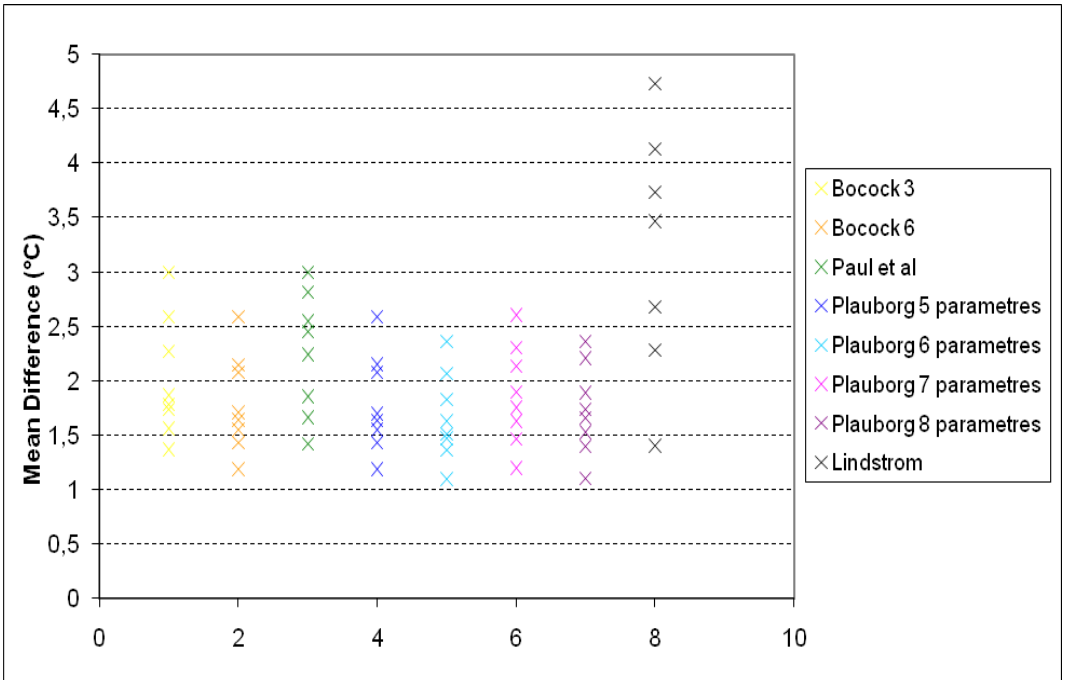

Fig. 6.13 Mean differences calculated on days with Tobs<1°C obtained by the different models with calibration on all the data. One Lindström value, superior to 60°C, was excluded

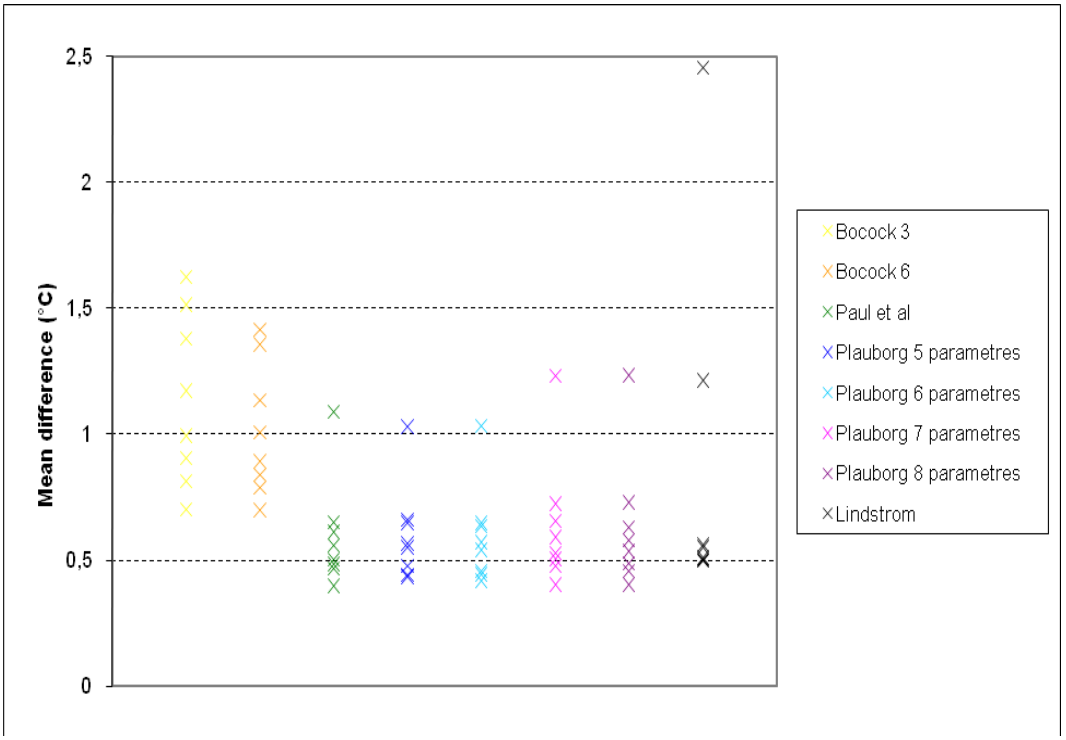

Fig. 6.14 Mean differences calculated on days with Tobs<1°C obtained by the different models with calibration on days with Tobs<1°C.

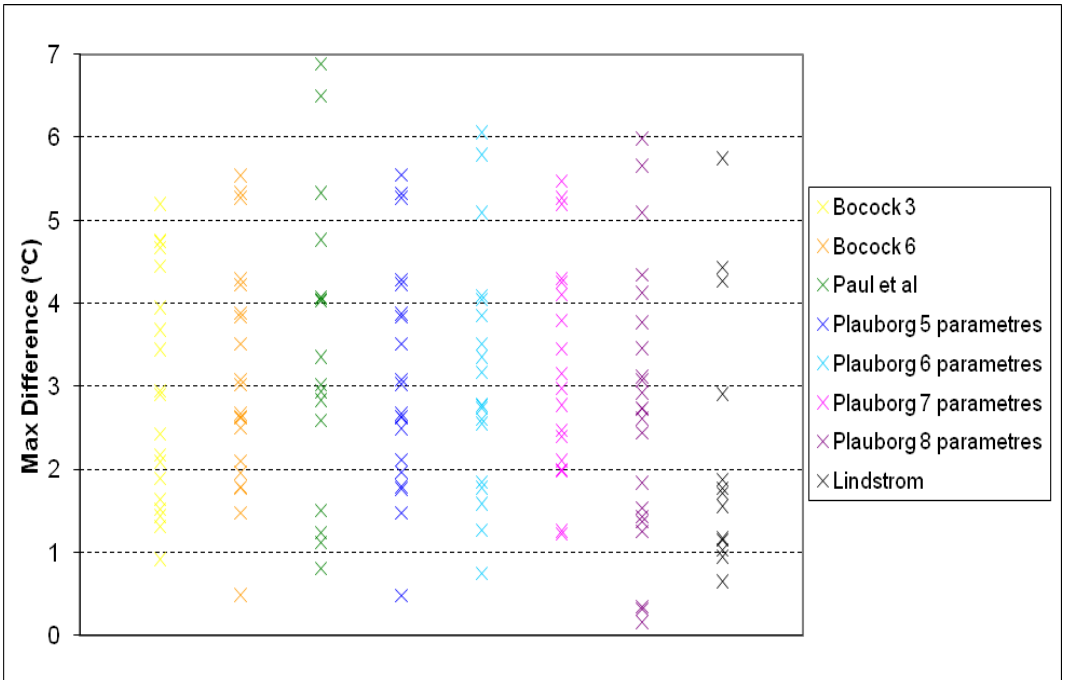

Fig. 6.15 Maximum differences calculated on days with Tcalc<1°C obtained by the different models with calibration on all the data. 3 values obtained by Lindström and superior to 15°C. were excluded.

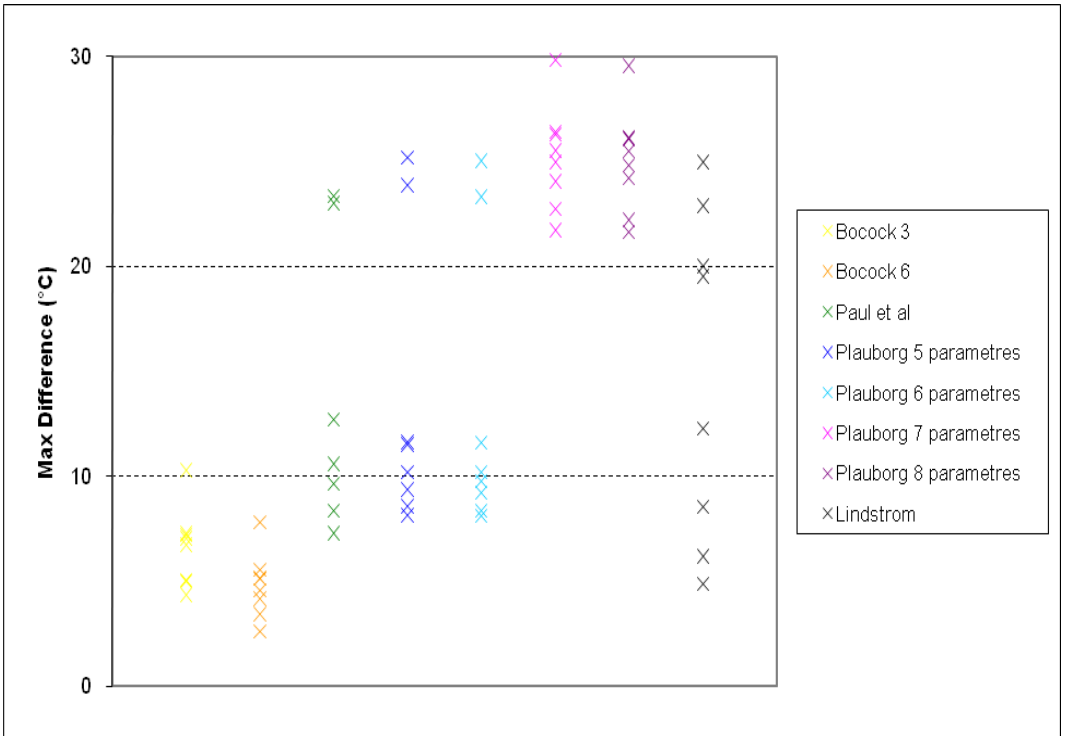

Fig. 6.16 Maximum differences calculated on days with Tcalc<1°C obtained by the different models with calibration on days with Tobs<1°C. One Paul et al value was excluded as it was equal to 39,8°C;.

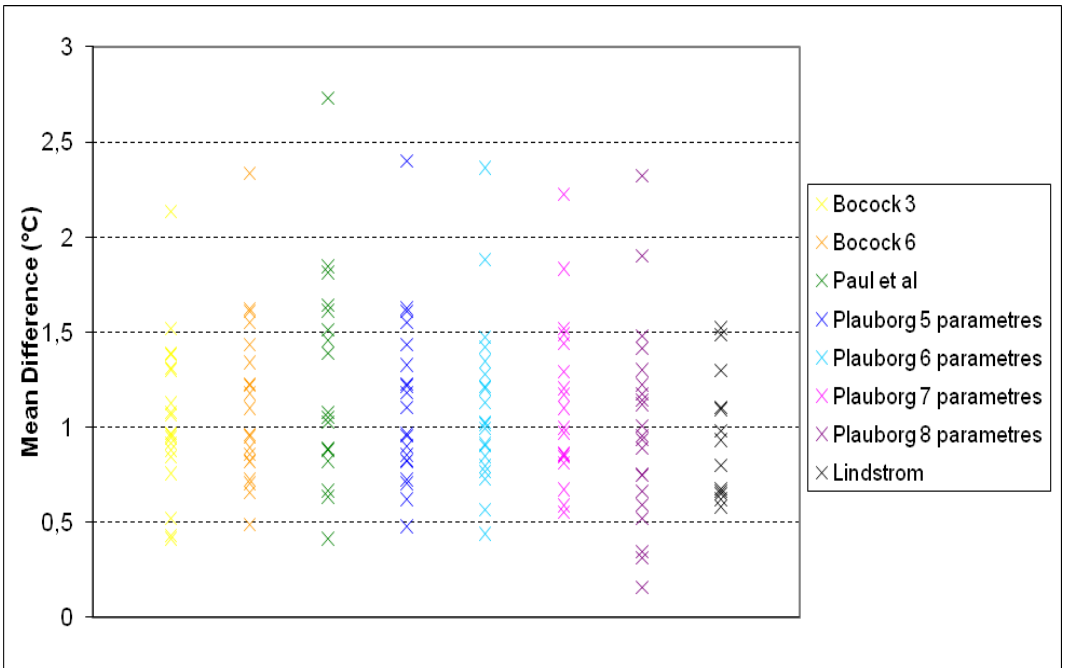

Fig. 6.17 Mean differences calculated on days with Tcalc<1°C obtained by the different models with calibration on all the data. 3Lindström values, superior to 5°C, were excluded

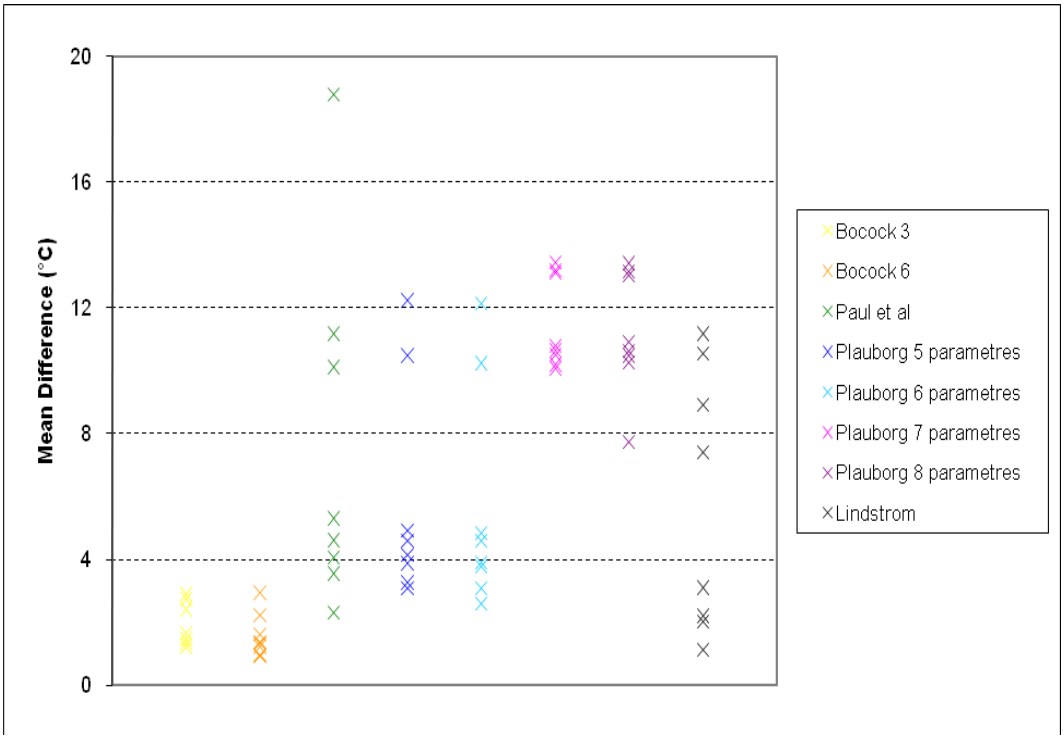

Fig. 6.18 Mean differences calculated on days with Tcalc<1°C obtained by the different models with calibration on days with Tobs<1°C.

Table 6.2 Means of the results obtained on the different stations for each model and each criterion

Criterion	Bocock 3	Bocock 6	Paul et al	Plauborg 5	Plauborg 6	Plauborg 7	Plauborg 8	Lindström
NSE calculated on all the data Calibration on all the data	0,94	0,94	0,91	0,94	0,95	0,94	0,95	-24,24
NSE calculated on all the data Calibration on days with Tobs<1°C	0,79	0,8	-3,25	-1,85	-1,78	-3,33	-3,26	-2,35
Maximum difference (°C) calculated on all the data Calibration on all the data	6,17	5,88	6,5	5,88	5,66	5,96	5,73	312,11
Maximum difference (°C) calculated on all the data Calibration on days with Tobs<1°C	7,52	6,72	22,22	19,45	19,25	25,19	25,01	20,72
Mean difference (°C) calculated on all the data Calibration on all the data	1,2	1,12	1,48	1,12	1,08	1,12	1,08	4,5
Mean difference (°C) calculated on all the data Calibration on days with Tobs<1°C	2,27	2,22	10	8,65	8,54	10,53	10,42	9,32
NSE calculated on days with Tobs<1°C Calibration on all the data	-21,45	-16,62	-31,1	-16,58	-14,28	-17,73	-15,15	-62443,04
NSE calculated on days with Tobs<1°C Calibration on days with Tobs<1°C	-7,02	-5,4	-1,44	-1,25	-1,22	-1,71	-1,68	-3,57
Maximum difference (°C) calculated on days with Tobs<1°C. Calibration on all the data	5,5	5,33	6,05	5,33	5,12	5,44	5,17	809,32
Maximum difference (°C) calculated on days with Tobs<1°C. Calibration on days with Tobs<1°C	4,26	2,8	1,92	2,01	1,99	2,12	2,1	2,59
Mean difference (°C) calculated on days with Tobs<1°C. Calibration on all the data	2,02	1,79	2,25	1,79	1,67	1,87	1,74	10,79
Mean difference (°C) calculated on days with Tobs<1°C. Calibration on days with Tobs<1°C	1,14	1,02	0,6	0,6	0,59	0,64	0,63	0,85
Maximum difference (°C) calculated on days with Tcalc<1°C. Calibration on all the data	2,95	3,1	3,47	3,1	3,07	3,19	2,74	38,61
Maximum difference (°C) calculated on days with Tcalc<1°C. Calibration on days with Tobs<1°C	6,62	4,81	16,84	13,56	13,21	25,19	25,01	14,9
Mean difference (°C) calculated on days with Tcalc<1°C. Calibration on all the data	1,05	1,12	1,26	1,13	1,11	1,11	1	3,44
Mean difference (°C) calculated on days with Tcalc<1°C. Calibration on days with Tobs<1°C	2,06	1,58	7,49	5,83	5,65	11,5	11,21	5,81

6.3.4 Discussion

It can be seen on figure 6.1 that, in validation, all the models except the Lindström model follow the general trend of the observed soil temperature curve when calibrated on all the data. The Lindström model does not manage to follow the whole observed temperature curve but catches it on low temperatures that are the temperatures of interest.

On figure 6.2, the results seem less good : in validation, only the two Bocock models are able to follow the general trend of the observed temperature curve. However most of the other models manage to catch it on low temperatures, namely, the Paul et al model, the Lindstöm model and the Plauborg models 5 and 6 parameters. Plauborg models 7 and 8 parameters, that have 2 harmonics, get very low temperatures around the month of June that are totally inaccurate and that would artificially create frost conditions if they appear in the frost module.

Those results are confirmed by figures 6.3 and 6.4. The NSE calculated on all the data in validation after a normal calibration are superior to 0,9 for every model except for Lindström's –with pretty low results – and Paul's which anyway always gets NSE higher than 0,8. After calibration on the days with Tobs<1°C however, the NSE –calculated on all the data – obtained in validation are pretty bad for all models with very few –and very low- positive values except for the two Bocock models that only get pretty high positive values. It is thus clear that – except for the Bocock models - the calibration on days with Tobs<1°C is unable to ensure a good estimation of the soil temperature in general, whatever the model used. But it can be seen on figures 6.9 and 6.10 that the calibration on days with Tobs<1°C actually gives a better estimation of the soil temperature on days with Tobs inferior to 1°C – with sometimes positive NSE - than calibration on every data – with NSE inferior to -5 for every model. With this calibration, the Plauborg models with 5 and 6 parameters are the one getting the best results in validation on days with Tobs<1°C while the Bocock models seem less effective (Fig. 6.10).

The same conclusions can be drawn from the study of the differences – in absolute values - between observed and calculated soil temperatures. When calibrated on every data, all the models –except Lindström's – have most of their maximum differences between 4 and 7°C – except on one station where all models have a maximum difference of 18°C (Fig. 6.5).The same range of maximum differences can be observed on figure 6.11 where only days with Tobs<1°C are taken into account. Thus when calibrated on all the data, the models tend to make their largest error on the low temperatures in validation. The study of the mean differences give the same conclusion : when calculated on all data, they are between 1 and 1,5°C for all models calibrated on all data – except for Paul model with mean differences up to 2°C and Lindström's with far largest mean differences (Fig. 6.7) but when only days with Tobs<1°C are taken into account the mean differences get higher value - mostly from 1 to 2,5 or 3°C depending on the model for all models except Lindström's (Fig. 6.13). The only model that get lower mean differences when only days with Tobs<1°C are taken into account is Lindstrôm's that seem to get better results on low temperatures.

But when calibrated on days with Tobs<1°C, the models have the opposite behaviour. The maximum differences calculated on all the data in validation - with values between 10 and 30°C except for Bocock models that stay between 5 and 10°C - are far higher than the ones obtained with models calibrated on all the data (Fig. 6.6). The mean differences calculated on all the data - with values between 5 and 15°C

except for Bocock models that stay around 2°C - are also 10 times higher than the ones obtained with a calibration on all the data,(Fig. 6.8). However, when only the days with Tobs<1°C are taken into account, the maximum differences –with values between 1 and 4°C - are significantly lower than when the models are calibrated on all the data (Fig. 6.12) and the mean differences – with values mostly around 0,5°C with a maximum at 1 or 1,5°C depending on the model, which is totally acceptable for an estimation to be included in a frost module for GR4J – are also significantly lower than the ones obtained by a calibration on all the data (Fig. 6.14).

It thus appears that a calibration on the days with Tobs<1°C would give better results in validation when estimating soil temperature on those days that are the only ones of interest. However when only the days with Tcalc<1°C are taken into account, it can be seen that both for maximum and mean differences, the calibration on days with Tobs<1°C gets far worst results than when calibration is done on all the data except for the Bocock models that get similar results with both calibration techniques. Indeed with calibration on all the data most of the maximum differences range from 1 to 6°C (Fig. 6.15) and the mean differences from 0,5 to 2,5°C (Fig. 6.17) while with calibration on the days with Tobs<1°C, most of the maximum differences for models other than Bocock's range from 8 to 26°C (Fig. 6.16) and the mean differences range from 3 to 14°C (Fig. 6.18). Those errors are particularly serious because, on some days, estimations made by the models would create frost conditions in the GR4J model while the real soil temperatures would be largely above the freezing point, which would result in wrong flow calculations.

Thus even if the calibration on days with Tobs<1°C gives better results when Tobs<1°C, the occasional too large underestimation of the soil temperature for models other than Bocock's, resulting in an overestimation of the number of frozen days may prevent the use of this technique.

According to the different results, the Bocock and the Plauborg models 5 and 6 parameters seem to be the ones giving the best results in validation but, with calibration on all the data, the difference with the other models is not very large except for the Lindström model that presents very poor results and that should not be kept for integration in the GR4J model. Finally, the Paul et al model is often getting less good results than other models and thus it may not be necessary to keep it in the study.

6.4 Conclusions

These investigations have allowed the elaboration of 4 different models that have been tested on 11 stations. The aim was to reproduce low temperatures as accurately as possible without creating false frost conditions (i.e. low calculated soil temperatures while the observed temperatures are significantly higher than the freezing point). 2 calibrations techniques were tested, one taking into account all the data and the other focusing on the data from days with an observed soil temperature inferior to 1°C. The second techniques appeared to be unreliable for most of the models – but not for Bocock models - because of too many false frost alerts. Finally, with the calibration on every data, the Lindström and Paul et al models did not appear to be reliable enough and should not be studied further.

In the following steps, the different remaining models will be integrated in a frost module that will be joined to GR4J. They will be used on

stations were calibration will not be possible and will thus be calibrated on the 11 stations so as to maximise the mean of the NSE values calculated on each one of them.

References

BOCOCK, K. L., JEFFERS, J. N. R., LINDLEY, D. K., ADAMSON, J. K. & GILL, C. A. (1977) Estimating Woodland Soil-Temperature from Air Temperature and Other Climatic Variables. *Agricultural Meteorology,* 18**,** 351-372.

BOCOCK, K. L., LINDLEY, D. K., GILL, C. A., ADAMSON, J. K. & WEBSTER, J. A. (1974) Harmonic analysis and synthesis: basic principles of the technique and some applications to temperature data. *Merlewood Research and Development Paper,* 54**,** 1-29.

DINGMAN, S. L. (1976) HYDROLOGIC EFFECTS OF FROZEN GROUND, Literature Review and Synthesis. *CRREL Special Report (US Army Cold Regions Research and Engineering Laboratory)*.

GUARAGLIA, D. O., POUSA, J. L. & PILAN, L. (2001) Predicting temperature and heat flow in a sandy soil by electrical modeling. *Soil Science Society of America Journal,* 65**,** 1074-1080.

GUPTA, S. C., RADKE, J. K., LARSON, W. E. & SHAFFER, M. J. (1982) Predicting Temperatures of Bare-Covered and Residue-Covered Soils from Daily Maximum and Minimum Air Temperatures. *Soil Science Society of America Journal,* 46**,** 372-376.

GUPTA, S. C., RADKE, J. K. & LARSON, W. E. (1981) Predicting Temperatures of Bare and Residue Covered Soils with and without a Corn Crop. *Soil Science Society of America Journal,* 45**,** 405-412.

HASFURTHER, V. R. & BURMAN, R. D. (1974) Soil temperature modeling using air temperature as a driving mechanism. *Transactions, ASAE,* 17**,** 78-81.

ISARD, S. A. & SCHAETZL, R. J. (1995) Estimating Soil Temperatures and Frost in the Lake Effect Snowbelt Region, Michigan, USA. *Cold Regions Science and Technology,* 23**,** 317-332.

LI, X. & KOIKE, T. (2003) Frozen soil parameterization in SiB2 and its validation with GAME-Tibet observations. *Cold Regions Science and Technology,* 36**,** 165-182.

LINDSTROM, G., BISHOP, K. & LOFVENIUS, M. O. (2002) Soil frost and runoff at Svartberget, northern Sweden - measurements and model analysis. *Hydrological Processes,* 16**,** 3379-3392.

NIU, G. Y. & YANG, Z. L. (2006) Effects of frozen soil on snowmelt runoff and soil water storage at a continental scale. *Journal of Hydrometeorology,* 7**,** 937-952.

PAUL, K. I., POLGLASE, P. J., SMETHURST, P. J., O'CONNELL, A. M., CARLYLE, C. J. & KHANNA, P. K. (2004) Soil temperature under forests: a simple model for predicting soil temperature under a range of forest types. *Agricultural and Forest Meteorology,* 121**,** 167-182.

PLAUBORG, F. (2002) Simple model for 10 cm soil temperature in different soils with short grass. *European Journal of Agronomy,* 17**,** 173-179.

ROODENBURG, J. (1985) Estimating 10-cm soil temperatures under grass. *Agricultural and Forest Meteorology,* 34**,** 41-52.

ROTH, K. (2007) *Soil Physics, Lecture Notes*, Institute of Environmental Physics, University of Heidelberg.

THUNHOLM, B. (1990) A Comparison of Measured and Simulated Soil-Temperature Using Air-Temperature and Soil Surface-Energy Balance as Boundary-Conditions. *Agricultural and Forest Meteorology,* 53**,** 59-72.

WANG, L., KOIKE, T., YANG, K., JIN, R. & LI, H. (2010) Frozen soil parameterization in a distributed biosphere hydrological model. *Hydrology and Earth System Sciences,* 14**,** 557-571.

WILLIAMS, G. P. & GOLD, L. W. (1977) Les températures du sol. *Digests de la construction au Canada,* 180F.

ZHANG, Y., CAREY, S. K., QUINTON, W. L., JANOWICZ, J. R., POMEROY, J. W. & FLERCHINGER, G. N. (2010) Comparison of algorithms and parameterisations for infiltration into organic-covered permafrost soils. *Hydrology and Earth System Sciences,* 14**,** 729-750.

ZHANG, Y., CHEN, W. J., SMITH, S. L., RISEBOROUGH, D. W. & CIHLAR, J. (2005) Soil temperature in Canada during the twentieth century: Complex responses to atmospheric climate change. *Journal of Geophysical Research-Atmospheres,* 110.

7 TEST OF THE FROST MODULE ON THE 1910 FLOOD

In chapter 5, two frost modules were developed to integrate frozen soil influence within the GR4J model. After testing these two modules, it was decided that the linear one, being simpler and giving better results without unrealistic parameters values, would be preferred for tests on the 1910 flood.

However this linear frost module requires the input of soil temperature data averaged on the basin surface. These data are not available for the 1910 flood and had to be estimated from air temperatures data. Several such models were thus tested in chapter 6, using recent air and soil temperature series. The Bocock 3, Bocock 6 and Plauborg 5 and 6 parameters models were the ones presenting the best results in validation. They will thus be used for the 1909-1910 soil temperatures estimation.

In chapters 3 and 4, three basins were shown to present problems when GR4J is used to estimate the flow in 1910 : the Marne at Ferté, the Seine at Bazoches and the Seine at Paris Austerlitz. This chapter will describe the 1910 flood simulation test on those three basins with the linear frost module using soil temperatures estimated with the two Bocock models and the Plauborg models with 5 and 6 parameters. The best results obtained will be presented and discussed. The aim of these tests is to know whether this addition of models will improve the simulation of the 1910 flood and thus, whether it is possible to conclude about the frost hypothetical role during this phenomenon.

7.1 Data

Only the three basins of the Marne at Ferté, the Seine at Bazoches and the Seine at Paris Austerlitz were tested.

Concerning the soil temperature models :

- In calibration, the same data as in chapter 6 were used (see table 6.1 and part 6.3.1)
- In 1909-1910, 3 sets of daily mean air temperature data (in °C) were provided by *Meteo France* :
    - In Châlons, from 01/12/1909 to 31/01/1910
    - In Langres, from 01/12/1909 to 28/02/1910
    - In Paris Montsouris, from 01/01/1909 to 28/02/1910

Concerning GR4J and the linear frost module :

- In calibration, the same data as in chapter 5 were used (see table 5.1 and part 5.3.1)
- Also for calibration, the daily mean air temperature data (in °C) were provided by *Meteo France* on the period from 01/01/1994 to 31/07/2009
- In validation on the 1910 flood, the same data as in chapter 4 were used (see table 4.1 on the right part and part 4.1.1).

7.2 Method

For calibration of the soil temperature models, the FORTRAN software was used. At each step of the calibration, the parameters were chosen in order to maximise the mean of the Nash-Sutcliffe Efficiencies obtained on each of the 11 stations. These Efficiency criteria were first calculated

on all the data and then calculated only on days with Tobs<1°C. Thus only two sets of parameters (for normal calibration and for calibration on days with Tobs<1°C) were obtained at the end for each of the four chosen models (Bocock 3 and 6, Plauborg 5 and 6).

The calibrated models were then used on the three air temperature sets for 1909-1910 in order to get three estimated soil temperature sets that would be used by the frost module.

The GR4J + linear frost model was calibrated first using the observed soil temperatures available, exactly as explained in chapter 5.3.2 (thus with three efficiency criteria and on two periods for each basin). The model was then validated on the 1910 flood using the calculated soil temperatures. In the Châlons and Langres cases, soil temperatures data were not covering the whole 1909-1910 period and thus the frost module was just operating when data were available and was not used on the other days.

On a second test, soil temperatures at Paris Montsouris were calculated from air temperatures on the recent years using the calibrated soil temperature models. The GR4J + frost model was then calibrated using those calculated soil temperature as input data. The validation was then done on the 1910 flood by using soil temperatures calculated by the same model. With this technique, the bias between the soil temperature at Paris Montsouris and the 11 stations was the same in calibration and validation and thus its influence on the final results was eliminated.

Finally on a last test, daily soil temperatures calculated on recent years in Paris Montsouris by the Plauborg model with 6 parameters calibrated on every data were linked to the daily soil temperatures of the pixel with the lowest annual mean temperature (calculated by inverse distance weighting from the 11 stations, see chapter 5.3.2) using the equation :

$$T_{PM} = AT_{CP} + B \qquad \text{(Eq. 7.1)}$$

Where :

- T_{PM} is the calculated daily soil temperature at Paris Montsouris, in °C.
- T_{CP} is the daily soil temperature of the coldest pixel, in °C.
- A and B are parameters that were calibrated on the recent years.

The GR4J + frost model was then calibrated on recent years using the coldest pixel temperatures (just like in chapter 5.3.2). The validation was made by estimating those temperatures in 1909-1910 from Paris Montsouris calculated temperatures by using equation 7.1.

7.3 Results

In the first test, when calibration is made with observed soil temperatures, many simulations were launched for each basin. On 1909-1910, 24 calculated soil temperatures sets were available (3 air temperature sets * 4 soil temperature models * 2 calibration type). On the recent years, 6 calibrations were done (3 criteria * 2 periods). Thus 144 tests were possible.

In the second test, only the Paris Montsouris air temperatures could be used as they were the only ones with data in 1909-1910 and 1994-2009. Furthermore, the GR4J simulation was made on one period only, thus only 24 tests were to be launched.

Finally, in the last test, calibration was made on the coldest pixel temperatures that was calculated on 1910. Thus the soil temperature data set in 1910 was unique and only 6 tests corresponding to the 6 GR4J calibrations could be launched.

In all those cases, it would be unnecessary to present every result in this section and for every step only the best and the worst ones will be shown here and discussed afterwards.

7.3.1 Marne at Ferté basin

On chapter 4, the simulation of the 1910 flood on the Marne at Ferté basin got very bad results with a maximum of -0,154 for the Nash-Sutcliffe Efficiency calculated on the flow values in validation (see chapter 4.3.1). This result is to be compared with the ones obtained with the frost module.

Using observed temperatures data for calibration

On the Marne at Ferté basin, the best result was obtained with soil temperatures calculated from **Châlons** air temperatures with the **Plauborg model at 6 parameters** calibrated on **days with Tobs<1°C**. The GR4J + linear frost model was calibrated by maximisation of the **KGEmod** criterion on **1994-1998**.

The worst result was obtained with soil temperatures calculated from **Paris** air temperatures with the **Plauborg model at 6 parameters** calibrated on **days with Tobs<1°C**. The GR4J + linear frost model was calibrated by maximisation of the **NSE** criterion on **1994-1998**.

The results obtained in validation in those two cases are presented in table 7.1.

The hydrographs of those 2 results are shown on figure 7.1.

Using calculated soil temperatures in Paris for calibration

The best result was obtained with soil temperatures calculated by the **Plauborg model at 6 parameters** calibrated on **days with Tobs<1°C**. The GR4J + linear frost model was calibrated by maximisation of the **KGEmod** criterion on **1994-2002**.

The worst result was obtained with soil temperatures calculated by the **Bocock 3 model** calibrated on **all days**. The GR4J + linear frost model was calibrated by maximisation of the **NSE** criterion on **1994-2002**.

The results obtained in validation in those two cases are presented in table 7.2.

The hydrographs of those 2 results are shown on figure 7.2.

Using the coldest pixel temperature

The best result was obtained after **KGEmod** calibration on **1994-1998** and the worst result after **NSE** calibration on **1998-2002**. They are presented in table 7.3.

The hydrographs of those 2 results are shown on figure 7.3 :

Table 7.1 Marne at Ferté : best and worst results obtained in validation on the 1910 flood by GR4J + linear frost using observed temperatures in calibration.

Criterion	Best Results	Worst Results
NSE(Q)	0,005	-0,71
NSE(VQ)	-0,11	-1,002
NSE(lnQ)	-0,279	-1,43

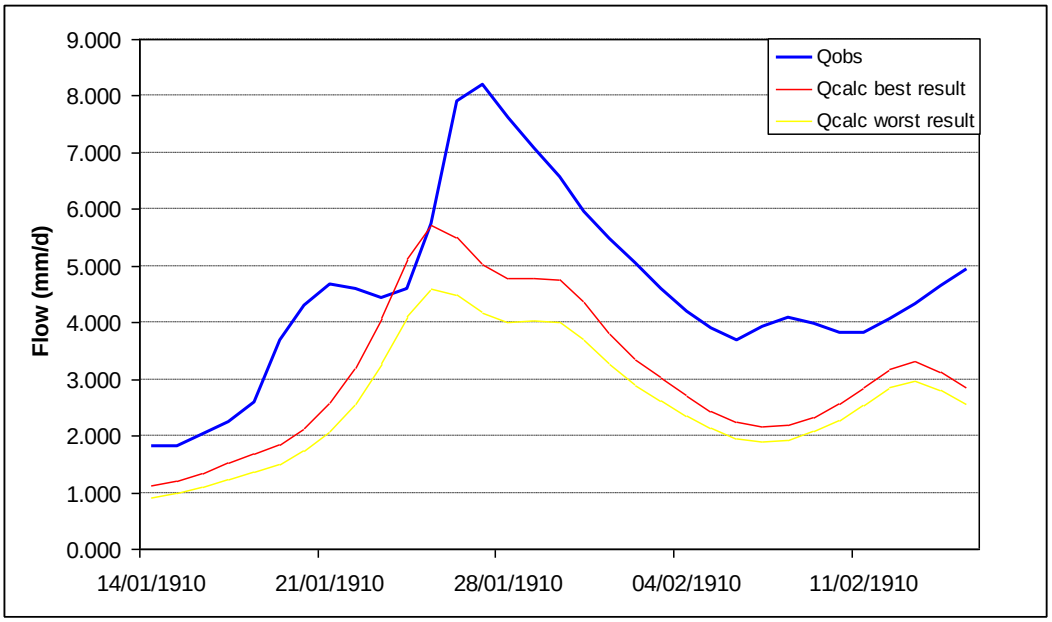

Fig. 7.1 observed hydrograph and best and worst results obtained on the Marne at Ferté station by GR4J + linear frost after calibration on observed temperatures.

Table 7.2 Marne at Ferté : best and worst results obtained in validation on the 1910 flood by GR4J + linear frost using calculated Paris soil temperatures in calibration and validation.

Criterion	Best Results	Worst Results
NSE(Q)	-0.090	-0,483
NSE(VQ)	-0,224	-0,67
NSE(lnQ)	-0,433	-0,943

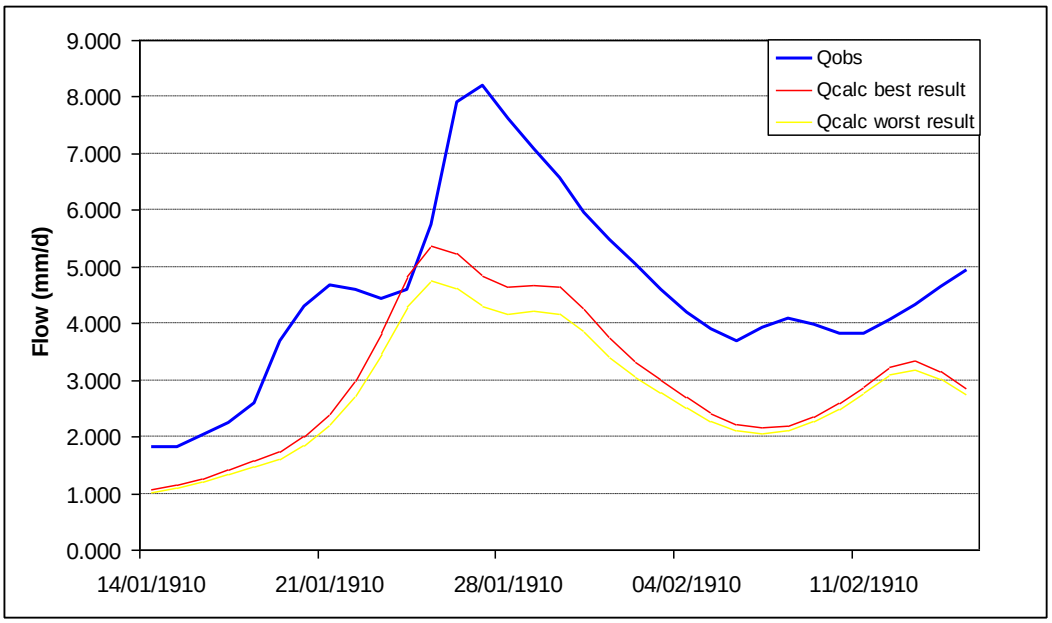

Fig. 7.2 observed hydrograph and best and worst results obtained on the Marne at Ferté station in validation on the 1910 flood by GR4J + linear frost after calibration on calculated Paris temperatures

Table 7.3 Marne at Ferté : best and worst results obtained in validation on the 1910 flood by GR4J + linear frost using coldest pixel temperature in calibration and validation.

Criterion	Best Results	Worst Results
NSE(Q)	-0.043	-0,705
NSE(VQ)	-0,162	-0,95
NSE(lnQ)	-0,336	-1,291

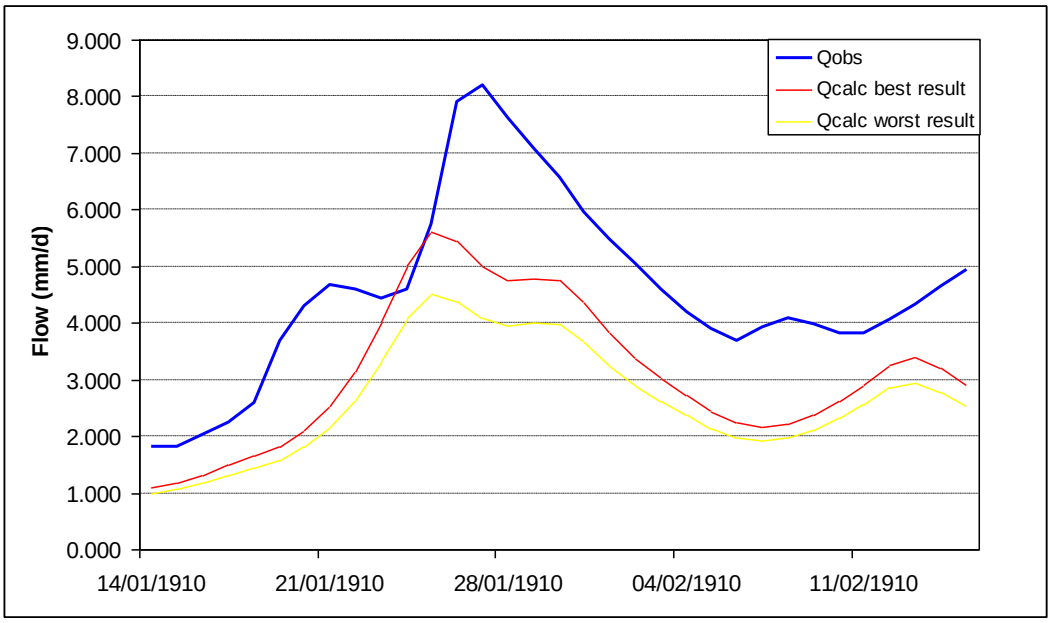

Fig. 7.3 observed hydrograph and best and worst results obtained on the Marne at Ferté station in validation on the 1910 flood by GR4J + linear frost after calibration on the coldest pixel temperature

7.3.2 Seine at Bazoches basin

The new results that will be displayed here should be compared with the ones obtained in chapter 4 on this basin for the simulation of the 1910 flood. On that section a maximum of 0,506 was obtained for the NSE calculated on the flow values (see chapter 4.4.1).

Using observed temperatures data for calibration

On the Seine at Bazoches basin, the best result was obtained with soil temperatures calculated from **Paris** air temperatures with the **Bocock 3 model** calibrated on **days with Tobs<1°C**. The GR4J + linear frost model was calibrated by maximisation of the **KGEmod** criterion on **2003-2009**.

The worst result was obtained with soil temperatures calculated from **Paris** air temperatures with the **Plauborg model at 6 parameters** calibrated on **days with Tobs<1°C**. The GR4J + linear frost model was calibrated by maximisation of the **NSE** criterion on **2003-2009**.

The results obtained in validation in those two cases are presented in table 7.4.

The hydrographs of those 2 results are shown on figure 7.4.

Table 7.4 Seine at Bazoches : best and worst results obtained in validation on the 1910 flood by GR4J + linear frost using observed temperatures in calibration.

Criterion	Best Results	Worst Results
NSE(Q)	0,675	0,136
NSE(VQ)	0,657	-0,097
NSE(lnQ)	0,566	-0,607

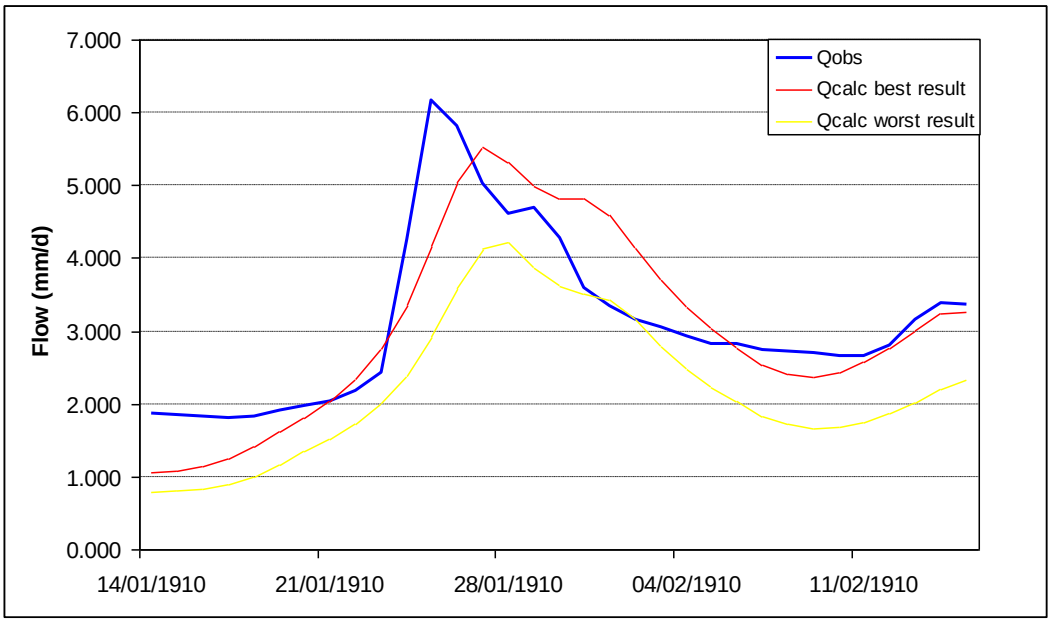

Fig. 7.4 observed hydrograph and best and worst results obtained on the Seine at Bazoches station by GR4J + linear frost after calibration on observed temperatures.

Using calculated soil temperatures in Paris for calibration

The best result was obtained with soil temperatures calculated by the **Bocock 6 model** calibrated on **days with Tobs<1°C**. The GR4J + linear frost model was calibrated by maximisation of the **KGEmod** criterion on **1998-2002**.

The worst result was obtained with soil temperatures calculated by the **Plauborg model with 6 parameters** calibrated on **all days**. The GR4J + linear frost model was calibrated by maximisation of the **NSE** criterion on **1998-2002**.

The results obtained in validation in those two cases are presented in table 7.5.

The hydrographs of those 2 results are shown on figure 7.5.

7.3.3 Seine at Paris Austerlitz basin

In chapter 3, the best result that could be found on the Seine at Paris Austerlitz basin in validation on the 1910 flood was obtained by KGEmod calibrating taking the reservoirs into account. A maximum of 0,489 for the NSE criterion was then found. This result should now be compared to the new results that will be obtained in this section.

Table 7.5 Seine at Bazoches : best and worst results obtained in validation on the 1910 flood by GR4J + linear frost using calculated Paris soil temperatures in calibration and validation.

Criterion	Best Results	Worst Results
NSE(Q)	0,556	0,427
NSE(VQ)	0,534	0,381
NSE(lnQ)	0,413	0,206

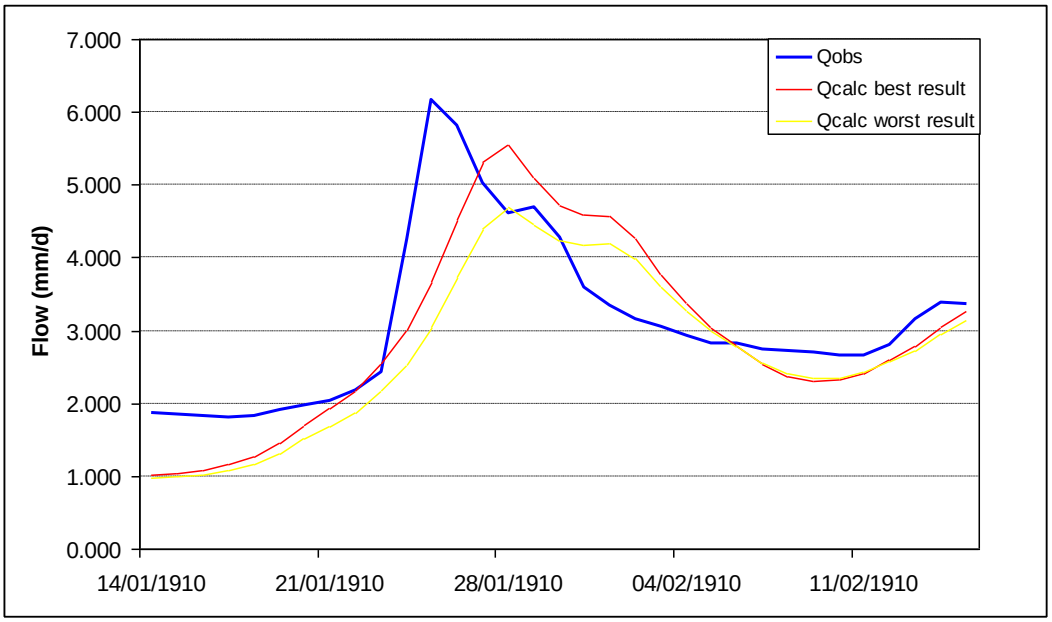

Fig. 7.5 observed hydrograph and best and worst results obtained on the Seine at Bazoches station in validation on the 1910 flood by GR4J + linear frost after calibration on calculated Paris temperatures

Using observed temperatures data for calibration

On the Seine at Paris Austerlitz basin, the best result was obtained with soil temperatures calculated from **Langres** air temperatures with the **Plauborg model at 6 parameters** calibrated on **all days**. The GR4J + linear frost model was calibrated by maximisation of the **KGEmod** criterion on **1994-1998**.

The worst result was obtained with soil temperatures calculated from **Paris** air temperatures with the **Plauborg model at 6 parameters** calibrated on **days with Tobs<1°C**. The GR4J + linear frost model was calibrated by maximisation of the **NSE** criterion on **1994-1998**.

The results obtained in validation in those two cases are presented in table 7.6.

The hydrographs of those 2 results are shown on figure 7.6.

Using calculated soil temperatures in Paris for calibration

The best result was obtained with soil temperatures calculated by the **Bocock 6 model** calibrated on **days with Tobs<1°C**. The GR4J + linear frost model was calibrated by maximisation of the **KGEmod** criterion on **1994-2002**.

The worst result was obtained with soil temperatures calculated by the **Plauborg model with 6 parameters** calibrated on **all days**. The GR4J + linear frost model was calibrated by maximisation of the **NSE** criterion on **1994-2002**.

The results obtained in validation in those two cases are presented in table 7.7 .

The hydrographs of those 2 results are shown on figure 7.7.

Table 7.6 Seine at Paris : best and worst results obtained in validation on the 1910 flood by GR4J + inear frost using observed temperatures in calibration.

Criterion	Best Results	Worst Results
NSE(Q)	0,446	0,171
NSE(VQ)	0,483	0,176
NSE(lnQ)	0,502	0,155

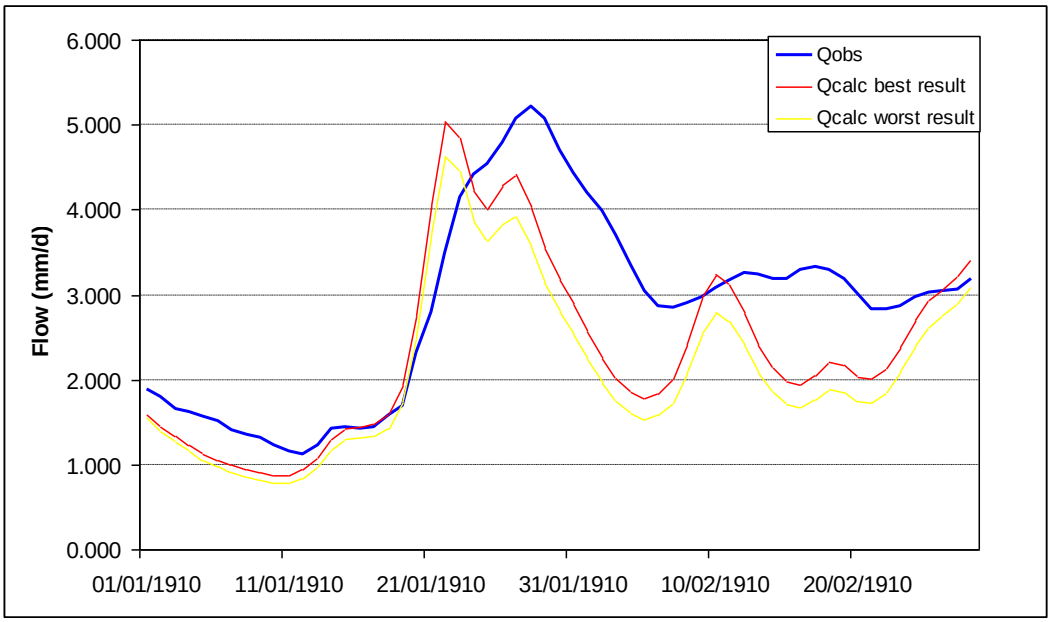

Fig. 7.6 observed hydrograph and best and worst results obtained on the Seine at Paris station by GR4J + linear frost after calibration on observed temperatures.

Table 7.7 Seine at Paris : best and worst results obtained in validation on the 1910 flood by GR4J + linear frost using calculated Paris soil temperatures in calibration and validation.

Criterion	Best Results	Worst Results
NSE(Q)	0,47	0,355
NSE(VQ)	0,51	0,396
NSE(lnQ)	0,533	0,408

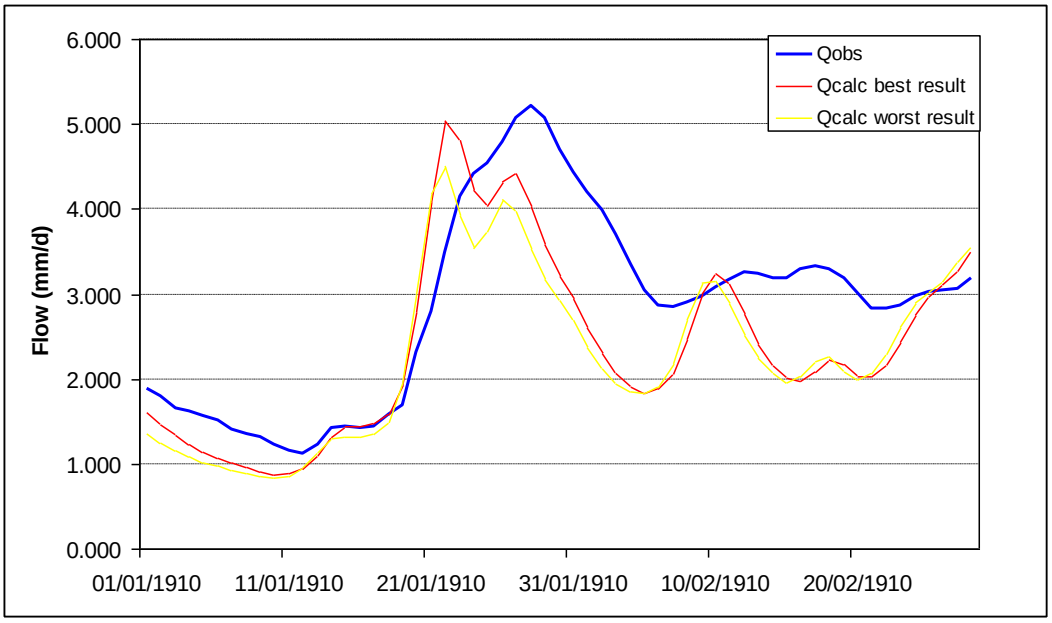

Fig. 7.7 observed hydrograph and best and worst results obtained on the Seine at Paris station in validation on the 1910 flood by GR4J + linear frost after calibration on calculated Paris temperatures

Using the coldest pixel temperature

The best result was obtained after **KGEmod** calibration on **1998-2002** and the worst result after **NSE** calibration on **1994-1998**. They are presented in table 7.8.

The hydrographs of those 2 results are shown on figure 7.8.

Table 7.8 Seine at Paris : best and worst results obtained in validation on the 1910 flood by GR4J + linear frost using coldest pixel temperature in calibration and validation.

Criterion	Best Results	Worst Results
NSE(Q)	0,54	0,37
NSE(VQ)	0,581	0,4
NSE(lnQ)	0,604	0,416

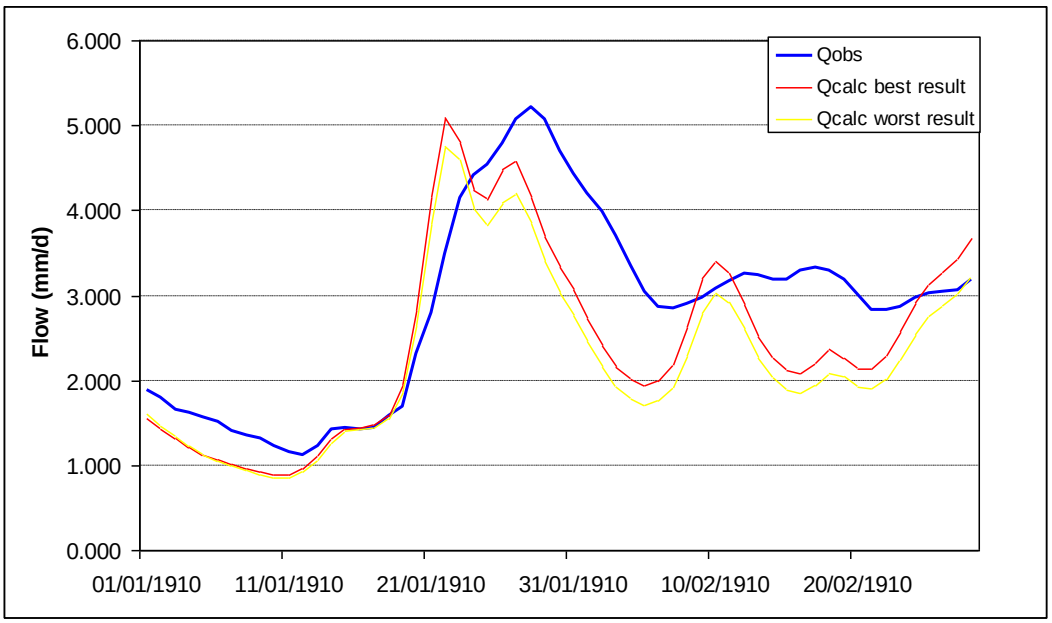

Fig. 7.8 observed hydrograph and best and worst results obtained on the Seine at Paris station in validation on the 1910 flood by GR4J + linear frost after calibration on the coldest pixel temperature

7.4 Discussion

On each one of the basins, for each of the tests, the best result is always obtained after a KGEmod calibration for GR4J and the worst result after a NSE calibration. But no tendency can be observed for the best soil temperature model, nor the best air temperature station to use. It depends on the basin and on the test undertaken. For example, soil temperatures calculated with **Paris** air temperatures by **Plauborg model with 6 parameters** calibrated on **days with Tobs<1°C** will give the best results on the Marne at Ferté basin when using the calculated Paris soil temperature for GR4J calibration but will give the worst results on the Seine at Paris Austerlitz basin when using observed soil temperature for GR4J calibration. Thus a unique model that would give the best result – or at least one of the best – in every situation, could not be identified and an application in flood prediction is not possible at this state. However it is still interesting to see the results obtained on the 1910 flood.

On the Marne at Ferté basin, the results should be compared with the ones obtained on chapter 4 (Table 4.6 and Fig. 4.3). In this comparison, only the results obtained after calibration accounting for the water reservoir will be taken into account as in this chapter testing the frost module, all calibrations were accounting for it on the Marne at Ferté basin. In tables 7.1, 7.2 and 7.3, it can be seen that, for all tests, when the best result is considered, the 3 criteria - NSE(Q), NSE(VQ) and NSE(lnQ) - values are higher than the best obtained result without the frost module on chapter 4 (KGEmod calibration accounting for the water reservoir). But when the worst result is considered, then the criteria values are actually lower than the worst obtained result without the frost module (NSE calibration accounting for the water reservoir). Thus no real conclusion can be drawn. Furthermore, even the best results are still very far from a satisfactory result with only one case with a positive NSE(Q) value (Table 7.1). From the hydrographs (Fig. 7.1, 7.2 and 7.3) it can be seen that a large volume of water is still missing. In this

basin, the frost module does not manage to solve the 1910 flood problem.

On the Seine at Bazoches basin, the results should also be compared with the ones obtained in chapter 4 (Table 4.9 and Fig. 4.4). Here again the best obtained results (Tables 7.4 and 7.5) are much higher than the ones obtained on chapter 4. But the worst obtained results are comparable to the worst results obtained without the frost module. On this basin, the frost module thus seems to have improved the simulation of the 1910 flood. However, even the best results are still not very satisfactory and it can be seen on the hydrographs that the peak flow is still underestimated and simulated later than what was observed (Fig. 7.4 and 7.5). In this case, even if it improves the simulation, the frost module does not totally solve the problem.

On the Seine at Paris Austerlitz basin, the results should now be compared to those obtained on chapter 3. As for the Marne at Ferté basin, in this comparison, only the results obtained with calibration accounting for the water reservoirs will be taken into account : table 3.6 and figure 3.3 for NSE calibration and table 3.8 and figure 3.4 for KGE and KGEmod calibrations. This time the best and worst results are lower than their corresponding results obtained on chapter 3 when the frost module is calibrated on the observed temperatures (Table 7.6), they are comparable when the frost module is calibrated on the calculated Paris soil temperatures (Table 7.7) and they are higher when the coldest pixel temperatures are used (Table 7.8). However, once again, even the best results are not satisfactory. On the hydrographs it can be seen that, if the peak flow is acceptably estimated, it is still in advance related to what was observed. The plateau observed around January, 15th is still not simulated (Fig. 7.6, 7.7 and 7.8).

7.5 Conclusion

This addition of models - one for the soil temperature and the other for the frost influence on hydrology – is not giving stable results and should thus not be applied in forecasting at this point.

On the 1910 flood, the results obtained are not remarkably different from those obtained by GR4J alone. In many cases, they are even comparable. But even in the few cases where an improvement in the flood simulation can be noticed, the results are still far from being satisfactory. Thus it is not possible to conclude about a predominant role of frozen soil on the 1910 flood.

However, the inverse conclusion still cannot be made either : it is still possible that the model could not replicate the effect of frost on the hydrological cycle. Indeed, as shown on chapter 4, the frost formation is too scarce during the recent years to allow for a good calibration and validation of the model. It is thus not even possible to conclude about the correctness of the linear frost model.

Thus this approach failed but "in everyday scientific practice, model failures are the rule rather than the exception. It takes any number of dead-end explorations before one hits on a suitable way to move forward"(Andréassian et al., 2010). This frost modelling approach was worth trying, and it is now obvious that frost is not a common problem within the Seine at Paris Austerlitz basin. In the next, conclusive chapters, some new perspectives to solve the 1910 flood problem will be described.

Reference

ANDRÉASSIAN, V., PERRIN, C., PARENT, E. & BARDOSSY, A. (2010) The Court of Miracles of Hydrology: can failure stories contribute to hydrological science? *Hydrological Sciences Journal,* 55**,** 849 - 856.

8 CONCLUSION AND PERSPECTIVES

In the previous chapters, a new module was developed in order to take the frost effects on hydrology into account in the GR4J model. However this module was unable to solve the problem encountered in the simulation of the 1910 flood.

In this chapter, additional tests were performed in order to get more information about this problem. In a first part, a new – ad hoc – hypothesis was used : the undercatch (or under-collection) of rain water that can occur during snowy windy weather. Then in a second part, a delay was introduced in the simulated data and rain water was added on some specific days.

Finally, in a third part, new perspectives were introduced to develop new, more reliable models.

8.1 Rain undercatch

On snowy, windy days, the falling snowflakes can be diverted by the wind and thus may not enter into the measuring devices cones thus leading to an underestimation of the rain water. This phenomenon mostly occurs in the mountains where up to 80% of the precipitation may not be measured.

In 1910, it snowed as one can see on many pictures from that time and the measuring devices were less reliable than today. However, no information about wind and snow conditions is available and it is thus impossible to give a measure of the undercatch influence. A simple model was thus designed.

8.1.1 Principle

During the 1910 flood the measured precipitation was thus multiplied by a factor X_{UC} that is supposed to represent the rain water that could not be collected and thus measured. To calculate X_{UC}, it was considered that the first snowflakes are formed when air temperature reaches 3°C and that there is no more liquid water in the rain when air temperature reaches -1°C. Thus X_{UC} was calculated as a linear function of air temperature given by the equation :

$$X_{UC} = \begin{cases} 1 & if\ T_{air} > 3 \\ 1{,}3 - \frac{0{,}3}{4} \times (T_{air} + 1) & if\ -1 \le T_{air} \le 3 \\ 1{,}3 & if\ T_{air} < -1 \end{cases} \qquad \text{(Eq. 8.1)}$$

Where :

- X_{UC} is the multiplying factor for precipitation
- T_{air} is the air temperature in °C.

Equation 8.1 does not take wind conditions into account because those data are not available during the 1910 flood. Thus under-catch is considered to happen on each snowy day. However, to counterbalance this error, a low value of 1,3 was set for the maximum multiplying factor compared to the 80% missing water that can occur is some cases.

8.1.2 Data

In calibration and validation, the same data like in chapters 3 and 4 were used on the Seine at Bazoches, Seine at Paris and Marne at Ferté basins. The same data like in chapter 7 were used for air temperature.

8.1.3 Method

The Excel software was used as in chapters 3 and 4.

In validation on 1910 the precipitations data from December, 1st 1909 to February, 28th 1910 were multiplied by an undercatch factor calculated as explained in part 8.1.1. The air temperature used for calculation of this factor was the mean of the 3 air temperature sets of data in Châlons, Langres and Paris.

8.1.4 Results

The results obtained in validation on the 3 basins with different calibration and validation methods are presented in table 8.1.

The observed and simulated flows obtained on the Marne at Ferté basin on the 1910 flood are shown on figure 8.1.

Table 8.1 Results obtained on the 3 basins with different calibration and validation techniques.

Method	NSE obtained in validation on the 1910 flood		
	Marne at Ferté basin	Seine at Bazoches basin	Seine at Paris basin
KGEmod calibration taking water reservoirs into account	-0,154	0,506	0,489
NSE calibration taking water reservoirs into account. Validation taking undercatch into account	-0,196	0,394	0,502
KGE calibration taking water reservoirs into account. Validation taking undercatch into account	-0,054	0,403	0,596
KGEmod calibration taking water reservoirs into account. Validation taking undercatch into account	0,068	0,379	0,616

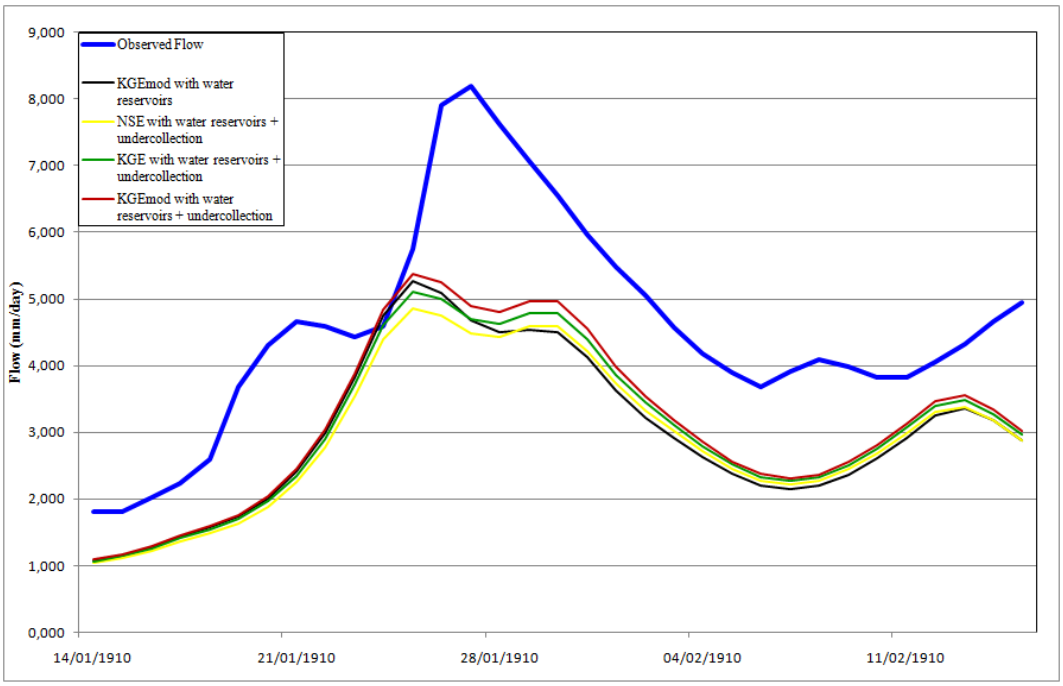

Fig. 8.1 observed and simulated flow on the Marne at Ferté basin after different calibration and validation methods

The observed and simulated flows obtained on the Seine at Bazoches basin on the 1910 flood are shown on figure 8.2.

Finally, the observed and simulated flows obtained on the Seine at Paris Austerlitz basin on the 1910 flood are shown on figure 8.3.

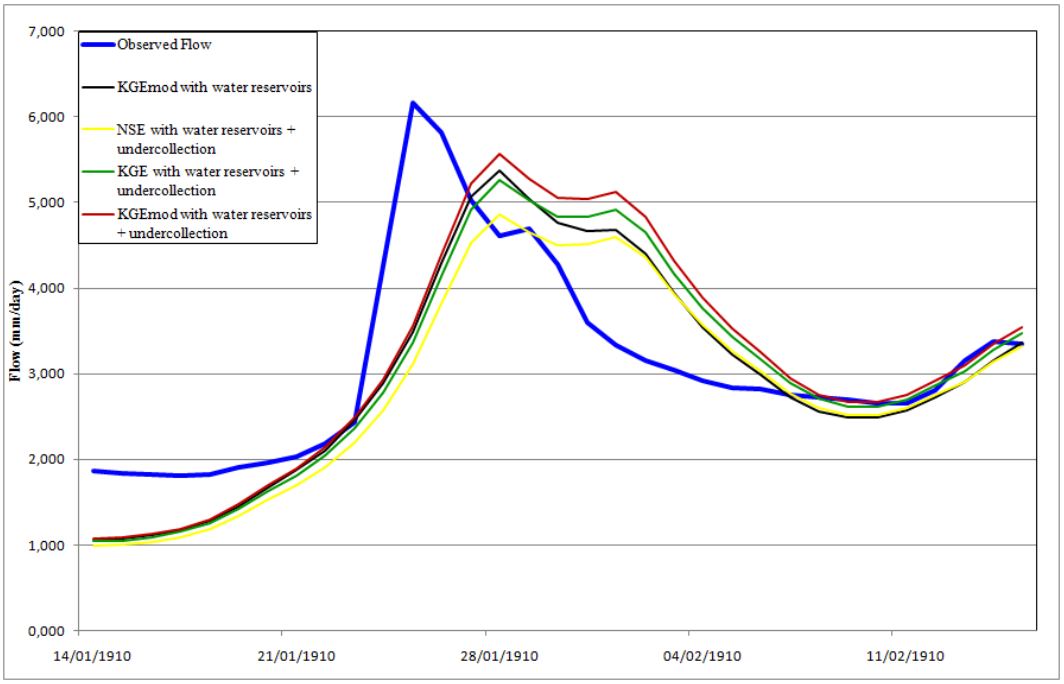

Fig. 8.2 observed and simulated flow on the Seine at Bazoches basin after different calibration and validation methods

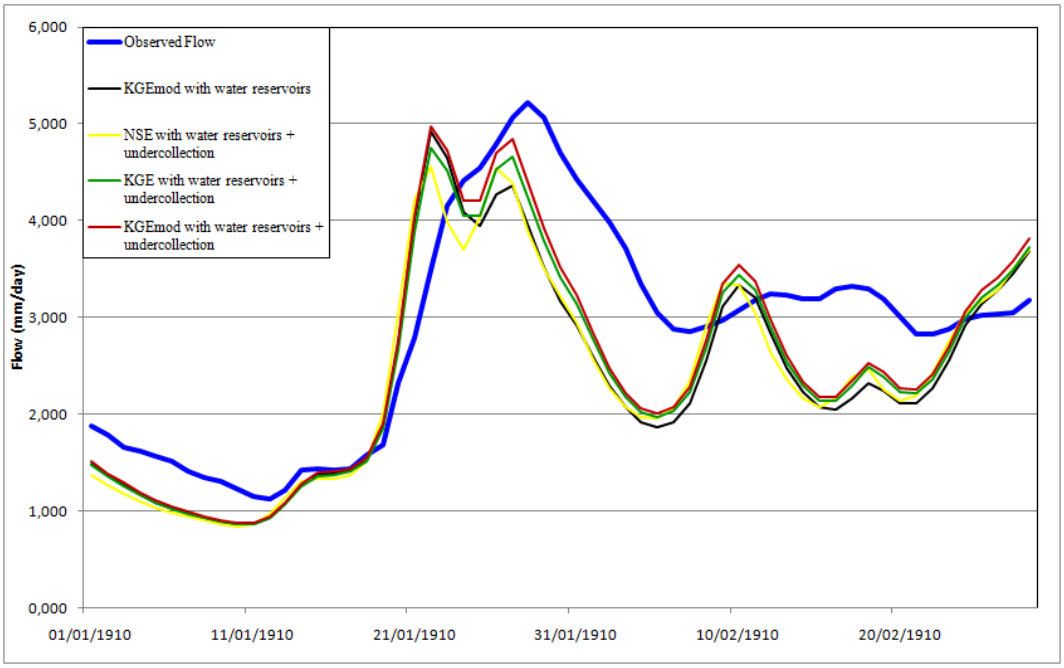

Fig. 8.3 observed and simulated flow on the Seine at Paris Austerlitz basin after different calibration and validation methods

8.1.5 Discussion

It can be seen in table 8.1 that taking into account the undercatch by the addition of some water in the precipitation on 1910 has improved the results obtained in validation for the Marne at Ferté and the Seine at Paris Austerlitz basin. The same result can be seen on the hydrographs on figures 8.1 and 8.3. However those results are still far from being satisfactory.

The Seine at Bazoches basin has a different behavior and the addition of water when taking into account the undercatch is not bringing any improvement in the simulation with a Nash-Sutcliffe efficiency that is actually decreased (table 8.1). The reason can be seen on the hydrograph (Fig. 8.2), after January, 28th, the simulated flow is superior to the observed one and an increase in the precipitation leading to an increased simulated flow is thus leading to a larger error.

On figures 8.1, 8.2 and 8.3, it can finally be seen that taking into account the undercatch does not change the shape of the simulated hydrographs but is just increasing a little the calculated flow values. Thus this ad hoc hypothesis of a general underestimation of the precipitation in 1910 due to a snowy windy weather is not bringing any solution nor explanation to the problem encountered when simulating the 1910 flood.

8.2 Delays and modified precipitations

In chapter 8.1, an ad hoc hypothesis – the undercatch of rain water – was used to add extra precipitation on the 1910 set of data. But this hypothesis could not be verified and, more importantly, the amount of extra precipitation was set arbitrarily.

In this chapter, the same approach was used in a more radical way. The data and the results obtained in validation were modified in order to fit more the reality. then a comparison with the real data and results would give hits about the model failures.

8.2.1 Delays

It could be seen on the results of the propagation model (Chapter 4.6) that the Yonne river peak flow was simulated a bit in advance related to what 2.4was observed. This phenomenon was explained by an increase of the river water celerity on this river between 1910 and the recent period on which the calibration was made. This increase of celerity was explained by the removal of 3 locks.

On all simulation of the 1910 flood on the Seine at Paris Austerlitz basin (see for example figures 3.4, 7.8 or 8.3), the simulated peak flow is also in advance related to the observed one. It is thus possible that the water celerity has raised on the whole Paris Austerlitz basin due to several recent development on the river such as lock removal. In this case, the advance in the peak flow could be explained by a difference in the celerity between the calibration period and the validation in 1910.

A delay D was thus introduced on the 1910 simulated results. D is a float parameter expressed in days and the new flow $F_{delay}(d)$ at day d is given by the equation :

$$\begin{aligned} F_{delay}(d) = &\left[1-\left(D-Int(D)\right)\right]\times F_{calc}\left(d-Int(D)\right) \\ &+\left(D-Int(D)\right)\times F_{calc}\left(d-\left(Int(D)+1\right)\right) \end{aligned} \quad \text{(Eq. 8.2)}$$

Where :

- $F_{delay}(d)$ is the new calculated flow including the delay at day d in mm/day

- D is the delay in days
- Int(D) is the Integer part of D in days
- $F_{calc}(d)$ is the simulated flow, calculated by GR4J in validation at day d, in mm/day

8.2.2 modification of the precipitations

On the observed hydrograph of the Seine at Paris Austerlitz basin on the 1910 flood, a plateau can be seen from around February, 11th to February 18th. None of the simulated hydrographs is able to replicate this plateau (figures 3.4, 7.8 or 8.3 for example). In the absence of rain, such a plateau can be caused by snow melting –but this hypothesis was tested and did not give any satisfactory result – or by a positive groundwater exchange with another neighboring basin.

To get an estimation of the water that was brought to the basin to explain such a plateau, the precipitation data were modified in order to replicate it as accurately as possible.

8.2.3 Data

The same data like in chapter 7 were used on the Seine at Paris Austerlitz basin.

8.2.4 Method

The Excel software was used. First the calibration and validation were done as in the previous chapters. The results obtained in validation were then modified to give a delayed simulated flow using equation 8.2. The delay D was then calibrated so as to maximize the Nash-Sutcliffe efficiency calculated by comparison of the delayed simulated flow and the observed Flow.

Then, precipitations were modified in February 1910 and calibrated in order to get the best result possible in validation on the 1910 flood. The goal was also to modify precipitation on as few days as possible. Those new calculated flows obtained with modified precipitations were then delayed using equation 8.2. The delay D was then optimized again.

8.2.5 Results

The best compromise between the Nash-Sutcliffe Efficiency and the number of days with modified precipitations was obtained by modifying only 2 days : Februray, 11th and 12th 1910 :

- On February, 11th, instead of the 1,31 observed mm of rain, 10,12mm were put.
- On February, 12th, instead of the 0,55 observed mm of rain, 7,54mm were put.

Only the results obtained with those modifications will be presented in this part.

The different Nash-Sutcliffe Efficiencies calculated - with and without delays, with and without the modified precipitations described above - are summarized in table 8.2.

The different hydrographs obtained with KGEmod calibration taking water reservoirs into account are shown on figure 8.4.

And the different hydrographs obtained with KGEmod calibration, taking the water reservoirs into account, with the frost module using the coldest pixel temperature, are shown on figure 8.5.

Table 8.2 Obtained Nash-Sutcliffe Efficiencies with different calibration method, with and without delays, with and without precipitation data modifications.

Method	NSE obtained in validation without delay	Delay (in days)	NSE obtained in validation with delay
KGEmod calibration taking water reservoirs into account, without precipitation modifications	0,489	2,31	0,66
KGEmod calibration taking water reservoirs into account, with 2 days precipitation modifications	0,589	2,28	0,761
KGEmod calibration taking the water reservoirs into account with the frost module using the coldest pixel temperature, without precipitation modifications	0,54	2,32	0,722
KGEmod calibration taking the water reservoirs into account with the frost module using the coldest pixel temperature, with 2 days precipitation modifications	0,63	2,29	0,815

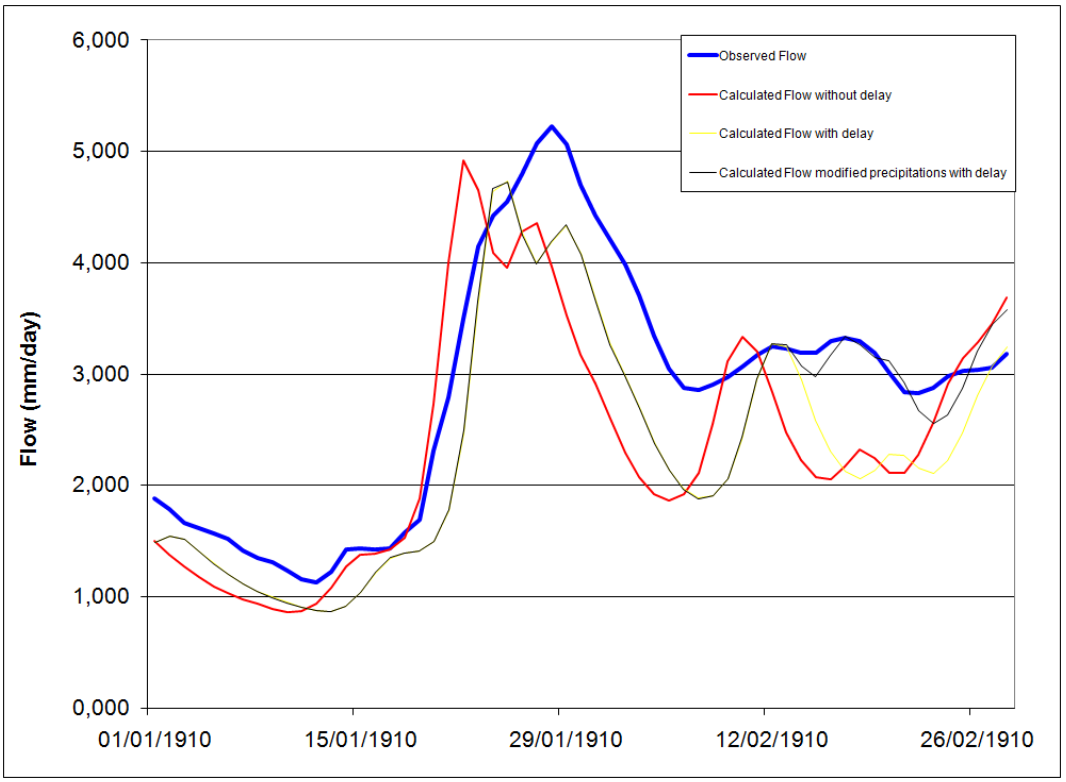

Fig. 8.4 Observed hydrograph and calculated hydrographs obtained after KGEmod calibration taking water reservoirs into account, without delay, with delay and with 2 days precipitation modifications and delay.

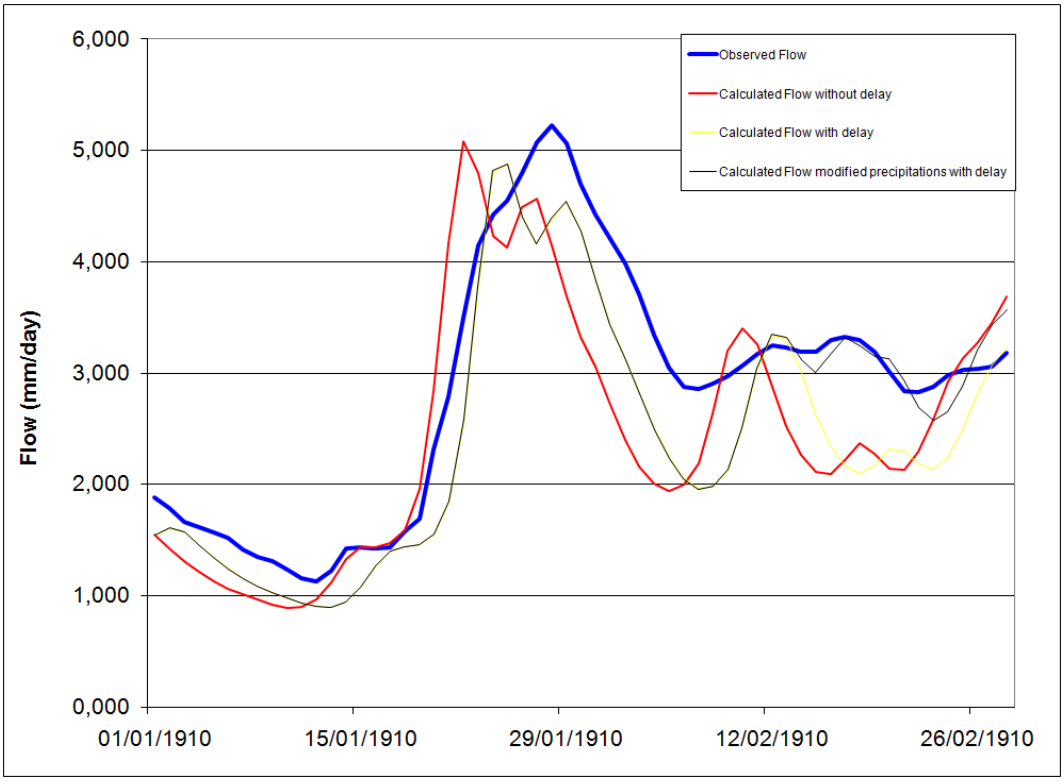

Fig. 8.5 Observed hydrograph and calculated hydrographs obtained after KGEmod calibration taking water reservoirs into account, with the frost module using the coldest pixel temperature, without delay, with delay and with 2 days precipitation modifications and delay.

8.2.6 Discussion

It can be seen that the results obtained by putting a delay to the calculated flows are much better than the normal calculated flows for all calibration methods with a NSE increase of around 0,18 points in each case (Table 8.2). Furthermore, the delays, that are calibrated in each case to maximize the Nash Sutcliffe efficiency calculated on the observed low and the calculated flow with delay, are very similar for each calibration technique and get a value around 2,3 days (Table 8.2). This quasi-equality in the calibrated delays may suggest that the hypothesis of a water celerity change on the basin between 1910 and the recent years and that would influence GR4J results could be true and that, in average, on the Seine river, peak flows are now reaching Paris Austerlitz station more than 2 days in advance related to what was happening in 1910.

Furthermore, precipitations values modifications on only 2 chosen days (February, 11th and 12th) also leads to better results in validation with a NSE increase of around 0.1 in each case (Table 8.2). However, the hypothesis of failures in the data is not acceptable as more than 100 stations were used to calculate the average precipitations and it is not possible that all of them were giving false results on those particular 2 days. However, this may suggest that a certain amount of water - that can be estimated from the new values put for precipitations – was brought to the basin on those 2 days, maybe by groundwater exchange with another basin.

In any case, the results obtained with delayed calculated flow obtained with precipitation values modified on only 2 days are relatively satisfactory with a NSE value superior to 0,75 - the addition of the frost module still not bringing much improvement (Table 8.2). The

hydrographs (Fig. 8.4 and 8.5) are confirming this conclusion : the delayed calculated peak flow is closer to the Observed one than the normal calculated peak flow, even if it is still a bit in advance. The 2 days precipitation modifications are leading to a satisfactory simulation of the plateau in February 1910. However, the Flow is still underestimated during the period between the peak flow and the plateau.

Even if those results are based on unjustified hypothesis, they should be considered as they give important clues about what brings GR4J's inability to reproduce the 1910 flood. Those delays and water surplus may have physical causes that are not taken into account in the model and that, obviously, may have critical influences on its results.

8.3 Linking error and temperature

On figure 5.1, it could be seen that the Seine peak flow was corresponding to a water temperature drop which led to the hypothesis of frozen soil as a cause of the 1910 flood. However it was not possible to study the reliability of this hypothesis since the frozen soil module that was designed could not really be calibrated nor assessed.

But it may not be necessary to model frost as it was done in this study. A new perspective would be to assess a possible correlation between the model error and the water or air temperature. If such a correlation exists then it could be assumed that when the water temperature –or maybe even air temperature – are relatively low – in a way that should be more precise – then "something" happens – that could be frost or any other phenomenon – that is not taken into account by GR4J and that wil thus create error that can be automatically corrected.

In this part, the link between GR4J error and water and air temperatures will be studied on the 1910 flood to assess if such a correlation could be exploited to improve the model.

8.3.1 Data

The observed flow on the Seine at Paris Austerlitz basin was used. The calculated flow was obtained by NSE calibration taking water reservoirs into account (Part 3.2).

The same air temperatures in Paris data like in chapter 7 were used from January, 1st to February, 28th 1910. The water temperatures data in the Marne river on the same period were furnished by the *DIREN*.

8.3.2 Method

On each day from January, 1st to February, 28th 1910, the error was calculated as the difference between the observed and the calculated flow. This error was then matched to the air and the water temperatures at this day.

In a second step, the cumulated error was calculated for each day and drawn against cumulated air and water temperatures. For calculation of the cumulated errors and temperatures, negative values were replaced by 0.

8.3.3 Results

The scatter plot showing daily air and water temperatures against daily errors are shown on figures 8.6 and 8.7 respectively.

The graphs showing the cumulated error as a function of the cumulated air and water temperatures are shown on figures 8.8 and 8.9 respectively.

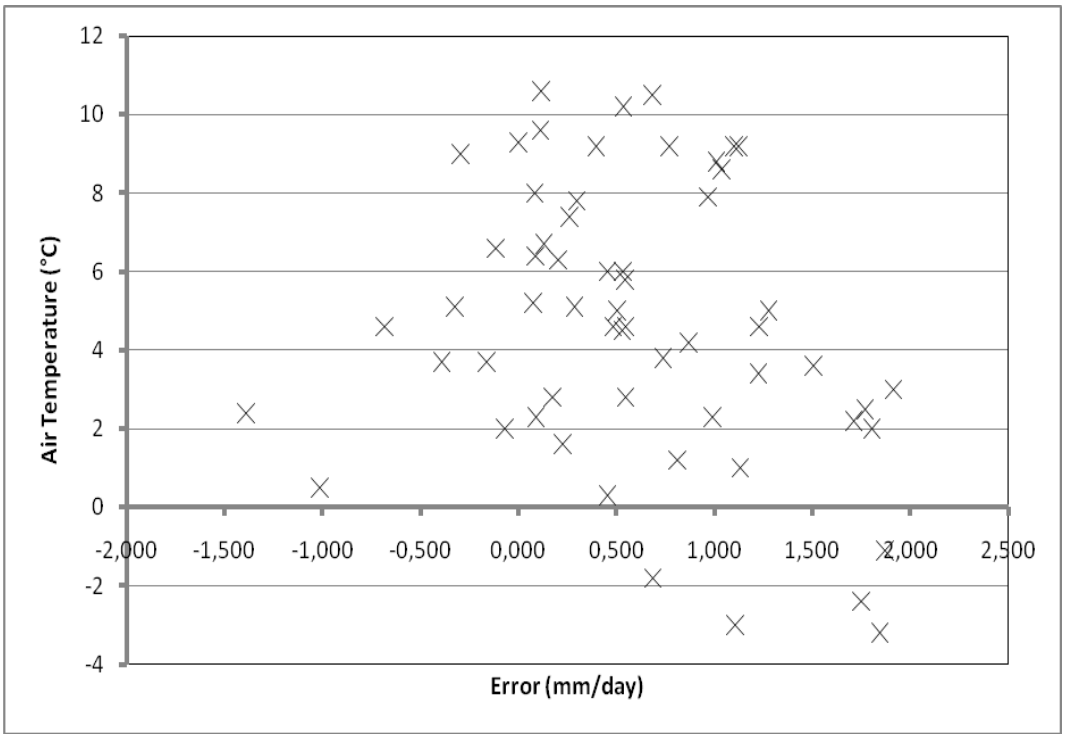

Fig. 8.6 scatter plot of the air temperatures against errors (observed flow - calculated fow with NSE calibration taking water reservoirs into account)

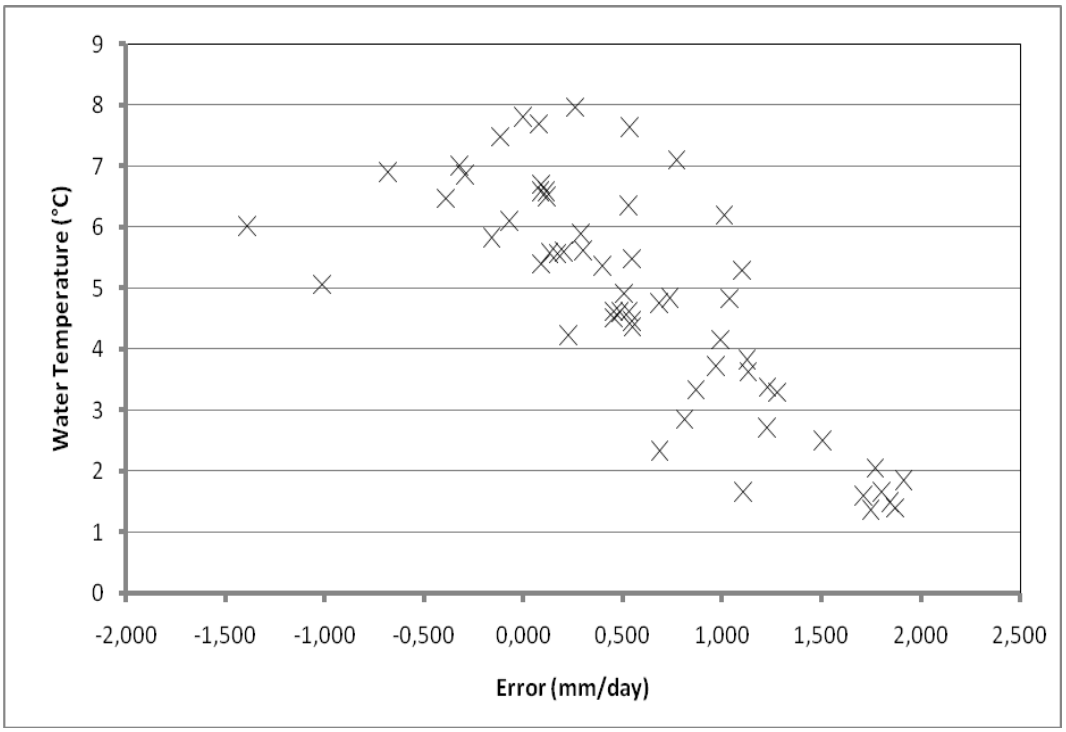

Fig. 8.7 scatter plot of the water temperatures against errors (observed flow - calculated fow with NSE calibration taking water reservoirs into account)

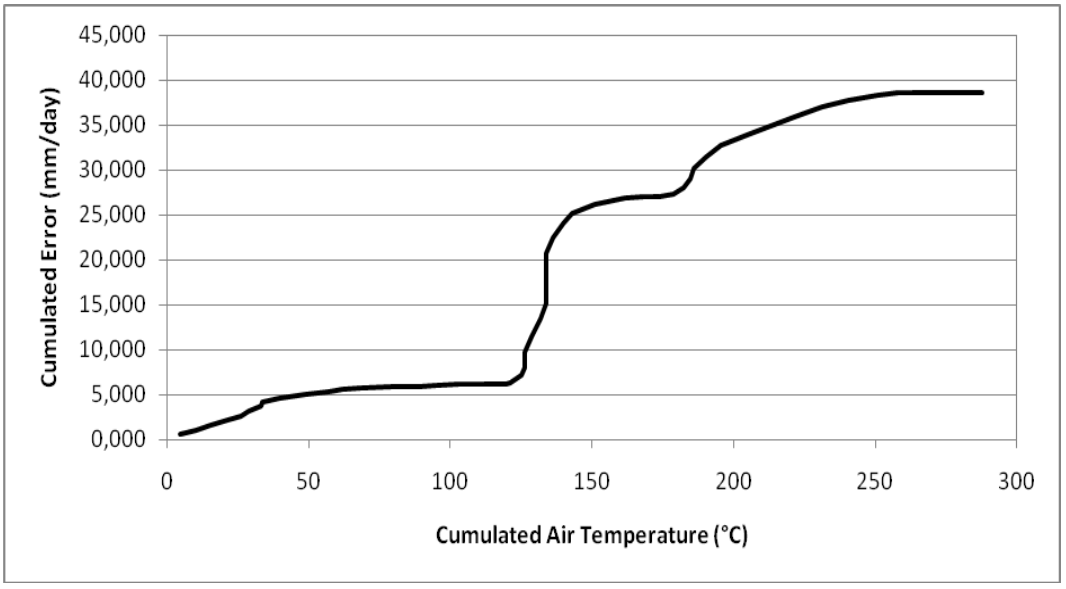

Fig. 8.8 cumulated error (observed flow - calculated fow with NSE calibration taking water reservoirs into account) function of cumulated air temperature.

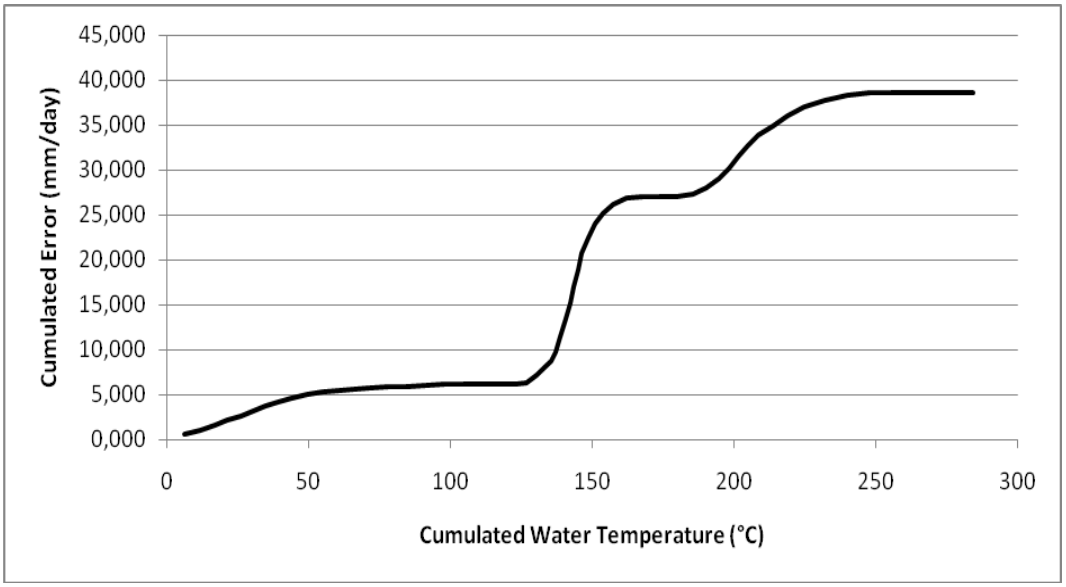

Fig. 8.9 cumulated error (observed flow - calculated fow with NSE calibration taking water reservoirs into account) function of cumulated water temperature.

8.3.4 Discussion

The correlation between air temperature and GR4J error on the 1910 flood is not obvious on figure 8.6 even if it can be seen that all errors superior to 1,5 mm/day happened on days with an air temperature inferior to 2°C. However on figure 8.8, an almost vertical slope can be observed in the middle of the graph. This slope represents a period of time with very low air temperature (and thus a small increase in cumulative air temperatures) but large daily errors (and thus a large increase in cumulative errors). This phenomenon is happening from January, 23rd to February, 3rd 1910 i.e. during the peak flow of the flood.

The correlation between water temperatures and errors is much more visible. The scatter plot on figure 8.7 clearly shows the tendency of larger errors happening when water temperature is low. Furthermore, the same

almost vertical slope can be observed on figure 8.9 at the same period of time than for air temperatures with the same interpretation.

Those graphs are thus clues that GR4J errors could be linked to air or water temperatures with a more obvious correlation with the last one. It may not be necessary to model any physical phenomenon and a simple corrective term, function of air or water temperatures, could be added to the model to correct those errors if they happen to be recurrent. That would be a new perspective to continue the investigation on the 1910 flood problems for GR4J simulations.

8.4 General Conclusion

On chapters 2 and 3 the GR4J problems to reproduce the 1910 flood were identified and some firs approach hypothesis were then tested to solve them. It appeared that taking the water reservoirs into account or changing the statistical tools during the calibration, if it improved the results, did not lead to satisfactory results on the main basin of the Seine at Paris Austerlitz and 2 of 4 of its sub-basins : the Marne at Ferté-sous-Jouarre and the Seine at Bazoches-lès-Bray.

The hypothesis was then made that frost could be a the origin of those problems as it is not taken into account in the model and that it has an influence on the hydrology of the basins. A frost module, linked to a soil temperature estimation model using air temperatures data in input was then designed specifically. However, this additional module did not give significant improvement on the 1910 flood simulations. However, no conclusion could be drawn on the frost role on the 1910 flood from those results. Indeed, the lack of relevant data on recent years had prevented a good calibration and assessment of the model.

This study has thus shown that improvements could be brought to the 1910 simulation by taking into account water reservoirs and using the KGEmod criterion in calibration. It has also permitted to isolate the problem on 2 of the 4 sub-basins. However it did not manage to show any evidence concerning the role –or absence of role - of frost on this flood and on GR4J errors. this should not be considered as a failure, but as the first steps of an investigation that should now be continued with new modules.

This last chapter has thus shown some new perspectives of development for the continuation of this study. Indeed, if the addition of a certain amount of rain – that could be justified by an hypothetical undercatch in 1910 – did not bring any significant improvements on the simulation, other results are worth studying. First, it was shown that the addition of a delay on the calculated flow –that could be justified by a change in water velocity between 1910 and recent years – brought significant improvement on the simulation. Furthermore, an addition of rain on only 2 days was also bringing significant improvements. It is thus worth investigating on the possibility of such a transfer on those days. Finally, a last study showed apparent correlations between the model errors and air or particularly water temperatures. If this correlation happens to be recurrent on other basins or periods of times, a new model that would not be based on physical phenomenon like the frost module developed on this study but only on those statistical correlations, could be designed to improve GR4J.

As a conclusion, this study has thus shown that none of the suggested hypotheses listed in chapter 1.4 could lead to a satisfactory simulation of the 1910 flood, even if some of them significantly improved it, and the causes of the flood are still unclear. There are several reasons for this,

especially the lack of relevant data for the frost hypothesis testing. However this study has also shown new hypothetical explanations that should now be tested and could lead to the solution of the 1910 flood simulation problem.